

802209

A MINERALOGICAL AND GEOCHEMICAL STUDY
OF THE ZONAL DISTRIBUTION OF ORES IN
THE HUDSON BAY RANGE, BRITISH COLUMBIA

By

RODNEY VICTOR KIRKHAM

A thesis submitted in partial fulfillment of the
requirements for the degree of

DOCTOR OF PHILOSOPHY
(Geology)
at the
UNIVERSITY OF WISCONSIN

1966

ABSTRACT

Sulfide-sulfosalt vein and replacement ores rich in Fe, As, Ag, Zn, Pb, and Au; a stockwork-type molybdenum deposit; a Au-Bi-Te- vein and replacement deposit; and some small Cu-Fe-Ag deposits in the Hudson Bay Range of west-central British Columbia are zonally arranged about felsic porphyritic Tertiary intrusions. The ores are apparently temporally and genetically related to the intrusions.

A study has been made of the geologic setting of the deposits, the chemistry of the ores, and the geochemistry of sphalerite, pyrrhotite, arsenopyrite, and other minerals in an attempt to define the zoning more closely and to evaluate processes controlling its development.

The 60 or so known deposits of the district have been divided into groups based on their mineralogy, metal content, and structural features. Small "sulfide" vein deposits with variable amounts of sulfosalt and gangue minerals are by far the most common type. Arsenopyrite, pyrite, pyrrhotite, sphalerite, galena, quartz, carbonate, marcasite, chalcopyrite, tetrahedrite, bournonite, and ruby silvers are the most common minerals. Sulfide replacement bodies, that have many of the mineralogic features of the veins, occur at sulfide vein intersections in limestone lenses.

The molybdenum deposit, which is centrally located, is essentially a very extensive stockwork of small quartz veins containing variable amounts of ore and other gangue minerals. Quartz, magnetite, pyrite, molybdenite, hornblende, biotite, chlorite, potash feldspar, muscovite, calcite, dolomite, pyrrhotite, chalcopyrite, scheelite, and gypsum are the most important vein minerals. The Au-Bi-Te deposit, consisting of native Au and Bi, bismuthinite, Bi-Te sulfides, and molybdenite in quartz veins and replacement pods in highly altered rocks, occurs near the fringe of the molybdenum deposit.

The Cu-Fe-Ag ores are a special type of outer zone deposit. They are mostly small veins, with little associated alteration, containing variable amounts of chalcopyrite, bornite, magnetite, hematite, pyrite, and unidentified silver minerals.

Metal content, mineralogy, and structural features of the ores outline the zoning. The distribution of iron sulfides has been used to divide the district into an inner (pyrite), an intermediate (pyrrhotite) zone, and an outer (pyrite) zone. The inner zone is approximately coincident with the molybdenum deposit and the intermediate and outer zones

cover the areas that contain sulfide deposits. An area containing mostly barren quartz veins, between the inner and intermediate zones and somewhat overlapping the two, has been designated the "barren" zone.

Metal content, mineralogy, structural features, and spatial arrangement of deposits suggest that all ores were emplaced under the same regional thermal-hydrothermal regime. But the sulfide ores were probably formed before the molybdenum deposit during or just after the period of thermal metamorphism. The molybdenum deposit was formed largely after the period of thermal metamorphism during a stage of more restricted magmatic activity in the Glacier Gulch area. The thermal-hydrothermal regime established by the emplacement of the Tertiary porphyries could have been the main factor controlling the zonal arrangement of ores.

TABLE OF CONTENTS

	Page
INTRODUCTION	1
Location and Topographic Features of the District	3
Previous Studies	5
Mining History	6
Acknowledgements	6
GENERAL GEOLOGY	8
Stratigraphy	8
Felsic Intrusions	11
Thermal Metamorphism	15
Geologic History of the Range	16
ORE DEPOSITS	19
General Description	19
Sulfide Vein and Replacement Deposits	20
Molybdenum Deposit	22
Hypogene Zoning	26
Statistical Study of Assays	30
Introduction	30
Statistical Methods and Computing Pro- cedures	31
Nature of the Samples	33
Selected Results	36
Vein and Mineral Paragenesis	45
Features of Selected Minerals	56
Tetrahedrite-Tennantite	56
Bournonite	56
Galena	57
Chalcopyrite	57
Gypsum	59
Scheelite	59
Vein Feldspars	63
Vein Carbonates	63
Precious Metals	70
Pyrrhotite	72
Distribution and Description	72
Experimental Techniques	75
Interpretation of the Results	78
Sphalerite	82
Introduction	82
Distribution and Description	82
Chemically Analyzed Sphalerite Standards	85
Electron Microprobe Analyses	87
Instrumentation and Analytical Procedures	92
Discussion of the Results	97

District-wide Variations in the FeS Content of Sphalerite	103
Arsenopyrite	108
Distribution and Description	108
Arsenopyrite Geothermometer-Geobarometer	110
Chemical Analyses	111
X-ray Analyses	113
Discussion of the Results	115
District-wide Variations in the Composition of Arsenopyrite	119
Fluid Inclusions	122
 SOME THEORETICAL CONSIDERATIONS OF ORE GENESIS	127
Pressure Estimates of Ore Formation	127
Thermal Pattern in the District	129
The Concept of Monoascendent and Polyascendent Zoning	131
Chemical Character of Ore Solutions in Terms of Activity of Sulfur and Temperature	132
Possible Mechanisms of Deposition	134
Mixing of Solutions	134
Throttling	135
Chemical Control of Host Rocks	138
Structural Control	139
Possible Model of Ore Formation	140
 CONCLUSIONS	143
 BIBLIOGRAPHY	145

Tables

	Page
1 Table of Formations	10
2 Index to Properties	28
3 Summary of Assay Data	32
4 Chemical Analyses of Tetrahedrite	56
5 Chemical and X-ray Data for Scheelite	60
6 Chemical Analyses of Calcites	65
7 Summary of X-ray and Staining Data for Vein Carbonates	67
8 Precious Metal Contents of Mineral Concentrates . .	71
9 Summary of Pyrrhotite Data	76
10 Chemical Analyses of Sphalerite Standards	87
11 Sphalerite Analyses Corrected for Impurities and Recalculated to 100 Weight Per Cent	88
12 Calculated Mole Per Cent Sulfides in Sphalerite Standards	89
13 Summary of Electron Microprobe Data for Sphalerite	98
14 Chemical Analyses of Arsenopyrite Standards	113
15 Summary of X-ray Data for Arsenopyrite	114

Figures

1 Index Map	3
2 Aerial View of Hudson Bay Mountain	4
3 Generalized Geologic Map	9
4 Typical Specimens from the Granodiorite Sheet	13
5 Typical Tertiary Porphyry	14
6 View of a Thrust Fault	17
7 Dome Vein	21
8 Area of Prominent Jointing in the Molybdenum Deposit	23
9 Typical Quartz Vein Stockwork of the Molybdenum Deposit	23
10 Sparsely Mineralized Fine Grained Quartz, Molyb- denite Veinlet	24
11A Quartz, Magnetite Veinlet with a Prominent, Pyritic, Bleached Halo	25
11B Bleached Alteration Halos along a Quartz, Hornblende Veinlet and a Pyrite Veinlet	25
12 Properties and Mineral Zones	27
13 Generalized Diagram of the Mineral Zoning	29
14 Ag-Pb Regression Curve for 3920 Level Henderson Vein	37
15 Selected Ag-Pb Regression Curves	38
16 Gold Content of Deposits from Assay Data	41
17 Silver Content of Deposits from Assay Data	41
18 Lead Content of Deposits from Assay Data	41
19 Zinc Content of Deposits from Assay Data	41
20 Silver-Gold Ratios Calculated from Assay Means . . .	43

21	Silver-Gold Ratio of Ores Shipped from Central City District	43
22	Silver-Lead Ratios Calculated from Assay Means	43
23	Lead-Zinc Ratios Calculated from Assay Means	43
24	Barren "Wormy" Quartz Veins Cut by Tabular Quartz Veins	48
25	Type I Molybdenum Veins	49
26	Type I Veins Cut by Type II Veins	49
27	Paragenetic Diagrams	51
28	Pyrite from Small Veinlet in the Molybdenum Deposit.	53
29	Arsenopyrite from the Copper Queen Claim	53
30	Poikilitic Pyrite Crystal	55
31	Pyrrhotite Partly Replaced by Lamellar Marcasite	55
32	Row of Sphalerite Inclusions in Chalcopyrite	58
33	Calcite Vein Cutting Volcanic Host Rock and Banded Ferroan Dolomite	64
34	Subsolidus Relations in the System $\text{CaCO}_3 \cdot \text{MgCO}_3 \cdot \text{FeCO}_3$	68
35	"Zig-Zag" Troilite Lamellae in Hexagonal Pyrrhotite.	79
36	Intergrowth of Monoclinic Pyrrhotite in Hexagonal Pyrrhotite	79
37	Monoclinic Pyrrhotite Formed in Hexagonal Pyrrhotite	80
38	Lamellae of Monoclinic Pyrrhotite in Hexagonal Pyrrhotite	80
39	Oriented Lamellae and Blebs of Chalcopyrite in Unetched Sphalerite	84
40	Oriented and Unoriented Lamellae of Chalcopyrite in Etched Sphalerite	84
41	Calibration Curve for Sphalerite Microprobe Analysis	96
42	Frequency Distribution of FeS in Sphalerite from Sample 63-174A	96
43	FeS Contents of Sphalerites in Mole Per Cent	103
44	Variation in FeS Content of Sphalerite Away from the Metamorphic Front	105
45	Variation in FeS Content of Sphalerite Away from Point "A"	105
46	Schematic Contour Map of the Average FeS Content of Sphalerite	106
47	Twinned Arsenopyrite Crystals Veined by Pyrrhotite, Chalcopyrite, and Quartz	109
48	Zoned Arsenopyrite Crystals from the Iron Vault Property	109
49	Dependence of the $d(131)$ Spacing of Arsenopyrite on the As Content.	115
50	Variation in the As Content of Arsenopyrite Away from the Metamorphic Front.	120
51	Lines of Constant Spacing of Arsenopyrite on PT Projection	121
52	Fluid Inclusion with a NaCl Daughter Mineral	125
53	Typical Fluid Inclusions in Sphalerite	125
54	$a\text{S}_2$ -T Diagram for Selected Sulfidation Reactions	133
55	Isothermal P-X Projection of the L-V Boundary in the System $\text{NaAlSi}_3\text{O}_8\text{-H}_2\text{O}$	141

INTRODUCTION

During the past two decades the understanding of geochemical processes of hydrothermal ore deposition has been tremendously advanced. The recent book "Geochemistry of Hydrothermal Ore Deposits" (ed. Barnes, 1967) is ample testimony to this fact. Most of the advances have been made through laboratory study of pertinent phase equilibria, solution chemistry, and by the application of thermodynamic principles to the understanding of natural systems. Because of the nature of these studies most of the work has been carried out by physical-chemists and laboratory-oriented geologists. However, if we are to gain a more accurate impression of the processes of ore deposition, geochemically oriented field studies which guide, supplement, and ultimately test the laboratory work should keep pace with experimental studies. It was with this consideration in mind that the present study was undertaken.

When the study was initiated in 1963, it was thought that temperatures of ore formation could be determined by application of sulfide solid-solution geothermometers and that the importance of temperature as a control on district-wide mineral zoning could be evaluated. The compositions of sphalerite and pyrrhotite were to be used as "sliding-scale" geothermometers. Work since this study was initiated has shown that these geothermometers, as originally proposed, are invalid. However, the same studies have added greatly to our knowledge of the conditions of formation of these minerals.

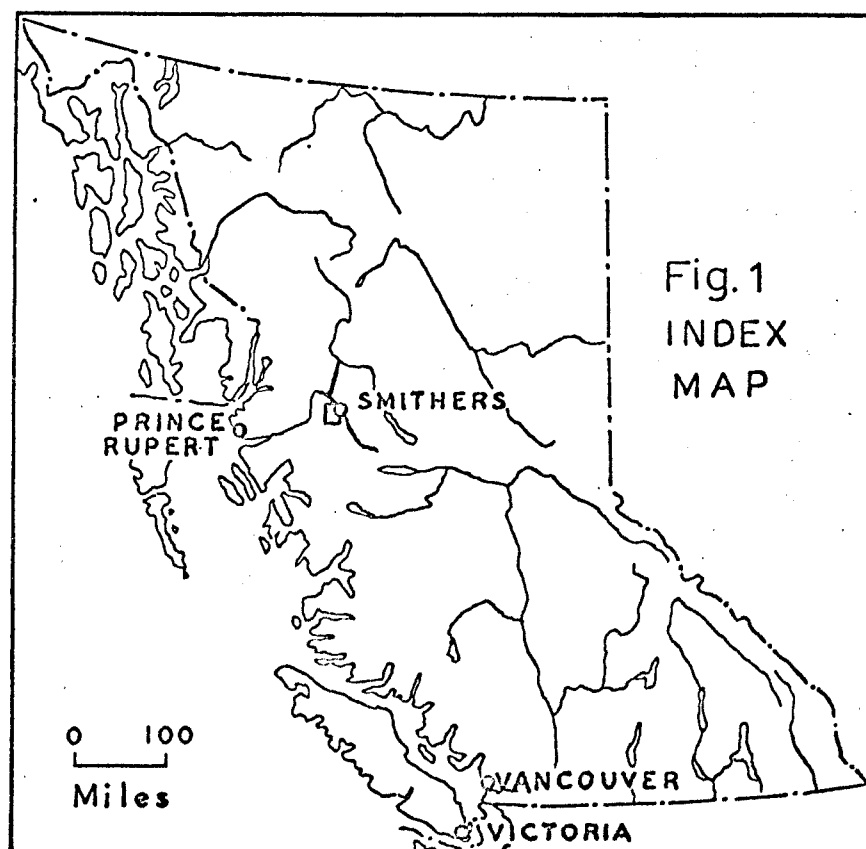
Thus, even though at this time quantitative geothermometry using these minerals is not possible, study of their compositions and associated minerals can set some general restrictions on conditions which prevailed during ore deposition, and hence, give greater insight into the processes of deposition.

Since it was first studied, the Hudson Bay Mountain area has been considered to be a district displaying prominent zonation of mineral deposits. This study was designed to define the zoning more closely and to shed light on the processes of ore deposition. The study of sphalerite has been strongly emphasized because sphalerite is widespread and shows considerable chemical variation, and because its phase relations are fairly well known. In general its chemical variations conform with the zonal pattern of the ores; hence, they should reflect some of the changes in conditions of ore deposition. Variations in other major minerals such as pyrrhotite, arsenopyrite, and vein carbonates, have been studied, but detailed studies of wall rock alteration and minor constituents of the deposits have been deferred. It is hoped that by concentrating on major aspects of the mineralogy and the associated regional geological study, a foundation will be established from which other studies can be carried out. Field studies of all the deposits considered here and a study of the regional geology have been carried out by the writer, but general geological aspects of these studies are only summarized in this thesis. They will be presented later as

a bulletin of the British Columbia Department of Mines.

Location and Topographic Features of the District

The fifty to sixty known mineral deposits that lie within the Hudson Bay Mountain mining district occur in the eastern half of the Hudson Bay Range in west-central British Columbia. The area is about 900 miles by road north of Vancouver and about 230 miles east of the port of Prince Rupert. It is immediately west of the Bulkley River at the town of Smithers and lies about 40 miles east of the Coast Mountains. B.C. Highway 16 and a line of the Canadian National Railway pass along the eastern margin of the district.



The range is one of a group collectively called the Hazelton Mountains. These isolated ranges lie immediately east of the main chain of the Coast Mountains just north of the Interior Plateau. To the east they are flanked by more small ranges that form the southern end of the Skeena Mountains and northern end of the Nechako Plateau (Holland, 1965).



Figure 2 - Aerial view of Hudson Bay Mountain from the northeast. Glacier Gulch is in the foreground and Toboggan Creek is to the right. The center of the molybdenum deposit is marked by an "x".

The Hudson Bay Range is an isolated group of ridges and peaks about 200 square miles in extent. Hudson Bay Mountain, 8497 feet in elevation, is the dominant topographic feature. Valleys and passes bounding the mountain mass range from 1300 to 3500 feet in elevation.

Three small glaciers are present in the upper reaches of Hudson Bay Mountain and there are a few rock glaciers in some of the west and north-facing cirques. In general, outcrop is excellent above 5000 feet at tree-line, but some areas below this level have very sparse exposures and thick conifer forests.

Previous Studies

All mining properties of the area have been examined from time to time by officers of the British Columbia Department of Mines and are described in the Annual Reports of the Minister of Mines. The prime purpose of these reports was to record any exploration activity on the properties; some of them therefore contain little or no geological information. The only comprehensive reports on the geology and mineral deposits of the area have been published by the Geological Survey of Canada.

R.H. Jones (1925 and Univ. of Wis. Ph.D. thesis) published the first comprehensive report on the geology and mineral deposits of the district. He spent one summer on field work, mapping about 200 square miles and studying selected mineral properties. A geological map at a scale of one inch to two miles that includes the Hudson Bay Range was compiled by J.E. Armstrong of the Canadian Geological Survey in 1944. There are few changes on this map from Jones' original work. E.D. Kindle (1954) published a report on the mineral resources of the area but he mainly restricted his study to individual deposits and made no attempt to study the areal geology.

The writer (1966) has described briefly the geology in the vicinity of the molybdenum deposit.

Mining History

The Hudson Bay Mountain mining district has not been an important source of metals, but its future prospects are promising. Since 1905, when extensive exploration in the district began, the only significant producer has been the Sil Van Mine (earlier the Duthie Mine and the Henderson Mine). From 1923 to 1954 it produced about 80,000 tons of ore, bearing values in lead, silver, zinc, gold, and copper. Other properties of the district have only yielded tonnages of ore insufficient to sustain mining operations.

Interest in the district was renewed in 1956, when the molybdenum deposit was staked. American Metals Climax (Southwest Potash and Climax Divisions) has since been exploring the deposit. The company first did extensive diamond drilling from surface, and then in 1966 continued exploration from underground workings. This deposit should become a major source of molybdenum, tungsten, and possibly copper.

Acknowledgements

The field work was sponsored by the British Columbia Department of Mines and Petroleum Resources, which also kindly provided chemical analyses of several rock and mineral samples. Helpful assistance in mapping was given by Messers. Thomas Burgess (1963), David Haegert (1964), Robert Thorburn (1964 and 1965), and Alan Foster (1967).

The writer is indebted to the Geological Survey of Canada

for performing four K-Ar age determinations on vein and porphyry minerals from the Glacier Gulch area, for spending much time on selection of proper samples, and for continued interest in the study.

Climax Molybdenum (B.C.) Ltd., Sil Van Mines, Ltd., and Hudson Bay Mountain Silver, Ltd. generously provided access to their drill core, geological records, and assays. Messers. H. Gilleland, J. Allan, R. Anderson, R. Barker, J. Jonson, D. Davidson, and Dr. S. Wallace were particularly helpful.

Dr. P. Barton of the United States Geological Survey kindly provided the synthetic sphalerite samples used in preliminary electron microprobe studies, and Mr. E. Glover of the University of Wisconsin helped the writer with many aspects of the microprobe work.

Mr. K. Billingsley of the Political Science Department of the University of Wisconsin helped tremendously in the computational aspects of this thesis. Mr. B. Lewis of the Geophysics Department also helped in the computational work. The Wisconsin Alumni Research Foundation provided the funds for computer use. These funds are made available by the National Science Foundation which supports the University of Wisconsin Computing Center.

A grant from the Union Carbide Research Corporation supported completion of this thesis from December 1967 to April 1968.

The writer is also indebted to Dr. E.N. Cameron and other members of the faculty of the Department of Geology of the University of Wisconsin for guidance and constructive criticism.

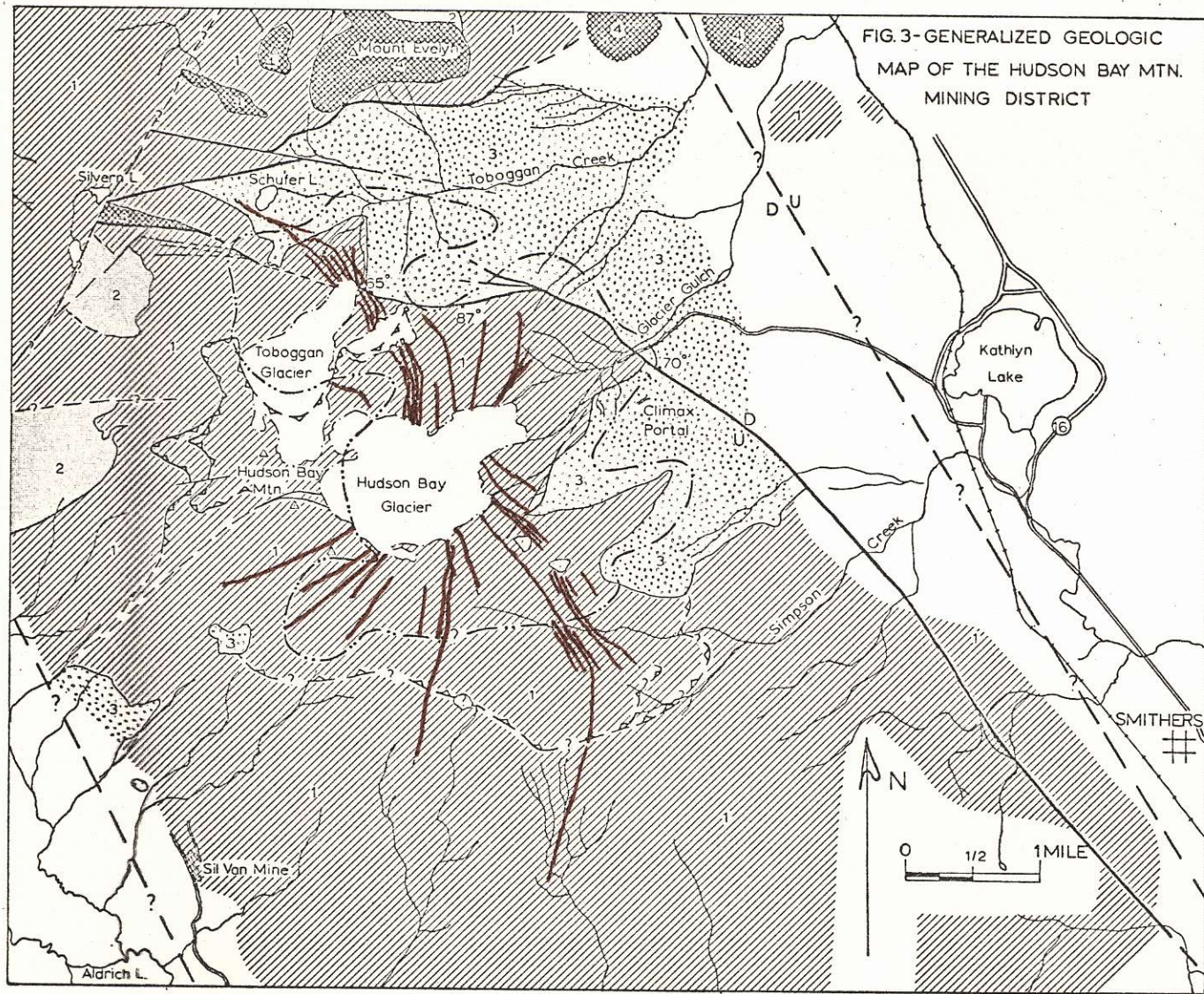
GENERAL GEOLOGY

The district is underlain mainly by volcanic and sedimentary strata of the Hazelton Group and sedimentary strata of the Bowser Group (Figure 3), both probably of Jurassic age. A few small bodies of Jurassic or Cretaceous (?) granodiorite and quartz monzonite are exposed in the northern and western parts of the district, and numerous early Tertiary porphyry dikes and some small plugs and stocks occur near the molybdenum deposit in Glacier Gulch. Covered Tertiary porphyry intrusions are probably responsible for the thermal metamorphism in the central part of the district. There has been no regional metamorphism above lowest greenschist facies. Although there has been extensive faulting, including thrusting, in general, folding has not been intense.

Stratigraphy

Stratigraphic relations in the district are summarized in Table 1.

Hazelton volcanic rocks include many diverse types but pyroclastic rocks, especially lapilli tuff, of intermediate composition are most abundant. Welded tuffs and lava domes have been recognized in some units. Some sequences are composed almost entirely of massive units whereas some contain a high percentage of bedded rocks. Many sequences are composed mainly of rocks that are shades of red, purple or brown, owing to hematite pigment; however, rocks that have been hydrothermally altered or thermally metamorphosed are



LEGEND







-  - Granodiorite
-  - Bowser sedimentary rocks
-  - Hazelton sedimentary rocks
-  - Hazelton volcanic rocks
-  - Tertiary porphyry dike
-  - Limit of thermal metamorphism

Table 1 - Table of Formations

Era	Period or Epoch	Unit	Lithology	
Cenozoic	Pleistocene & Recent		Glacial till; glacio-fluvial sand, gravel, and silt; recent talus and alluvium	
	Unconformable contact			
	Paleocene		Felsic, porphyritic dikes and stocks	
Mesozoic	Jurassic or Cretaceous(?)	Bulkley intrusions	Intrusive contact	
			Granodiorite and quartz monzonite	
	Fault and intrusive contacts			
	Upper Jurassic and Lower Cretaceous (?)	Bowser Group	Poorly sorted conglomerates, graywacke siltstone, mudstone, minor impure coal, and hornfelsic equivalents	
	Unconformable contact			
	Middle Jurassic (?)	Volcanic Division	Andesitic, dacitic, rhyolitic, and basaltic tuffs, breccias, flows, and intrusions, and hornfelsic equivalents	
	Bajocian (Lower Middle Jurassic)	Hazelton Group	Fault contact (?)	
			Sedimentary Division	Poorly sorted limy tuffaceous graywacke and siltstone, mudstone, cherty mudstone, and minor conglomerate and coal
	Lower Middle Jurassic or earlier	Hazelton Group	Conformable contact	
			Volcanic Division	Andesitic, dacitic, rhyolitic, and basaltic tuffs, breccias, flows, and intrusions and hornfelsic equivalents; minor limestone and tuffaceous graywacke

generally light or dark shades of green, gray or brown. Interlayered units of unquestionable sedimentary character are uncommon in the volcanic sequences. Nevertheless, it is quite possible that much of the pyroclastic debris has been reworked by sedimentary agents. Greenstone, diabase, and diorite dikes and felsitic intrusions are abundant in most volcanic sequences.

Bajocian sedimentary rocks of the Hazelton Group are definitely conformable with the underlying volcanic rocks on the western side of Hudson Bay Mountain but their upper contact relations have not been established.

Bowser sedimentary rocks unconformably overlie volcanic rocks of the Hazelton Group. Plant fossils in Bowser rocks mostly indicate an Upper Jurassic age but there is a possibility that some are Lower Cretaceous.

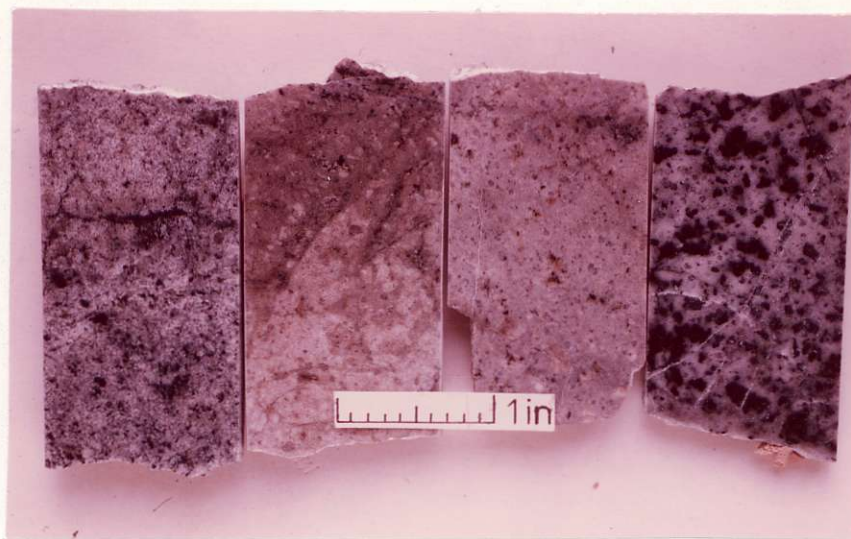
Felsic Intrusions

Three main groups of felsic intrusions have been recognized in the district: felsites, granodiorites, and Tertiary porphyries. The felsites are massive, spherulitic, flow banded, aphanitic, and/or slightly porphyritic. Where contacts are well exposed the intrusions seem to have had little effect on the country rock. Without seeing contact relationships one would tend to map most of the bodies as lava flows or domes. Most of the felsite intrusions are probably related to Jurassic volcanism, but their age(s) has not been established accurately. Some felsite intrusions outside the district have mineral deposits associated with them and may

be Tertiary in age (Brown, 1965 and 1966). In Figure 3 these intrusions have not been separated from their volcanic host rocks.

Both within and outside hydrothermally altered or thermally metamorphosed areas, the granodiorite is typically a highly altered granitic, aplitic, granophyric, and/or porphyritic rock. The largest known body of granodiorite is a thick, differentiated sheet that does not outcrop but occurs at depth in the vicinity of the molybdenum deposit. Small dike- and stock-like bodies also occur near Silvern Lake and on Mount Evelyn.

The writer (1966) suggested that because the granodiorite sheet and all Hazelton volcanic rocks are cut by mafic dikes and irregular bodies, and because the Bowser sediments are not cut by these intrusions, the granodiorite is probably pre-Upper Jurassic. The relationship between the mafic intrusions and the granodiorite was inferred from diamond drill cores. Subsequent underground work has shown that although a few mafic dikes certainly cut the granodiorite, many of the bodies logged as mafic dikes are actually large mafic blocks within the granodiorite. The earlier age interpretation is thus weakened, but the overall highly altered and deformed nature of this rock in all environments suggests that it was emplaced relatively early in the tectonic history of the area. Certainly this unit pre-dates the Tertiary porphyries, but the absence of unaltered primary biotite or hornblende has precluded use of conventional potassium-argon dating techniques.



A



B

Figure 4 - Typical specimens from the granodiorite sheet
Note how the mafic minerals have been redistributed in clots and veinlets, presumably by metamorphism.

A - most typical of the upper part of the sheet

B - most typical of the lower part of the sheet

The only Tertiary porphyries shown in Figure 3 are the dikes that form a somewhat radial pattern in the central part of the district. However, at least three small stock- or plug-like bodies are known in the Glacier Gulch area, and it is believed that Tertiary plutonism was responsible for the development of the thermal metamorphism and hydrothermal alteration that is so prevalent in the district. Typical Tertiary porphyry is a light-colored, massive, and markedly porphyritic rock, having an aphanitic to medium-grained granitic or aplitic matrix. The porphyries range from granite to quartz diorite. Most, however, are quartz monzonite or granodiorite. Quartz, feldspar, and less commonly biotite occur as phenocrysts.



Figure 5 - Typical Tertiary porphyry from small body exposed in a crevasse near the toe of the Hudson Bay Glacier.

Biotite from two porphyries has been dated by the Geological Survey of Canada; one at 67 ± 5 m.y., the other at 60 ± 5 m.y. The former intrusion is intra-mineral¹ (that is, emplaced between periods of mineralization) with respect to the molybdenum mineralization and the latter apparently post-dates the molybdenum mineralization. Since a hornblende from a molybdenite-bearing quartz vein in the same area has been dated at 65 ± 6 m.y., and biotite from a veinlet at 63 ± 4 m.y., the radiometric dates are consistent with the known geologic relations.

Thermal Metamorphism

An area of thermal metamorphism is present in the central part of the district. It was probably caused by the emplacement of Tertiary porphyries. Its outer limit is shown on Figures 3, 12, and 46. In volcanic rocks thermal metamorphism has resulted in marked color changes; crystallization of amphibole, chlorite, biotite, epidote, and/or garnet; and the formation of minor amounts of pyrrhotite and/or magnetite. Sedimentary rocks have become spotted or recrystallized to fine-grained metamorphic rocks containing amphibole, chlorite, epidote, and/or biotite. The detailed petrography of the metamorphosed rocks has not yet been studied.

Since the thermal metamorphism is thought to be due to the Tertiary porphyries, and the Tertiary porphyries were at least in part being emplaced at the time of hydrothermal ore

¹ This term was introduced by Wallace and others (1960).

deposition, it is conjectural whether or not there was any period of thermal metamorphism separate from the period(s) of hydrothermal activity. Mineral assemblages and rock appearances in areas that display thermal effects are distinct from those that have obviously been extensively hydrothermally altered. Most of the volcanic rocks have been metamorphosed to dark colors. The abundance of veins with bleached and altered halos cutting the dark metavolcanics of the molybdenum deposit indicates that the hydrothermal fluids that deposited this ore and caused the bleaching and alteration must have post-dated the metamorphism. The writer is convinced that the main period of thermal metamorphism preceded formation of the molybdenum deposit.

Geologic History of the Range

The range is structurally complex. Most of the major structural features are the result of doming, faulting and some folding. Thrust faulting may have been of major tectonic importance, although individual thrust faults are difficult to define. The lack of internal features in some volcanic units, absence of good marker horizons, scarcity of fossils in volcanic units, and presence of numerous alteration zones make a clear understanding of the regional structures and geologic history difficult.

Hazelton Group volcanic and sedimentary rocks were probably laid down on Jurassic volcanic islands and in shallow seas. Possibly the area was part of an island arc system (Tipper, 1959). These rocks were faulted and tilted and



Figure 6 - View of a thrust fault on the east side of the Toboggan Glacier. The fault separates massive volcanics. The light bands above the thrust are felsite dikes that have not been found below the thrust.

partly eroded prior to the deposition of the continental and marine strata of the Bowser Group. Possibly the thrusting and the intrusion of the granodiorites occurred during an orogenic episode at this time. The Bowser sediments were deposited in the south end of a large Jura-Cretaceous sedimentary basin, named the Bowser Basin (See Souther and Armstrong, 1966). There is evidence of some orogenic activity during Bowser time.

Since early Cretaceous, the area has been part of a large emergent, northeasterly trending structurally high belt called the Skeena Arch (Souther and Armstrong, 1966, and White, 1966). This belt is characterized by small mountain ranges, small silicic intrusions, and block faults.

Except for the fact that it has been extensively sculptured by glaciers, this area might have resembled parts of the Basin and Range province of the southwestern United States.

During the Early Tertiary, silicic porphyry intrusions were emplaced in various parts of the Hudson Bay Range. Intrusions in the east-central part of the Range were accompanied by block faulting, fracturing, broad gentle doming, thermal metamorphism, and extensive hydrothermal activity. Most ore deposits of the district were formed at this time. It is also possible that most of the uplift of Hudson Bay Range occurred then or somewhat later in the Tertiary. Tertiary volcanism, known to have been active in the area, was of major importance to the south.

ORE DEPOSITS

General Description

There is a great diversity of mineral deposits in the Hudson Bay Range. With the exception of coal deposits and possibly some small syngenetic or diagenetic iron sulfide deposits in black mudstones, the deposits appear to be genetically related to the Tertiary porphyry intrusions. Relatively small, complex sulfide-sulfosalt veins, rich in As, Zn, and Pb are the most common type of deposit in the district. The large stockwork-type molybdenum deposit in the east-central part of the district overshadows all others in economic importance.

The deposits of the district can be divided into five groups:

1. sulfide veins
2. sulfide replacement bodies in limestone
3. molybdenum deposit
4. gold-bismuth-tellurium deposit
5. copper-iron-silver vein and replacement deposits

The "sulfide" vein and replacement deposits are sulfide ores with variable amounts of sulfosalt and gangue minerals. The molybdenum deposit is essentially a very extensive stockwork of quartz veinlets with variable amounts of ore¹ and gangue minerals. The gold-bismuth-tellurium deposit is a unique occurrence of native gold and bismuth, bismuthinite, and

¹ The term "ore mineral" used in this thesis has no economic significance. It is used in its broadest sense to refer to metallic minerals whether or not they are economic.

bismuth-tellurium-sulfides, such as joseite, and molybdenite in quartz veins and replacement pods in altered rocks. The copper-iron-silver deposits are separated from the "sulfide" vein and replacement deposits because of their distinctive mineralogy and metal content. They contain iron oxides, chalcopyrite, and/or bornite, minor quantities of silver minerals, and some contain pyrite. Supergene(?) chalcocite, covellite, and bornite are also found in these ores. Their lack of Zn, Pb, and As distinguish them from the "sulfide" vein and replacement deposits. Typically they have very little associated alteration and are best considered a special group of outer zone deposits.

Sulfide Vein and Replacement Deposits

The sulfide veins, the most numerous and widespread type of deposit, are found in the intermediate and outer zones of the district. The main ore minerals in these veins are arsenopyrite, pyrite, pyrrhotite, sphalerite, galena, marcasite, chalcopyrite, bournonite, tetrahedrite, and pyrargyrite. Quartz, calcite, dolomite, siderite, and chalcidony are the main gangue minerals. The vein minerals were deposited as open-space fillings and replacements along sheeted and brecciated fracture zones. Many veins form anastomosing systems, some of which are over a mile in length. Cockade structures and drusy cavities lined with terminated quartz, calcite, pyrite, or arsenopyrite crystals are common in some veins. Mineralization within a given vein system is concentrated in ore shoots that generally range from a

few inches to about ten feet in width.



Figure 7 - Dome vein showing typical sheeted nature of the fracture zone. Most of the dark areas are sulfide mineralization.

Some parts of vein systems contain only an inch or two of sulfides, barren quartz, or calcite. All veins have bleached and altered borders. Propylitic alteration, with quartz, sericite, carbonates, chlorite, epidote, clays, and pyrite is the most abundant kind.¹

Apart from the replacement bodies that are integral parts of the sulfide veins, there are also some sulfide replacement bodies in limestone lenses on the Iron Vault claim near Silvern Lake. These irregular bodies, which occur at limestone vein intersections, have mineral assemblages that

¹ Wall rock alteration in the district was not studied in detail.

are very similar to those of the veins. Pyrrhotite and pyrite, however, predominate over the other sulfides.

Molybdenum Deposit

On surface molybdenum mineralization occurs over an area of about one by one-half miles in Glacier Gulch, on the east side of Hudson Bay Mountain. In places this mineralization is known to extend to depths greater than 3,000 feet. The molybdenum mineralization occurs in a quartz vein network that is far more extensive than the molybdenite mineralization. These quartz veins occur over an area of about 10 to 15 square miles. In this study the poorly mineralized outer part of this quartz vein network is referred to as the "barren" zone. Most veinlets are less than one-half inch wide, but some are greater than two to three feet wide. Molybdenum, tungsten, and copper are the main metals of economic interest.

Most of the veined area is underlain by a highly altered and metamorphosed volcanic sequence composed primarily of bedded pyroclastic rocks. Many types of intrusions occur in the area. The large, concealed, differentiated granodiorite sheet is the most favorable host rock and one or more early Tertiary silicic porphyries are probably the source of the hydrothermal fluids that deposited the ores of the district.



Figure 8 - Area of prominent jointing in the molybdenum deposit to the east of the Hudson Bay Glacier.



Figure 9 - Typical quartz vein stockwork of the molybdenum deposit, immediately east of the Hudson Bay Glacier. Note the absence of prominent alteration halos.

The main minerals found in the veins of the molybdenum deposit are quartz, magnetite, pyrite, molybdenite, hornblende, biotite, chlorite, potash feldspar, muscovite, calcite, dolomite, pyrrhotite, chalcopyrite, scheelite, and gypsum. Other minerals have been found in the veins but they are of minor importance.

Hydrothermal alteration and bleaching are extensive both inside and outside the area of molybdenum mineralization. There is a profusion of veinlet types and alteration and bleached halos (borders). Rocks with a high concentration of veins are markedly bleached over large areas. Quartz, sericite (muscovite), carbonate, potash feldspar, biotite, chlorite, hornblende, epidote, garnet, magnetite, and pyrite are widespread alteration minerals.

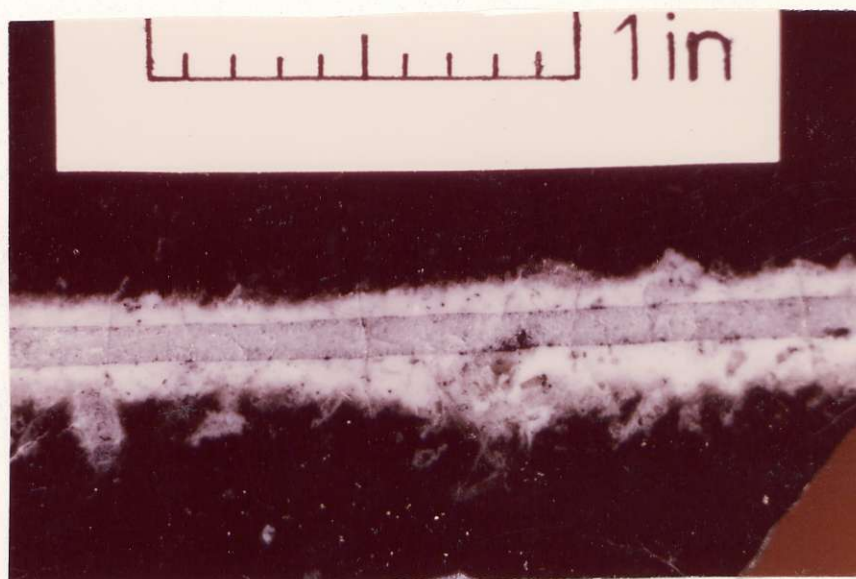


Figure 10 - Sparsely mineralized fine-grained quartz, molybdenite veinlet with a prominently bleached alteration halo. The host rock is dark, dense metamorphosed tuff from near the outer limit of molybdenum mineralization in Climax's exploration adit.

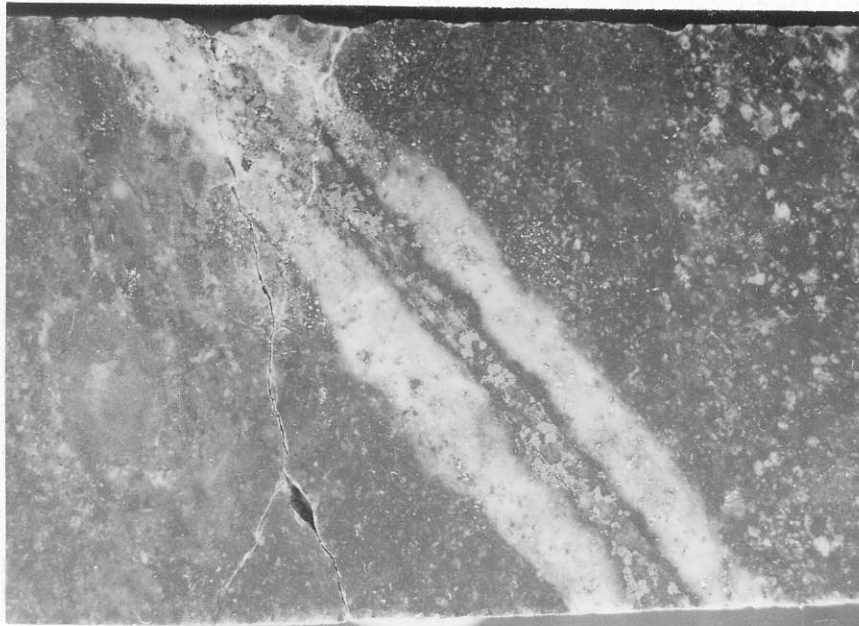


Figure 11A - Quartz, magnetite veinlet with a prominent, pyritic, bleached halo in a dark metamorphosed bedded pyroclastic rock from the molybdenum deposit. Mag. 2x.

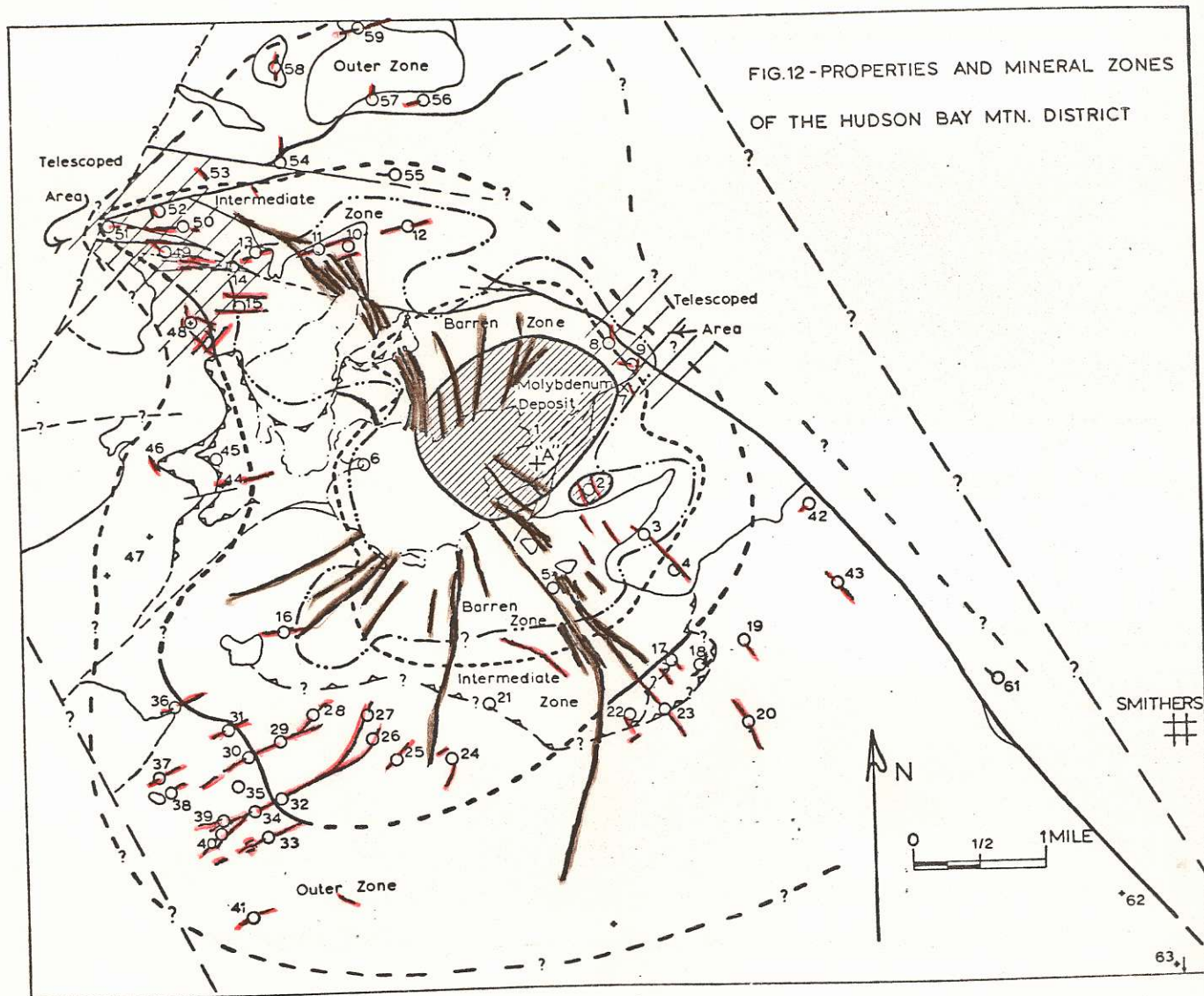


Figure 11B - Bleached alteration halos along a quartz, hornblende veinlet and a pyrite veinlet in dark metamorphosed volcanic rock from the molybdenum deposit. Note the difference in alteration halos. Mag. 2.5x.

Hypogene Zoning

District-wide hypogene zoning is manifested by variations of mineralogy, metal content, and structure of the deposits. The abundance and variation of iron minerals in the ores provide a very useful means for defining zones of the district. The district is divided into an inner (pyrite) zone, an intermediate (pyrrhotite) zone, and an outer (pyrite) zone with a "barren" quartz vein zone between and slightly overlapping the inner and intermediate zones (Figure 12). In ores with both pyrite and pyrrhotite the predominant one was used to define the zone. As defined the inner zone is essentially coincident with or slightly more extensive than the molybdenum deposit. Magnetite and other features of the mineralogy serve to distinguish the inner from the outer zone. The intermediate and outer zones cover those parts of the district containing sulfide vein and replacement deposits and Cu-Fe-Ag ores. Veins of the "barren" zone contain minor pyrite and pyrrhotite with pyrite generally being most abundant near the molybdenum deposit. Ores of the intermediate zone grade to ores of the outer zone but there is some question as to how the intermediate zone is related to the inner zone.

The generalized mineral zonation is shown in Figure 13. It is readily apparent that the inner zone is mineralogically distinct from the intermediate and outer zones. Chalcopyrite is the only ore mineral common to all zones and deposits. Telescoping is apparent in the Glacier Gulch area and on the northwest side of Hudson Bay Mountain west of the



LEGEND







-  -Tertiary porphyry dike
-  -Limit of thermal metamorphism
-  -Vein
-  "Sulfide" mineralization
-  -Cu-Fe-Ag mineralization
-  -Au-Bi-Te deposit

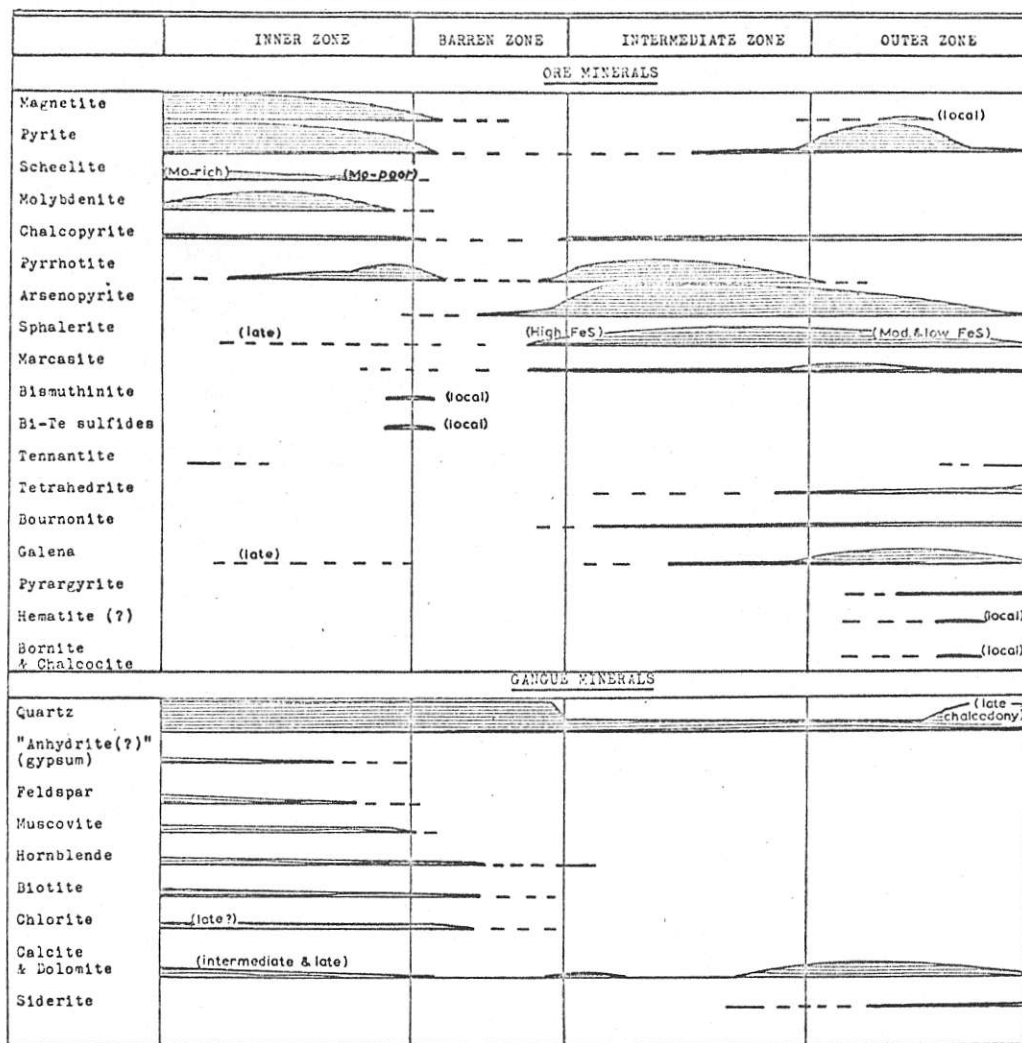
Table 2 - Index to Properties shown on Figure 12

Prop. No.	Property Name	Prop. No.	Property Name
1	Glacier Gulch Molybdenum	34	Hummingbird (Henderson vein system)
1A	Glacier Gulch Molybdenum 3500 Level	35	Pay roll
2	Unnamed	36	Victory
3	Unnamed	37	West Coronado
4	Yukon	38	East Coronado (Silver Star Claim)
5	Unnamed	39	Ashman and Gerrard Veins (Henderson vein system)
6	Unnamed	40	Henderson and Fault Plane veins (Henderson vein system)
7	Glacier Gulch Gold-Bismuth	41	King Tut
8	Glacier Gulch North Side	42	Unnamed
9	Glacier Gulch South Side	43	Vancouver Group (Lone Star)
10	Unnamed (Matuss vein system)	44	Unnamed
11	Matuss	45	Unnamed
12	Unnamed	46	Bonanza
13	Silver King Claim	47	Unnamed
14	Josie Claim	48	Silver Lake 1 and 2 and Gee Claims (Hudson Bay Mtn. Silver)
15	Bee Claim and "A" Fraction	49	Iron Vault and Van Anda Claims (Hudson Bay Mtn. Silver)
16	Iron King	50	Mammoth and Iron Mask Claims
17	Heather	51	Copper Queen Claim
18	Jessie	52	"T" Fraction and Copper Queen Claim
19	Cascade	53	Last Chance
20	Snowshoe	54	Rio Grande
21	Groundhog	55	Unnamed
22	Dorothy	56	Carroll East
23	Empire	57	Carroll West
24	Neepawa	58	Rico Aspen
25	Mayflower - Claims 1 and 3	59	Evelyn
26	Mayflower - Claim 2 (Henderson vein system)	60	Trixie
27	Mayflower - Claim 4 (Henderson vein system)	61	Zobnic
28	Sally Claim (Mamie vein system?)	62	Canadian Citizen and American Citizen Claims
29	Evinrude and Florence Claims (Mamie vein system)	63	Smithers Copper
30	Mamie (Mamie vein system)	64	Zeolite
31	Torrent		
32	Canary (Henderson vein system)		
33	Dome		

Toboggan Glacier. In these areas ores with outer zone features occur in the same area as ores with intermediate zone features.

The metal zonation is quite marked. Molybdenum and tungsten are essentially unique to the inner zone, whereas arsenic, zinc, lead, and silver are essentially unique to the intermediate and outer zones. Gold was preferentially concentrated to a limited extent in the intermediate zone and in parts of the outer zone; lead and silver were concentrated in the outer zone; and copper was deposited in about equal amounts in all zones. Iron and arsenic deposition was apparently significantly less near the periphery of the district.

FIGURE 13 - GENERALIZED DIAGRAM OF THE MINERAL ZONING



The change in character of the veining outward in the district is the structural manifestation of zoning. The inner (molybdenum) zone is essentially a stockwork of quartz veinlets. Attitudes of the veinlets generally become more uniform away from the central area. Most of these veins are less than an inch wide, have quartz as their main constituent, and occupy simple fractures. Although these veins occur in swarms, individual veinlets are usually fairly widely spaced. Veins of the intermediate and outer zones, on the other hand, range up to several feet in width; in many places contain more sulfides than quartz;

and typically occupy sheeted fracture zones which have reasonably well defined limits and are generally spaced a few hundred to a few thousand feet apart.

Statistical Study of Assays

Introduction

Assays from 2550 samples from 55 deposits in the district were available for study. It became apparent that generalizations made from scanning the assays would give little idea of the complexities and details of metal distribution in the district. The metal zoning is not simple or easily defined. Manual means of analyzing the data are prohibitively slow; hence a statistical analysis making full use of computers was selected as the best means of handling the data. The study was initiated with the firm belief that it would be possible to outline details of the zoning using statistical techniques and that some subjective elements of human bias could be eliminated. Because of the rather poor nature of some of the data (especially for district-wide studies) many of the statistics should be considered "descriptive" rather than "formal". The goal remains the same in either case--namely, to describe more fully the distribution of metals in the district. Statistical inferences from the numerical analysis, however, should not be applied too rigorously. The methods serve to illustrate a type of study of zoning that can be carried out. Only a summary of the salient features of this study are given; a more thorough

coverage of the results will be presented elsewhere.

Statistical Methods and Computing Procedures

Preliminary work consisted of correlation analyses supported by selected regression analyses; mechanically plotted scatter diagrams; and calculation of property assay means, standard deviations, and coefficients of variations. Property, local area, and district-wide studies were carried out separately. Property assay means and standard deviations are given in Table 3. For ease in computing $s = \sqrt{\frac{\sum(x-\bar{x})^2}{N}}$ rather than $s = \sqrt{\frac{\sum(x-\bar{x})^2}{N-1}}$ was used for the standard deviation. This significantly affects the results for small numbers of assays. Polynomial trend surfaces for selected metals and metal ratios were also calculated.

The 1604 and 3600 Control Data Corporation computers at the University of Wisconsin were employed for this study. Extensive use was made of standard statistical programs in STATJOB which is currently available as a 1604 CO-OP MONITOR library tape. UC PLOT library routine on the CDC 3600 computer was used to construct the scatter diagrams. Several small FORTRAN programs were written for special aspects of this work. A program for analyzing gravity data that was available in the Department of Geophysics was adapted by B. Lewis and to a lesser extent by the writer, to calculate and construct contour diagrams of polynomial trend surfaces for assay and other geological data.

Table 3 - Summary of Assay Data for the Hudson Bay Mountain Mining District

Property No.	Au			Ag			Pb			Zn			Cu			S			As		
	n	\bar{x}	s	n	\bar{x}	s	n	\bar{x}	s	n	\bar{x}	s	n	\bar{x}	s	n	\bar{x}	s	n	\bar{x}	s
1	5	.02	.01	6	.4	.7	1	.01	-	2	.81	.80	8	.48	1.22	7	1.95	4.11	-	-	-
3	1	.04	-	1	.1	-	1	.11	-	1	.13	-	1	.30	-	1	12.08	-	-	-	-
4	7	.21	.18	5	.2	.2	5	-	-	3	1.03	.42	1	.21	-	-	-	-	-	-	-
6	1	.01	-	1	.7	-	1	.75	-	1	5.60	-	1	.02	-	1	7.79	-	-	-	-
7	13	4.60	7.07	13	1.4	2.1	-	-	-	-	-	-	1	.18	-	-	-	-	-	-	-
8	6	.12	.12	5	55.9	70.7	3	14.20	10.68	3	18.73	11.76	3	.28	.22	-	-	-	-	-	-
9	5	.06	.04	5	21.3	4.6	5	3.97	3.26	5	6.11	5.10	1	.25	-	1	19.25	-	1	1.59	-
10	1	.24	-	1	.1	-	1	.01	-	1	2.80	-	1	.34	-	1	23.40	-	1	.50	-
11	1	.36	-	1	.1	-	-	-	-	-	-	-	-	-	-	-	-	-	-	-	-
12	1	.26	-	1	.1	-	-	-	-	-	-	-	1	.05	-	-	-	-	1	27.90	-
14	1	.01	-	1	.2	-	1	.11	-	1	6.00	-	1	.05	-	1	15.11	-	-	-	-
15	1	.01	-	1	7.3	-	1	5.24	-	1	12.90	-	1	.15	-	1	25.56	-	-	-	-
16	8	.15	.11	8	4.0	3.4	1	.08	-	3	8.43	5.27	3	.98	.53	1	12.81	-	1	9.01	-
17	1	.10	-	1	.5	-	-	-	-	1	3.40	-	-	-	-	-	-	-	-	-	-
18	6	.26	.07	6	8.1	9.7	6	6.00	8.22	6	9.02	2.97	2	.49	.26	2	13.16	3.84	2	9.20	4.80
19	5	.24	.12	5	2.3	2.3	4	20.04	8.58	1	8.80	-	1	.14	-	1	20.08	-	1	8.30	-
20	6	1.0	.07	6	97.3	59.3	6	22.24	17.16	5	11.09	3.27	4	.79	.46	2	17.36	3.56	2	1.87	.47
21	3	.08	-	3	7.1	1.4	2	2.65	.55	-	-	-	1	.75	-	-	-	-	-	-	-
22	2	.53	.23	2	6.5	.5	1	25.20	-	1	23.40	-	2	1.00	-	-	-	-	-	-	-
23	12	.14	.20	13	64.0	86.5	12	21.14	13.73	11	16.37	5.98	3	.73	.38	1	25.95	-	-	-	-
24	2	.38	-	2	3.8	-	-	-	-	2	6.20	-	-	-	-	-	-	-	-	-	-
26	2	.06	.04	2	3.3	1.6	2	.38	.26	2	1.75	1.45	2	.82	.16	2	22.74	.60	2	1.50	1.10
27	1	.01	-	1	.1	-	1	.01	-	1	.03	-	1	.02	-	1	4.69	-	1	12.00	-
28	1	.04	-	1	.2	-	1	.02	-	1	7.40	-	1	.15	-	1	15.97	-	1	5.80	-
29	2	.24	.04	2	1.5	.5	1	.11	-	2	7.74	2.27	1	.70	-	1	10.17	-	1	6.16	-
30	259	.36	.41	259	7.5	14.2	-	-	-	240	8.00	7.80	80	.89	.98	-	-	-	-	-	-
31	1	.22	-	1	2.0	-	1	.12	-	1	3.80	-	1	.30	-	1	16.55	-	1	20.15	-
32	106	.15	.12	106	12.1	12.1	98	8.63	7.37	99	8.25	4.97	-	-	-	-	-	-	-	-	-
33	13	.05	.05	14	15.4	22.5	13	14.78	21.86	11	3.78	3.16	2	.12	.08	2	7.22	1.74	2	7.55	.95
34	400	.13	.12	410	10.6	14.3	344	7.23	9.15	404	7.43	7.06	-	-	-	-	-	-	-	-	-
35	1	.04	-	1	.9	-	1	.42	-	1	6.20	-	1	.03	-	1	14.18	-	1	3.80	-
36	85	.18	.16	86	15.0	58.5	64	8.40	11.43	83	5.64	6.71	2	1.20	.30	-	-	-	-	-	-
37	16	.27	.16	16	30.1	31.2	15	14.48	11.42	15	16.78	9.12	-	-	-	-	-	-	-	-	-
38	5	.20	.16	5	32.8	17.4	4	21.29	9.70	4	15.36	4.93	1	1.11	-	1	16.61	-	1	3.10	-
39	44	.03	.04	428	34.7	102.6	214	4.01	6.78	211	4.72	5.84	-	-	-	-	-	-	-	-	-
40	164	.11	.48	951	51.5	121.0	727	6.32	10.74	723	6.33	7.38	-	-	-	-	-	-	-	-	-
41	1	.01	-	1	.3	-	-	-	-	-	-	-	-	-	-	-	-	-	-	-	-
43	2	.02	-	2	12.0	4.4	2	10.89	1.59	2	6.89	.99	1	.96	-	1	11.83	-	-	-	-
44	1	.02	-	1	3.0	-	-	-	-	1	2.70	-	1	2.70	-	1	2.05	-	-	-	-
46	1	.02	-	1	.6	-	1	.17	-	1	.03	-	1	10.73	-	-	-	-	-	-	-
47	-	-	-	1	.1	-	-	-	-	1	.22	-	1	.14	-	-	-	-	-	-	-
48	77	.25	.55	77	22.8	28.0	72	10.47	18.14	70	14.59	14.45	20	7.63	14.65	5	13.59	4.69	1	3.40	-
49	29	.37	.05	39	12.9	14.3	25	7.43	6.45	38	10.06	6.50	2	.51	.29	3	20.16	7.18	-	-	-
51	1	.15	-	1	2.9	-	-	-	-	-	-	-	-	-	-	-	-	-	-	-	-
52	1	.32	-	1	14.9	-	1	.75	-	1	.24	-	1	1.26	-	1	27.53	-	1	14.84	-
53	3	.01	.01	3	1.4	.9	-	-	-	1	.16	-	3	2.92	.59	-	-	-	-	-	-
54	1	.41	-	1	3.3	-	-	-	-	-	-	-	1	.68	-	1	23.61	-	1	8.60	-
55	1	.05	-	1	.1	-	-	-	-	-	-	-	1	.13	-	1	22.20	-	-	-	-
56	4	.18	.13	4	6.1	3.0	1	6.00	-	-	-	-	-	-	-	-	-	-	-	-	-
57	2	.04	.01	2	63.8	47.8	2	60.09	12.91	1	.20	-	1	.33	-	1	8.36	-	-	-	-
58	1	.01	-	1	53.7	-	1	.02	-	1	1.60	-	1	6.69	-	1	4.17	-	1	1.29	-
59	13	.01	.01	13	28.1	44.8	8	6.68	8.71	2	2.40	1.60	2	.19	.12	2	3.36	.42	2	2.60	.01
61	2	.01	-	2	104.0	-	-	-	-	2	.82	.68	-	-	-	-	-	-	-	-	-
62	2	.01	-	4	3.6	1.18	-	-	-	4	3.38	1.67	-	-	-	-	-	-	-	-	-
63	3	.01	-	3	2.8	1.13	-	-	-	-	-	-	3	1.53	.38	-	-	-	-	-	-

n = number of assays

Au and Ag - in ounces per ton

\bar{x} = mean value

Pb, Zn, Cu, S, and As - in per cent

s = standard deviation

Thirty variables and other miscellaneous information were coded on punched cards. The coded information is as follows: property number, sample identification number, sample width in inches, sample quality evaluation code, ounces per ton gold, ounces per ton silver, per cent lead, per cent zinc, per cent copper, per cent sulfur, per cent arsenic, mine horizontal co-ordinate, elevation, north-

south map co-ordinate, east-west map co-ordinate, distance to metamorphic "front"¹, distance to a point in the center of the molybdenum deposit ("A"), estimated average mole per cent FeS in sphalerite for the deposit, special code to identify samples from Cu-Fe-Ag deposits and samples taken by the writer (a total of 52), card sequence number, silver/gold ratio, gold/silver ratio, silver/lead ratio, lead/zinc ratio, copper/zinc ratio, gold/copper ratio, gold/lead ratio, copper/lead ratio, arsenic/sulfur ratio, silver/sulfur ratio, gold/sulfur ratio, gold/arsenic ratio, gold/zinc ratio, and silver/zinc ratio.

Nature of the Samples

In any statistical study one should define the "target population"--that is, the population about which one wants to gain information or make statistical inferences (see Krumbain and Graybill, 1965). The target population of this study is the ore deposits of the district. If valid inferences are to be made about the population, the samples should be randomly taken from the "sampled (accessible) population". As is typical for most geologic studies, the sampled population does not exactly equal the target population.

Unfortunately the available samples are not entirely suitable for rigorous statistical analysis because they are not representative "probability samples" (p. 149, Krumbain and

¹ Only values outside the metamorphic aureole were recorded and the front was considered to dip outwards at depth.

Graybill) of the sampled or target population. Therefore considerable subjective judgement has been used in evaluating the results. The main problem involved is the nature of the samples and the lack of a precise definition of a mineral deposit for sampling purposes. For instance, it is reasonable to ask if the samples are composed solely of ore minerals or if they contain various amounts of gangue, wall rock, or even oxidation products. Because of the variety of mineral occurrences in the district, it is difficult to define clearly the target population, the "ore deposit". It can be expected that most samples taken from surface exposures were oxidized to varying degrees. Samples could have been chipped from "representative" material across a massive sulfide vein, across a wide but sparsely mineralized sheeted fracture zone, or across an entire rock mass of stockwork ore. They could also have been grab samples from weathered high grade ore on mine dumps. Fortunately, in one respect, many of these problems have been avoided, since over 1900 of the assays are chip samples taken underground from the Sil Van Mine. Hence it can be expected that there was a certain degree of uniformity in collecting these samples. But this leads to another problem in the studying of zoning on a district-wide scale. There is a tremendous "clustering" of data from one area, and for many of the properties there is only meager data. Because of the greater amount of data available, more emphasis has been placed on studying the Sil Van Mine area than other parts of the district.

There are also other features of the assays that restrict their use in the study of zoning. Generally, unless a metal was obviously abundant in the ore, no assay was made for it. The absence of complete assay data causes the problem of handling "missing data" in the statistical analyses. Because gold and silver minerals could not be readily identified in hand specimen, and because they are economically important, generally, more assays are available for these metals. The Mamie property is a good example of one where there is ample assay data on gold, silver, zinc, and copper, but absolutely no information on lead. Yet galena, although sparse, is present in the ore.

Another problem arises from the fact that for some samples locations are only roughly known. Their "place" value is, therefore, considerably less than that of a series of assays whose relative locations are shown on a map.

Formidable as these problems seem, they can be evaluated to some degree. The use of metal ratios greatly alleviates some sampling problems in studying the zoning.¹ There are, however, problems that are much more difficult to account for, that may significantly affect the results.

¹ Koch and Link (1963), in a study somewhat similar to the present one, multiplied the assay value by the sample width in an attempt to circumvent sampling errors. Sound as this procedure may be for weighting assays for grade and tonnage calculations, it does not solve sampling problems for statistical studies. Moreover, it tends to cloud the results so that they cannot be directly compared with other areas.

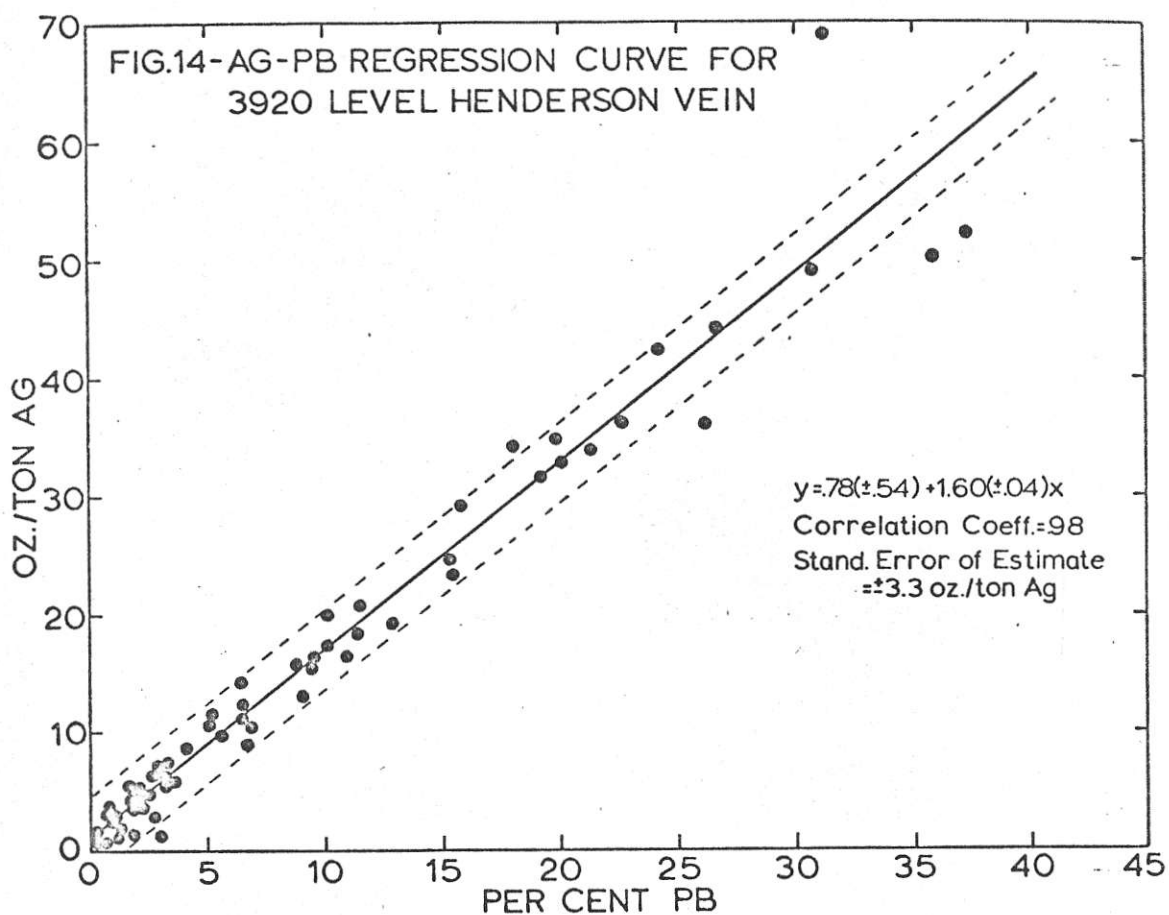
For instance, on underdeveloped properties there is no way of determining whether or not the sample was taken from a sulfide shoot. Assays from developed properties, of course, are mainly from the sulfide shoots. It is very possible that ores from shoots and ores from less highly mineralized portions of vein systems are significantly different. Supergene processes could possibly affect the results. Some high silver portions of the Henderson vein system were attributed by early workers to supergene deposition of native silver and ruby silver minerals. Although it is currently believed that these minerals are hypogene, the textural evidence for this consensus is not unequivocal.

Selected Results

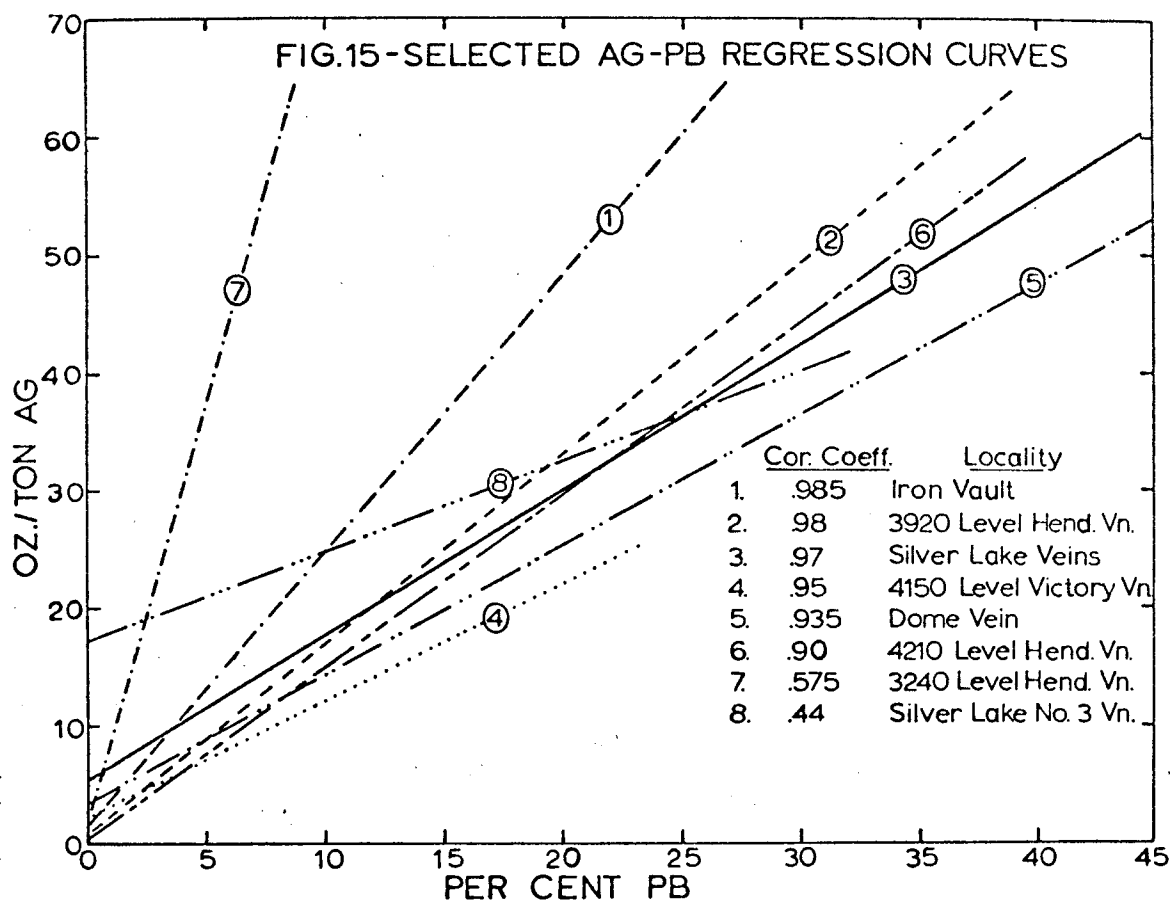
This study has produced a mass of data not yet completely analyzed. For example, one correlation run with 30 variables produces 900 correlation coefficients. The sheer volume of results will require a great deal more time for analysis; therefore, only some of the most obvious findings are presented.

The relationship between lead and silver is perhaps the most striking discovery of this study. For many of the deposits of the district there is a remarkably high correlation between the lead and silver contents of the ores. Correlation coefficients as high as .98(5) were found. Galloway (1924, p. 109) and other workers have suggested that there is a correlation between lead and silver of some ores. The former noted that there is about 1 to 2 ounces per ton silver

for every per cent lead in the Victory vein. However, the high degree of correlation had never been emphasized. Figure 14 shows a typical relationship between lead and silver.



When it was found that lead and silver showed a very close relationship in many of the deposits, the writer expected that a single relationship would hold for all these ores. However, when regression equations were calculated for these properties, it was discovered that each property or part of a property has its own characteristic relationship (Figure

15).¹

In sharp contrast to the high correlations found for many silver-lead ores, deposits or parts of deposits with high silver contents typically have low to moderate correlations with lead. For instance, the 3240 foot level of the Henderson vein and the Silver Creek No. 3 vein are high grade silver ores, in places containing as much as 50 to 100 ounces of silver per ton.

¹ It is easy to see how averaging of assay data would have obscured the relationships. Stanton and Richards (1961 and 1963) have discussed the problem of averaging assay data for correlation analyses.

It is very difficult to conceive of multi-stage processes on a district-wide scale that could account for the very high correlations between silver and lead. It is far more reasonable to assume that they were deposited together in silver-bearing PbS solid solutions. Oriented intergrowths of silver minerals in galena and the phase relations in the Pb-Ag-Bi-S system (Craig, 1967) support this conclusion. The high grade silver ores which show much lower correlations between silver and lead, on the other hand, suggest that there was a separate stage of silver mineralization in these areas. But the writer has not studied enough polished surfaces of these ores to substantiate this conclusion on mineralogical grounds. The variation in slope of the silver-lead regression curves is probably a reflection of variations in the silver/lead ratio in the ore solutions.

It is noteworthy that Koch and Link (1963) found very similar patterns in the Don Thomas vein of the Frisco Mine in Mexico. Unfortunately their data cannot be directly compared with the writer's, since they multiplied their assays by sample width. Variations in silver and lead contents of the Henderson vein system, moreover, would tend to cast doubt on their conclusion that since the mineralization is different on either side of the Frisco fault, faulting presumably took place before part or all of the ore was emplaced (p. 1070). There are no major faults off-setting the Henderson vein, yet it possesses variations in metal content very similar to those of the Don Thomas vein. The variations

they describe could equally well be due to lateral zonation within a single vein prior to faulting.

Correlations between other metals, metal ratios, and various distance parameters, in general, are much lower than those for silver and lead. This suggests that deposition of most metals was not as closely related as was the deposition of some of the silver and lead. Perhaps it merely reflects the lack of simple solid solution relationships of heavy metals in single minerals.

Although deposits of the district have been broadly grouped in zones, statistical studies have served to indicate that deposits within small areas have their own characteristics. For example, if we consider three veins that are fairly close together--the West Coronado, Mamie, and Henderson veins--we find they have distinct differences. The West Coronado vein is characterized by marked zonation over a distance of a few hundred feet; the Mamie vein by a low lead, and high gold and copper content; and the Henderson vein by a high silver and lead content and by very gradual zonation. These variations indicate that to some degree conditions of ore deposition in the various vein systems were significantly different.

Variations in absolute metal contents, as functions of distance from the metamorphic front (aureole), are shown in Figures 16 to 19. The mean value for each property listed in Table 3 was used for the graphs. In general "large" (greater than 30 assays) and "intermediate"-sized (greater

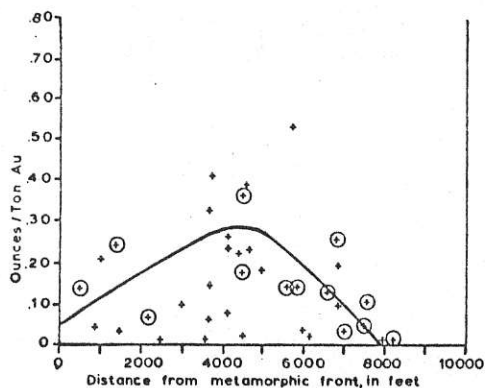


FIG.16-GOLD CONTENT OF DEPOSITS FROM ASSAY DATA

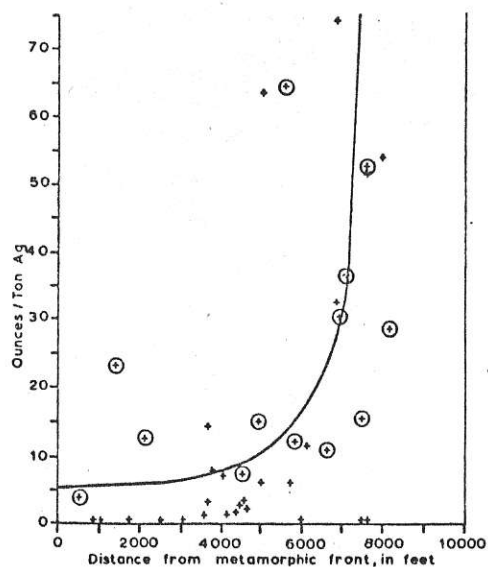


FIG.17-SILVER CONTENT OF DEPOSITS FROM ASSAY DATA

+ - small sample (<10 assays)

⊕ - intermediate-sized & large samples (>10 assays)

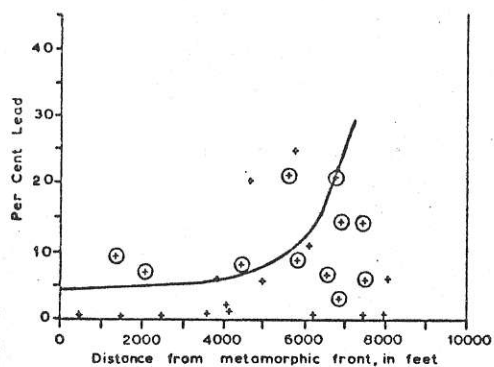


FIG.18-LEAD CONTENT OF DEPOSITS FROM ASSAY DATA

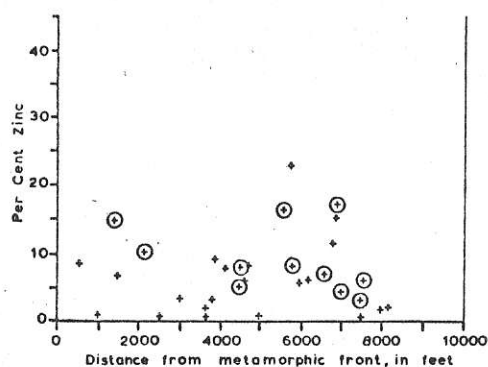


FIG.19-ZINC CONTENT OF DEPOSITS FROM ASSAY DATA

than 10 assays) samples, shown as large dots, outline the trends better than do the small samples. Some low values probably only signify poorly mineralized rock. From the plots it can be seen that gold values are highest in a zone about 3500 to 6000 feet from the metamorphic front; silver values in a zone about 5000 to 9000 feet from the front; lead values in a zone about 5000 to 8000 feet from the

front; and that zinc values show no discernible increase or decrease away from the front. It should be noted that the mole per cent FeS content of sphalerite (Figure 44, p. 105) and the atomic per cent arsenic in arsenopyrite (Figure 50, p. 120) also show definite trends away from the front.

Variations in selected metal ratios as functions of distance from the metamorphic front are shown in Figures 20, 22, and 23.

Again the large and intermediate sized samples outline the trends better than do the small samples. The ratios were calculated from the property assay means in Table 3. The same ratios determined by calculating the means of the ratios of the raw assay data, interestingly enough, yield very different values, but the trends are the same. The "mean of the ratios" is a function of assay variance but is not a function of the absolute values of the assays as is the "ratio of the means". Mathematically it is probably a better value than the "ratio of the means" used in this report. The silver/gold, silver/lead, and lead/zinc ratios all show marked increases in the outer part of the district. Variation in the silver/gold ratio is very similar to that given by Sims and Barton (1962) for the Central City district (Figure 21). Although the silver/gold ratios for the Hudson Bay Mountain district are somewhat larger, the striking similarity of the trends strongly indicates that the Hudson Bay Mountain trend is real. Sims and Barton used

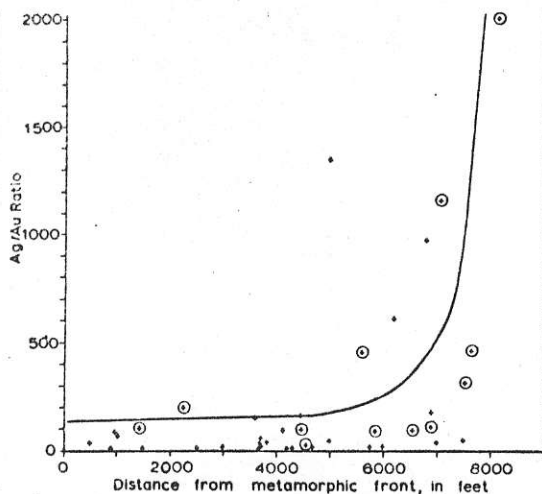


FIG.20-SILVER-GOLD RATIOS CALCULATED FROM ASSAY MEANS

for Figures 20, 22, & 23

• - small sample (<10 assays)

⊙ - intermediate-sized & large samples (>10 assays)

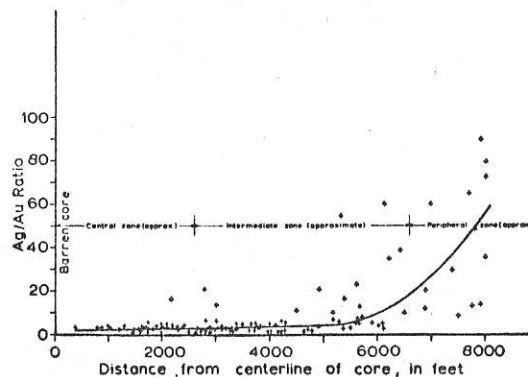


FIG.21-SILVER-GOLD RATIOS OF ORES SHIPPED FROM THE CENTRAL CITY DISTRICT (after Sims & Barton, 1962)

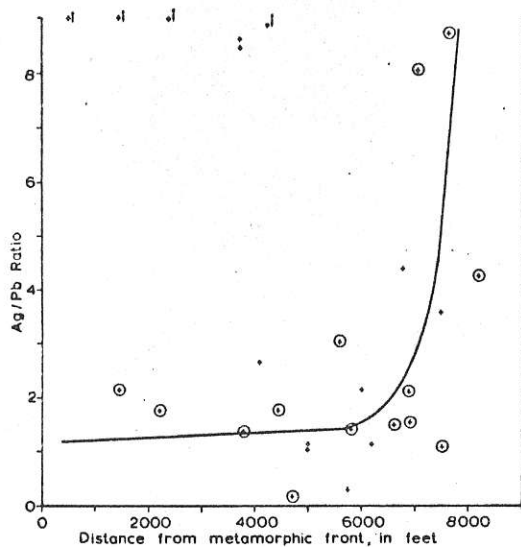


FIG.22-SILVER-LEAD RATIOS CALCULATED FROM ASSAY MEANS

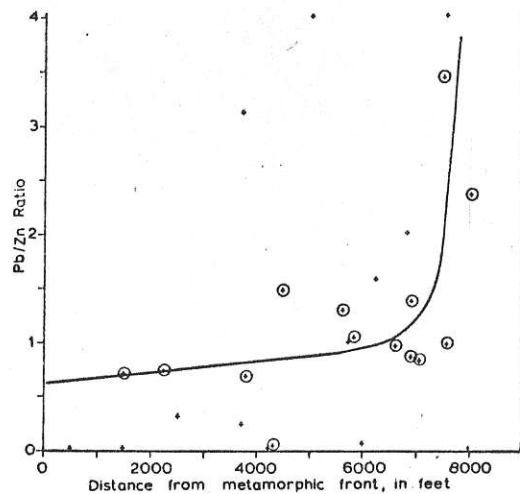


FIG.23-LEAD-ZINC RATIOS CALCULATED FROM ASSAY MEANS

production data and sampling-works assays for their calculations, and the distance they cite was measured from the centerline of the core of the district.

It can be noted that in the metal and metal ratio plots there is abrupt termination of properties at about 8000 feet from the metamorphic front. Figure 21 shows a similar abrupt

termination of properties about 8000 feet from the center-line of the Central City district. Sims and Barton (1962) have attributed the drastic changes in silver/gold ratio and presumably the termination of the mineralization to a zone of throttling (irreversible adiabatic expansion of the ore solutions) and possibly of mixing of the magmatically derived hydrothermal solutions with ground water. Similar depositional mechanisms are quite feasible for the Hudson Bay Mountain district, but the writer believes that mixing of solutions was probably the most important factor causing the drastic change in ratios and possibly the termination of mineralization.

Since much of the assay information comes from the southwest part of the district, and since the known extent of these veins is approximately coincident with the limit of outcrop, the abrupt termination of the mineralization as shown in Figures 16 to 23 should be viewed with caution. Exploration work done by Sil Van Mines Ltd. has shown that there are geophysical anomalies in the covered areas along strike from some of the veins. Possibly the veins could extend at least 1000 feet farther from the front.

Mole per cent FeS in sphalerite was plotted against assays and metal ratios, but due to clustering of data trends of only dubious value were outlined. Sympathetic variation of metal ratios and mole per cent FeS in sphalerite, of course, would support the contention that the

underlying causes for variation in both would be directly or indirectly the same. Since absolute metal content, metal ratios, mole per cent FeS in sphalerite, and atomic per cent arsenic in arsenopyrite all vary as a function of distance from the metamorphic front, it can be expected that they are all related to some degree.

Vein and Mineral Paragenesis

The main purpose of a paragenetic study is to reconstruct the depositional history of ores. Because of the problems involved in interpreting the temporal aspects of ore deposition for an entire mining district, a distinction has been drawn between vein and mineral paragenesis. Detailed mapping of deposits and district has shown that not all deposits were formed at the same time. Nevertheless, there is insufficient evidence to establish the exact chronology of each deposit. Since veins and deposits formed at different times, it is apparent that mineral paragenesis, the sequence of mineral deposition within a rock or vein, has only local significance. It would take thousands of polished surfaces and many field observations to establish the exact timing of the various mineralizing events, if in fact it can be established.

There are numerous examples of successive periods of ore deposition and more could probably be found if it were not for the fact that most ore exposures, whether on surface or underground, are covered by a layer of oxides or grime.

A summary of the relative age relationships of ores and intrusions in the district is as follows:

1. The porphyry dikes in the Glacier Gulch area shown in Figure 12 are intra-mineral with respect to the molybdenum mineralization (i.e., they cut and are cut by molybdenum-bearing veinlets), and to the north of the Toboggan Glacier they cut sulfide veins of the intermediate zone.
2. Aphanitic potash-rich dikes related to the stock below the ridge south of Glacier Gulch are also intra-mineral with respect to the molybdenum mineralization. These dikes post-date about 80 to 90 per cent of the quartz veinlets.
3. The small body of granodiorite porphyry exposed in a crevasse near the toe of the Hudson Bay Glacier apparently cuts the surface molybdenite mineralization, but is cut by numerous veinlets containing chalcopryite. This is an indication that there might have been a major stage of copper mineralization that at least in part followed the period of molybdenum mineralization.
4. The abundance of cross-cutting veins and the great diversity of vein and alteration types in the molybdenum deposit indicate that a variety of ore solutions under somewhat variable physicochemical conditions were responsible for ore formation in this area.
5. Post-sulfide chalcedony and chalcedony-kaolinite veins occur in the Henderson and Dome vein systems, and very fine grained quartz post-dates at least some of the sulfides in the Empire and Snowshoe veins.
6. Post-sulfide carbonate veins have been observed on the Henderson, Vancouver, and Glacier Gulch South Side properties.
7. A minute bournonite vein that cuts deformed galena and sphalerite was found in a hand specimen from the East Coronado vein.

8. On the Bee Claim a two to four inch galena, sphalerite vein is traversed for several feet by a $\frac{1}{16}$ to $\frac{1}{4}$ inch chalcopyrite vein.
9. Sulfide stringers with entirely different mineral assemblages which occur in the sheeted fracture zones, indicate that the ore solutions were of variable nature and passed through the fissures at different times.

In the molybdenum deposit there is a seemingly chaotic maze of cross-cutting veins which have been grouped by the writer (1966) as follows:

- A. "wormy" barren quartz veinlets in the contact region of the quartz monzonite stock (Figure 24)
- B. barren quartz vein stockwork ("high silica" rock) in the contact region of the quartz monzonite stock (veinlets have planar walls) (Figure 24)
- C. Type I molybdenum-bearing quartz veins (fine grained, sugary, well developed banded (ribbon) structure, high magnetite content) (Figures 25 and 26)
- D. Type II molybdenum-bearing quartz veins (medium and coarse grained, drusy, massive, low magnetite content) (Figure 26)
- E. Post-Type II barren and molybdenum-bearing quartz veins
- F. Post-quartz vein stockwork, quartz-carbonate veins (anastomosing, contain minor pyrite, sphalerite, galena and molybdenite which is present only in vein fragments from the quartz vein stockwork)

From relationships observed in diamond drill core it was concluded that these vein groups appear to represent successively younger periods of mineralization. However, from some of the vein relationships observed underground, it was discovered that the distinction between Type I and Type II veins is not clear-cut. Some Type I veins along strike

grade to veins that are more like Type II in character, and some Type I veins with a well developed banded structure contain clots of coarse grained drusy minerals. Even though a clear distinction between Type I and Type II molybdenum veins cannot be made for that part of the deposit exposed in the underground workings, it is still a definite possibility that there were at least two distinct periods of mineralization in other parts of the deposit. It should be remembered that a tremendous volume of rock has been mineralized and not all of it has been adequately studied.

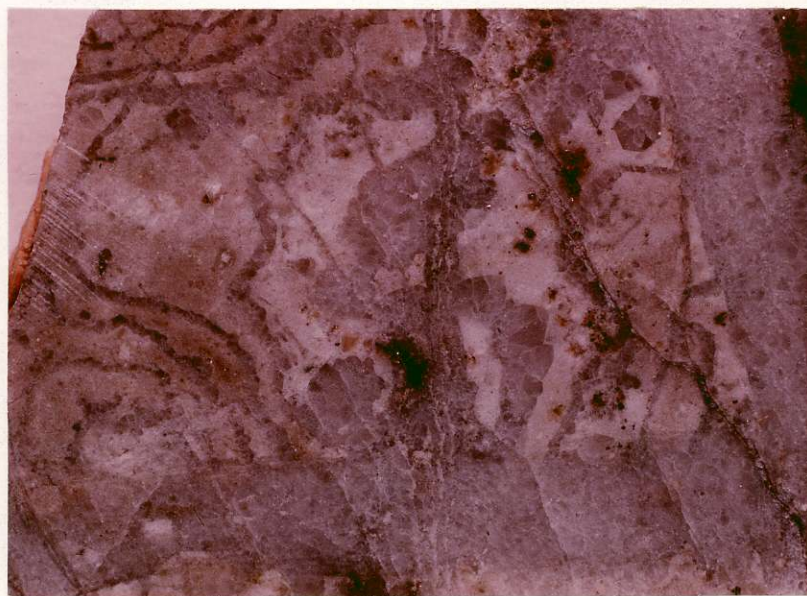


Figure 24 - Barren "wormy" quartz veins cut by tabular quartz veins in drill core specimen from the chilled contact zone of the quartz monzonite porphyry located approximately 3000 to 3500 feet below the ridge south of Glacier Gulch. Mag. 2x.

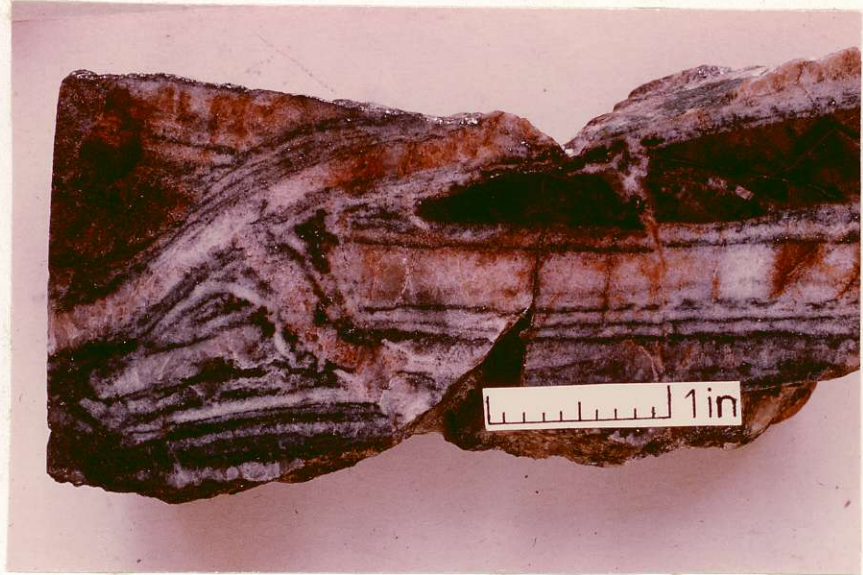


Figure 25 - Type I molybdenum vein showing the characteristic banded structure. Note the cross-cutting veins of the same type.

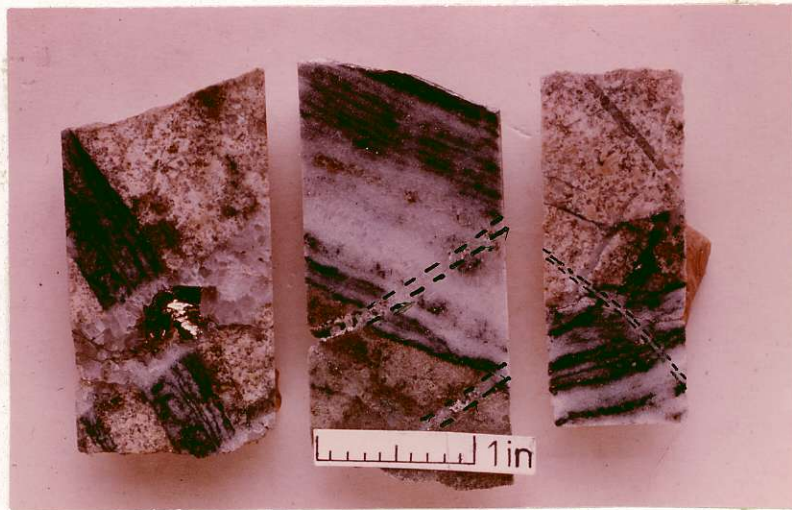


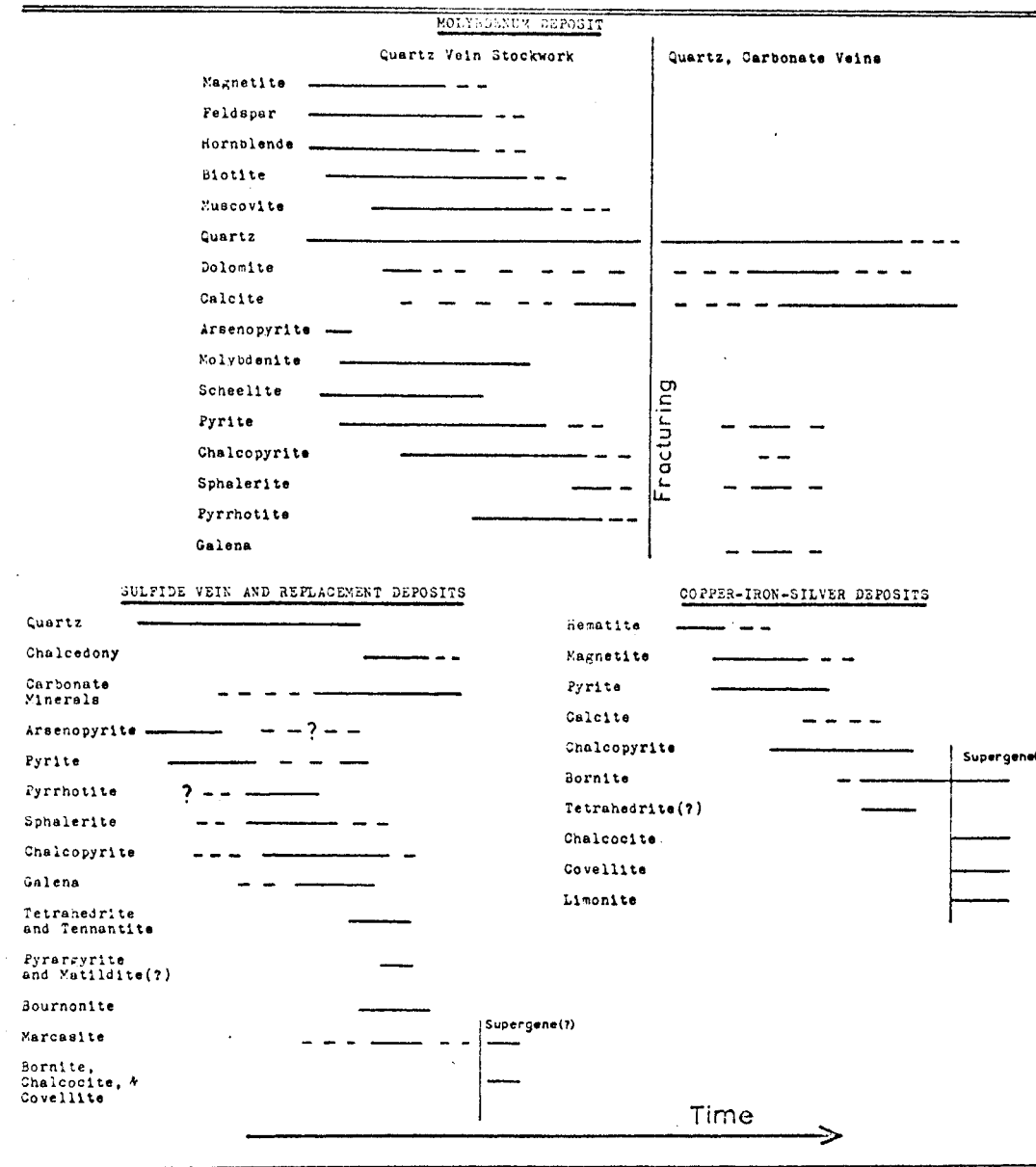
Figure 26 - Type I veins cut by Type II veins.

The field evidence cited above certainly indicates that there was at least some polyascendency (Kutina, 1957) of the ore solutions in the Hudson Bay Mountain district. If it were not for the generally poor quality of ore exposures it is almost certain that more such cross-cutting relationships could be observed.

Figure 27 shows conventional paragenetic diagrams for the main classes of deposits in the district. These types of deposits do not in general overlap or grade to one another so the relative timing of each is not known. It can only be inferred from the general geologic features of the district.

Caution should be exercised in interpreting these sequences. Recent work, such as that by Brett (1963), has cast doubt on the validity of certain microscopic textural relations as criteria for determining the paragenesis of ores. Recent studies of the kinetics of solid state sulfide reactions have shown that some soft sulfides continue to react far below their initial crystallization temperatures (see Skinner and Barton, 1967). It can be expected that such solid state reactions mask many of the original textural features of the ores. It is possible that a conventional paragenetic sequence determined from microscopic features may more closely parallel the "textural stability" rather than the initial sequence of deposition. That is, hard, stable minerals with high powers of crystallization would be indicated as relatively old; whereas, soft, "unstable" minerals with low powers of

FIGURE 27 - PARAGENETIC DIAGRAMS



crystallization would be indicated as relatively young. An example of this relationship is a simple one-quarter inch quartz, pyrite, chalcopyrite vein that can be traced for several hundred feet in the molybdenum deposit. Microscopically the chalcopyrite may vein the pyrite; however, intuitively it is very difficult to accept a complex deposi-

tional history for such a simple vein. It is far more reasonable to conclude that the vein minerals were precipitated at one time and subsequently underwent solid state changes that led to the apparent textural relations.

In the construction of Figure 27, through-going veins of one mineral in another were accepted as evidence that the vein mineral is younger. Crustification, breccia fragments, and some obvious replacement textures (e.g., pseudomorphs and veins with corroded borders) were also accepted as valid differential age criteria. Virtually all other textures were, however, interpreted to indicate simultaneous deposition. Unsatisfactory as this procedure may seem, it is considered to yield the most meaningful results. Some of the typical microscopic vein relationships are shown in Figures 28 and 29, and other textural features are shown in microphotographs in other parts of the thesis.

An extremely interesting relationship was discovered in ores from the sulfide veins. In these ores pyrite and arsenopyrite are typically highly fractured and veined and replaced by most other minerals, especially pyrrhotite. But some very anomalous relations were found in pyritic ores near the inner limit of the outer (pyrite) zone and in the intermediate (pyrrhotite) zone. These relations are as follows:

1. the sphalerite associated with the pyrite contains too high an iron content, as indicated by the known phase relations (Barton and Toulmin, 1966 and Boorman, 1967), to have crystallized in equilibrium with the pyrite (e.g., sample 64-30)



Figure 28 - Pyrite from small veinlet in the molybdenum deposit brecciated and veined by quartz (dark) and chalcopyrite (light). Mag. 150x.



Figure 29 - Arsenopyrite from the Copper Queen claim veined by chalcopyrite (light gray), pyrrhotite (medium gray), and quartz (black). Note that the quartz veins cut the chalcopyrite, pyrrhotite veins. Mag. 500x.

2. sphalerite in this area even though associated with pyrite contains blebs of pyrrhotite
3. lamellar marcasite is abundant in this area (Figure 31) - Edwards (1954) claims that this type of marcasite forms only by pseudomorphic replacement of pyrrhotite
4. a few small pyrrhotite inclusions are present both in the pyrite and marcasite

Even though the textural relations (vein) would lead one to believe that the pyrrhotite in the sulfide veins generally formed after the pyrite, the features cited above strongly suggest that pyritic outer zone ore actually formed at the expense of pyrrhotitic ore of the intermediate zone. If this is true then it follows that the general microscopic textural features of pyrite and pyrrhotite yield very misleading age data.

The presence of marcasite also indicates that these replacement reactions must have occurred below about 430°C (Kullerud, 1966). The intimate association of marcasite and pyrite supports the contention that the two minerals have different compositions and that both have stability fields somewhere below 430°C (Kullerud, 1966 and 1967). Under very high sulfur fugacities it would be expected that the marcasite would have decomposed to pyrite (Kullerud, 1967). Hence the sulfur fugacities were probably such that the stability field of pyrrhotite was only slightly exceeded.

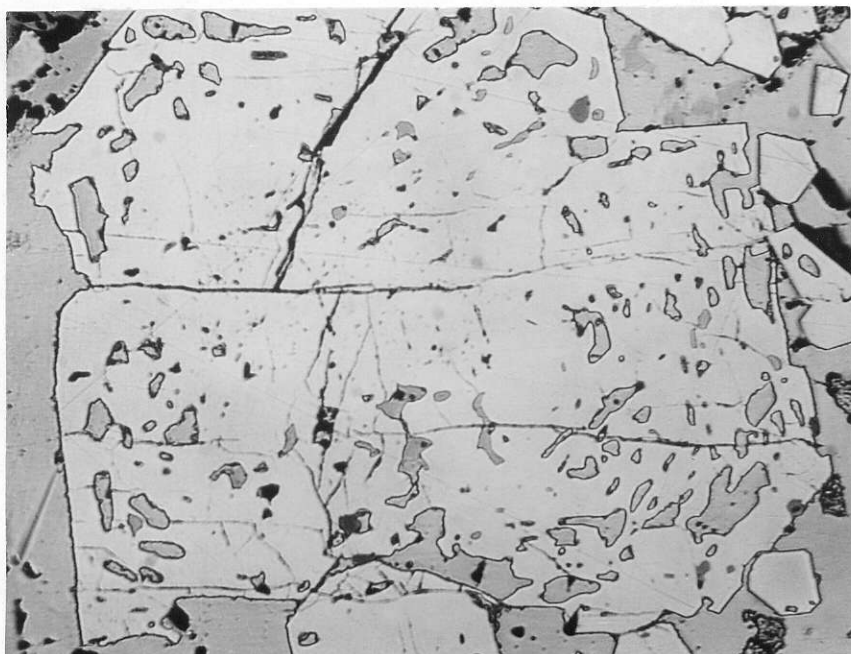


Figure 30 - Poikilitic pyrite crystal with included galena (light gray) and tetrahedrite (dark gray) from the Henderson vein. Mag. 130x.

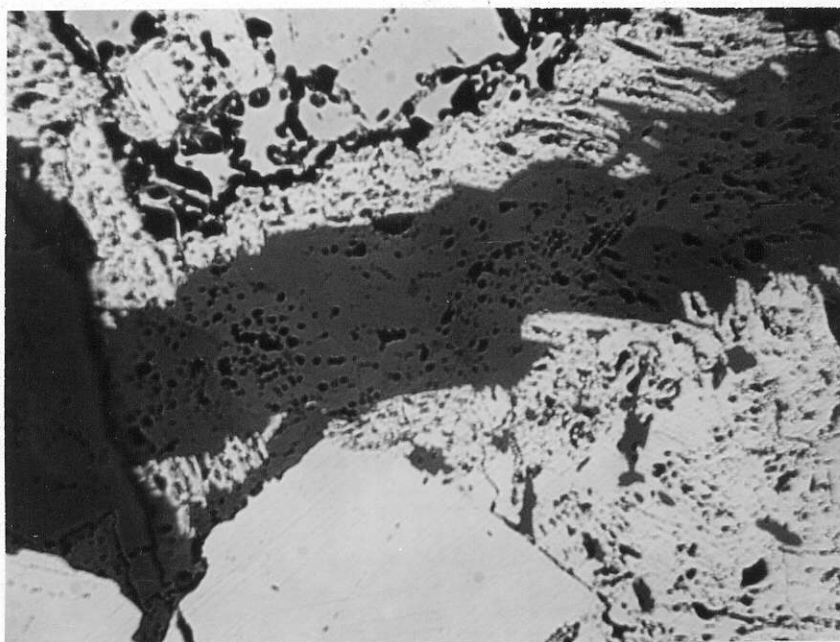


Figure 31 - Pyrrhotite partly replaced by lamellar marcasite along a carbonate vein. Light crystal in lower left is arsenopyrite. Copper Queen claim. Mag. 100x.

Features of Selected Minerals

Tetrahedrite-Tennantite

Both minerals occur in the district but tetrahedrite is the most abundant. Tennantite has been identified in only two samples: one from a small quartz vein in the molybdenum deposit, and the other (highly argentiferous) from a small carbonate, sulfide vein on the Rico Aspen property. Tetrahedrite (freibergite) occurs in many of the high-grade silver ores, and is probably the main silver mineral in them. Analyses of two tetrahedrites from the Henderson vein are given in Table 4.

Table 4 - Chemical Analyses of Tetrahedrite
from the Henderson Vein 1)

Sulfur	21.8	20.7
Antimony	25.0	25.5
Copper	19.0	18.0
Iron	4.0	5.0
Zinc	4.0	2.5 ³⁾
Silver	25.3 ²⁾	26.8 ³⁾
Gold	*	*
Bismuth	Nil	Nil
Arsenic	"	"
Tellurium	"	"
Specific gravity	5.1	5.2

1) after Galloway, 1923

2) Equals 7,384 oz. per ton

3) Equals 7,925 oz. per ton

* Equals 2.1 oz. per ton

Bournonite ($2\text{PbS} \cdot \text{Cu}_2\text{S} \cdot \text{Sb}_2\text{S}_3$)

Bournonite has not previously been reported from the district, but it is very widespread. It is most abundant in sulfide ores of the intermediate and outer zones. Previous

workers have probably mistaken it for tetrahedrite. X-ray films have a few characteristics of seligmannite, so there remains a distinct possibility that some arsenic has substituted for antimony.

Galena

Galena ranges from very coarse grained undeformed crystals to gneissic and steely deformed varieties. It occurs as large masses and as small grains intimately associated with other sulfides. In polished section it is typically free from intergrowths, but specimens from the Vancouver, Henderson, and East Coronado veins contain oriented intergrowths of tetrahedrite and matildite (?) formed by exsolution. Craig (1967) indicates that exsolution of matildite from galena only occurs below $215 \pm 15^{\circ}$ C. Unoriented blebs of pyrargyrite and native silver occur in galena from high-grade silver ores. Inclusions in some grains of galena from the Vancouver property are arranged in crude zones, which may be an indication that some galena was initially zoned in respect to silver.

Chalcopyrite

Chalcopyrite, although only a minor constituent in most deposits, is very widespread and shows much diversity in occurrence. It occurs as intergrowths, separate grains, and cross-cutting veins. Some is twinned, some is not; some contains isolated stars and blebs of sphalerite; some contains rows of rectangular blocks and crude stars of sphalerite that possibly could outline growth zones (Figure 32); and



Figure 32 - Row of sphalerite inclusions in chalcopyrite from scheelite-rich quartz vein (66-76) near fringe of the molybdenum deposit in Climax's exploration adit. Mag. 700x.

some does not contain any sphalerite or other inclusions. In some of the Cu-Fe-Ag ores it occurs as crystallographically oriented lamellae in bornite. Some of the chalcopyrite probably crystallized as cubic chalcopyrite or cubanite which at low temperature transformed to tetragonal chalcopyrite (Yund and Kullerud, 1966). Possibly the twinning is a record of such transformations. Chalcopyrite of the intermediate zone probably initially crystallized as cubanite (see Figure 54, p. 133). Since chalcopyrite is so widespread and occurs in every type of deposit, it would probably be fruitful to further study this mineral.

Gypsum

Gypsum, in the form of selenite, is present in many of the quartz veinlets of the molybdenum deposit. In some areas it has been found at depths as great as 2000 feet. Since it is stable only at relatively low temperatures and pressures, and since it is an integral part of many veins, it is probably an alteration product of primary anhydrite.

Scheelite

The economically important tungsten of the molybdenum deposit is contained mainly in scheelite, which occurs in quartz veinlets with molybdenite and alone. From available assay data it appears as if the zone of tungsten mineralization is approximately coincident with the zone of molybdenum mineralization.

Most of the scheelite fluoresces yellow-green suggesting Mo in solid solution (Greenwood, 1943), but some near the fringe of the molybdenum mineralization fluoresces white-blue and some crystals in the center of the molybdenum deposit exhibit irregular or crude zonal fluorescence. Although to the writer's knowledge the phase relations of the system scheelite (CaWO_4)-powellite (CaMoO_4) have not been studied, it can be expected that there would be considerable solid solution in the system, since scheelite and powellite are isostructural and since the radii of their +6 ions differ by only 9 per cent. Chemical and x-ray analyses show, however, that scheelite from the Hudson Bay Mountain district contains only minor Mo in solid solution.

To determine the extent of Mo substitution, two scheelites were chemically analyzed and two were x-rayed. The results are shown in Table 5.

Table 5 - Chemical and X-ray Data for Scheelite

A. Chemical Analyses of Scheelite ¹⁾					
	<u>67-157</u> ²⁾	<u>DDH57-533</u> ³⁾		<u>67-157</u>	<u>DDH57 533</u> ⁴⁾
Ca	14.15	-	CaO	19.80	19.23
W	61.22	58.50	WO ₃	77.20	73.77
Mo	1.35	2.52	MoO ₃	2.05	3.78
Ignition Loss	0.80	-	Ignition Loss	.80	-
			Totals	99.85	96.78

B. Cell Dimensions of Scheelite

	<u>DDH28-1743</u> ⁶⁾	<u>66-76</u>	<u>synthetic</u> ⁵⁾ <u>scheelite</u>	<u>synthetic</u> ⁵⁾ <u>powellite</u>
$a_0 =$	$5.243 \pm .003$	$5.242 \pm .003$	$5.242 \pm .005$	$5.226 \pm .005$
$c_0 =$	$11.376 \pm .002$	$11.369 \pm .002$	$11.372 \pm .005$	$11.43 \pm .007$

- 1) analyzed by the British Columbia Department of Mines
- 2) Sample 67-157 is from a drusy, pegmatitic scheelite-rich quartz vein which contains molybdenite, chalcopyrite, pyrite, feldspar, mica, chlorite, and calcite.
- 3) Sample DDH57-533¹ is from a relatively barren, coarse grained quartz, carbonate vein. Only a small amount of material was available for analysis.
- 4) by stoichiometry
- 5) after Swanson, Gilrich, and Cook, reported in the Handbook of Physical Constants, Clark, ed., 1966.
- 6) Samples 67-157, DDH57-533¹, and DDH28-1743¹ fluoresced yellow green. Sample 66-76 fluoresced white-blue.

If there is considerable Mo substitution, it should be reflected in the cell dimensions, since the cell dimensions of scheelite and powellite are significantly different. To test this possibility the writer, using a Norelco diffractometer and a NaCl internal standard, measured the position of the (020) and (004) scheelite peaks (to $\pm .012\theta$) of two scheelites--one with yellow-green fluorescence (DDH28-1743') and one with white-blue fluorescence (66-76). The "a" and "c" cell dimensions were calculated from these peaks using standard formulae for the tetragonal system (Table 5).

Several noteworthy features are shown by these cell dimensions. First, in view of the limits of accuracy of the methods, there is excellent agreement between Swanson et al.'s cell dimensions for scheelite and the writer's; however, the results are not in accord with Ferguson's ($a=5.26$ and $c=11.41$), (in Berry and Thompson, 1962). Also the fact that there is very little difference in cell dimensions of the yellow-green and white-blue fluorescing scheelite reinforces the conclusion that only minor Mo has substituted for W. Using Vegard's rule, the increase in the "c" dimension of DDH28-1743' scheelite over that of 66-76 corresponds to about 9 to 15 mole per cent CaMoO_4 , depending on whether 66-76 or the synthetic scheelite is used for the W end member. These tentative results serve to indicate that the "c" dimension may be

useful in determining the composition of scheelite, but some attempt should be made to determine the extent of Fe, Mn, Pb, and possibly other elements substitution and their effect on the cell dimensions.

There is some evidence to suggest compositional zoning of scheelite with respect to the molybdenum mineralization on the 3500 foot level. Near the fringe of molybdenum mineralization scheelite fluoresces white-blue; whereas, in most of the deposit it fluoresces yellow-green. Buseck, 1967, has noted zonation of scheelite fluorescence in respect to molybdenum mineralization at Tem Puite, Nevada. But the zoning he noted is the reverse of that at Hudson Bay Mountain. He interpreted this to indicate that where the molybdenum was incorporated in molybdenite it was unavailable to enter scheelite.

For a molybdenum-rich environment, indicated by the presence of abundant molybdenite, the molybdenum content of scheelite should be mainly controlled by the temperature and the fO_2/fS_2 ratio of the ore solution. A high temperature, sulfate-rich environment would favor an increased substitution of Mo in scheelite; whereas, a lower-temperature, sulfur-rich, oxygen-poor environment would tend to favor the formation of molybdenite and lessen substitution of Mo for W in scheelite. The presence of "anhydrite" and magnetite suggest that the molybdenum deposit was formed in an environment relatively high in $SO_4^{=}$. Future work may show that the Mo content of scheelite in molybdenum deposits is a very sensitive fO_2 indicator.

Vein Feldspars

Feldspar is abundant in the quartz vein stockwork of the molybdenum deposit. In places there is sufficient mica and hornblende with the feldspar to designate the veins as "pegmatitic", after the classification of Vokes' (1963). The feldspar which is typically white or light pink occurs mostly in medium- to coarse-grained anhedral and subhedral crystals. Some "flesh" pink feldspar has been identified as sodic plagioclase. X-ray analysis of 5 samples with a KBrO_3 internal standard (Orville, 1960 and 1967) showed that one is almost pure albite and the others are monoclinic (orthoclase?) potash feldspars containing about 10 per cent albite in solid solution. Stained potash feldspar from sample 66-76 showed that some zoning has been preserved. Preliminary work indicates that potash feldspar from associated porphyries does not contain as much albite in solid solution.

Vein Carbonates

Carbonate minerals are important gangue constituents in the quartz vein stockwork of the molybdenum deposit and of the sulfide vein and replacement deposits. They are also the main constituents of the quartz, carbonate veins that cut the quartz vein stockwork of the molybdenum deposit. In all these environments a definite sequence of carbonate deposition has been identified. Early buff or cream colored carbonate is cut by white, pale, or clear

carbonate (Figure 33). The buff carbonate is either siderite



Figure 33 - Calcite vein cutting volcanic host rock and banded ferroan dolomite from the Vancouver Group (Sample 65-62). Mag. 2x.

or dolomite-ankerite solid solution (Rosenberg, 1967), and the white, pale, or clear carbonate is calcite. Most of the carbonate occurs in compacted masses of medium to coarse grained anhedral crystals, but some of the calcite is present as terminated crystals lining vugs.

Twenty-two carbonates were studied by x-ray and staining techniques. The $d_{(211)}$ spacings were measured using NaCl as an internal standard. Hand specimens were stained with 0.5 per cent Alizarin Red S and 2 per cent HCl solution, and later with a 2 per cent potassium ferricyanide and 2 per cent HCl solution. According to Warne (1962),

in the Alizarin Red S solution, calcites stain red, dolomites do not stain, and ankerites and ferroan dolomites stain purple. Since many of the calcites stain purple instead of red this staining scheme is not applicable to carbonates of the Hudson Bay Mountain district. Similarly, Carpenter (1965) found that calcites from the Appalachian massive sulfide deposits stain purple instead of red. The potassium ferricyanide solution is a test for Fe^{++} ion. Samples of calcite, ferroan dolomites, and ankerites turn various shades of blue depending on the iron content, but siderites are not reactive to this solution. Although the writer did not test for it, small amounts of manganese can be expected in all samples.

Table 6 - Chemical Analyses of Calcites

	<u>65-62</u>	<u>65-98</u>
CaCO ₃	96.45%	96.76%
FeCO ₃	1.66	2.66
MnCO ₃	1.13	0.44
MgCO ₃	0.29	0.21
BaCO ₃	trace	trace
SrCO ₃	0.25	trace
Insoluble material	<u>0.37</u>	<u>0.35</u>
Totals	100.15	100.42

- analyzed by British Columbia Department of Mines
- 65-62-cross-cutting, coarse grained clear and white calcite from the Vancouver Group
- 65-98-coarse-grained, pale buff calcite from the Molybdenum Deposit

The results are given in Table 7 and schematically represented in Figure 34. The lower the d spacing of calcite and the higher for siderite and "dolomites", the greater the amount of minor element substitution that can be expected. The dependence of the $d_{(211)}$ spacing of natural dolomites and ankerites on regular substitution has not been adequately studied, so the results indicated in Figure 34 should be viewed with some caution. Figure 34 shows the probable compositional ranges of the carbonate minerals studied. Since any one of a number of cations can have a significant effect on the $d_{(211)}$ spacing, the exact compositions cannot be determined without chemical analyses. However, from the x-ray and staining results, and from two chemical analyses of calcite samples shown in Table 6, it is probable that carbonate minerals from the district are rich in Ca and Fe relative to Mg and Mn.

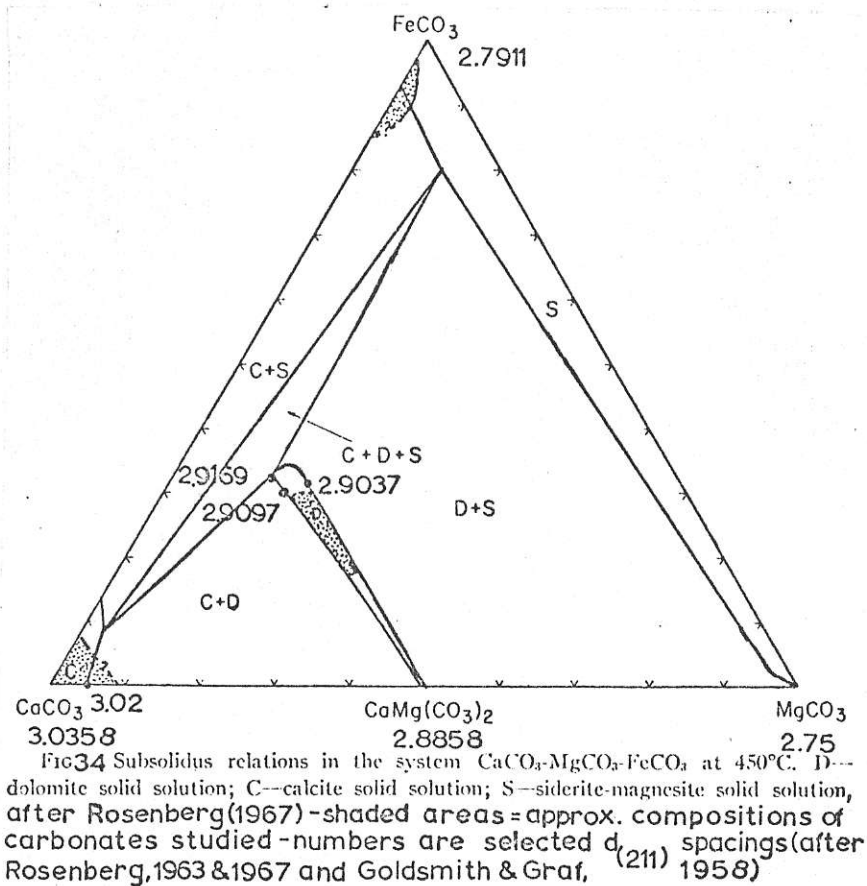
DDH29-1172' calcite and 65-98 ankerite (?) are of particular importance in geothermometry. If the shift of the $d_{(211)}$ spacing of DDH29-1172' calcite is primarily a function of iron substitution for calcium, its minimum indicated temperature of formation is 350°C (Rosenberg, 1963); however, if there is considerable magnesium substitution the minimum temperature would be even higher (Goldsmith and Graf, 1961). If the $d_{(211)}$ spacing of 65-98 ankerite (?) is indicative of a high iron content, then this ankerite (?) may have crystallized above 425° (Rosenberg, 1967). Since this carbonate vein cuts the quartz vein stockwork of the molybdenum de-

Table 7 - Summary of X-ray and Staining Data for Vein Carbonates

Prop. No.	Sample No.	d(211) spacing ± .002Å	Calcite Stain	Iron Stain	Occurrence
<u>Calcites</u>					
1	65-78	3.020	purple	strong	Type II py,mo,mus,gyps,carb,qz veinlet
	65-98	3.030	purple	strong	post-mo,qz,carb vein
	67-181	-	purple	faint	post-mo qz,carb vein
	DDH18-1482'	-	purple	faint	Type II mo,qz veinlet
	DDH21-1551'	3.022	purple	strong	coarse py,ccp,mus,kspar,carb,qz veinlet
	DDH29-5614'	3.018	purple	moderate	coarse py,mus,qz,carb veinlet
	DDH29-1172'	3.012	purple	strong	Type II mo,mus,carb,qz veinlet
	DDH29-1556'	3.025	purple	moderate	Pegmatitic, Type II ab,carb,mus,qz,mo, py veinlet sulfide vein
9	65-3	3.028	purple	strong	sulfide vein
43	65-62	3.028	red	faint	late crustiform carb veins
48	66-80	3.012	red	faint (anomalous)	sulfide vein
	Calcite reagent	3.034	-	-	x-ray calibration sample
<u>Ferroan Dolomites-Ankerites</u>					
1	65-78	2.912	purple	strong	Type II py,mo,mus,gyps,carb,qz veinlet
	65-98	2.914	purple	strong	post-mo qz,carb vein
	65-138A	2.907	dark purple	faint	post-mo qz,carb vein
	67-181	-	purple	strong	post-mo qz,carb vein
	DDH22-1983	2.8985	negative	strong	coarse py,mus,qz,carb vein
9	65-3	2.9085	-	-	sulfide vein
43	65-62	2.901	faint red	strong	late crustiform carb veins
5	65-91	2.9025	purple	strong	ccp,sp,tn,carb vein
<u>Siderites</u>					
9	65-3	2.794 ¹⁾	very faint	negative	sulfide vein
20	65-113	2.81(+?)	negative	very faint	sulfide vein
40	65-39	2.81(+?)	negative	very faint	sulfide vein
59	65-105	2.80	very faint	negative	sulfide vein

Abbreviations - ab-albite; carb-carbonate; ccp-chalcopyrite; DDH-diamond drill-hole; gyps-gypsum; kspar-potash-feldspar; mo-molybdenite; mus-muscovite; py-pyrite; qz-quartz; sp-sphalerite; tn-tennantite

¹ The d₍₂₁₁₎ spacings of the siderites are not accurate because the peaks overlap the NaCl(200) peak.



posit, this would be a minimum temperature for molybdenum deposition. Because the effects of manganese on the phase relations have not been studied, only minor information is available on the kinetics of carbonate solid state reactions, and since adequate studies of the relationship between composition and $d_{(211)}$ spacing have not been made for natural ankerites and ferroan dolomites, these results are only tentative.

Perhaps the most significant feature found in the present study is the relationship between carbonate composition and paragenesis. The paragenetic series from siderite, to ankerite or ferroan dolomite, to calcite is probably a re-

flection of the change in cation ratio of the ore solutions with time. Early solutions were probably rich in iron relative to calcium and magnesium while later solutions gradually increased in calcium relative to iron. Magnesium may have increased in respect to the other two when the ankerite or ferroan dolomites were forming. The Ca/Fe ratio probably increased as a natural result of iron being precipitated in sulfides and calcium being extracted from wall rocks by alteration (H^+ metasomatism).

In view of the paragenetic relations of the carbonates, it is interesting to note that siderite has not been found in the molybdenum deposit. A possible explanation for its absence is found in Holland's data (1959 and 1965). He has demonstrated that very high fugacities of CO_2 are required to stabilize siderite at high temperatures. In lieu of fluid inclusions exhibiting a separate CO_2 phase, it is most reasonable to consider that siderite crystallized only at moderate temperatures. Nevertheless, the presence of calcite with quartz in the molybdenum deposit would require relatively high CO_2 pressures to inhibit the formation of calcium silicates (Holland, 1965). It is also clear from Holland's work that in the presence of free silica, it is rather unlikely that such calcite formed above $500^\circ C$.

Precious Metals

Many deposits of the district contain economically important concentrations of precious metals, but very little work has been done to identify their exact occurrence. Moreover, it has been found that much of the gold is lost during concentration of the base metal sulfides. In many arsenopyrite-bearing ores it has been taken for granted that the gold is concentrated in arsenopyrite and not in the other minerals. Nevertheless, Thorpe (1967) has demonstrated convincingly that the gold of the Rossland district is contained mainly in chalcopyrite and not in arsenopyrite. Sims, et al. (1963) have shown that in the Central City district, chalcopyrite and tennantite contain more gold than pyrite, galena, and sphalerite, but that all metallic minerals contain some gold.

In order to better evaluate the precious metal distribution in the district, the writer made concentrates of minerals separated under a binocular microscope. The concentrates were analyzed for gold and silver. The analytical results are shown in Table 8. Except for 64-35 pyrite, most samples appeared reasonably pure. As might be expected, tetrahedrite and galena contain most of the silver. Moreover, the correlation analyses demonstrate the close association of lead and silver in many ores. It is also noteworthy that the chalcopyrite from the Mamie deposit contains considerable silver. From Table 8 it can be seen that the Mamie deposit contains about 7.5 ounces per ton silver, but

Table 8 - Precious Metal Contents of Mineral Concentrates

Mineral	Prop. No.	Sample No.	Approx. % Purity	Au oz./ton	Ag oz./ton	Associated Au oz./ton	Vein Assays ²⁾ Ag oz./ton
arsenopyrite	18	64-39	99	0.38	0.5	0.29	6.2
arsenopyrite	33	64-2	98	0.60	0.1	0.29	1.8
pyrrhotite	26	64-27	98	0.65	1.3	0.04	0.6
pyrite	19	64-35	80	0.14	2.3	0.15	8.9
sphalerite	30	65-24	97	0.10	2.0	0.10	1.7
pyrite	19	64-35	80	0.14	2.3	0.39	6.8
sphalerite	30	65-24	97	0.10	2.0	-	-
sphalerite	33	64-3	94	0.10	10.0	0.29	6.2
chalcopryrite	30	65-24	97	0.20	20.3	0.29	1.8
galena	33	64-3	98	trace	66.0	-	-
galena	33	64-3	98	trace	66.0	0.29	6.2
tetrahedrite ¹⁾	40	-	-	2.1	7384.0	0.29	1.8
tetrahedrite ¹⁾	40	-	-	2.1	7925.0	-	-

-analyzed by the British Columbia Department of Mines

1) after Galloway, 1923

2) grab and channel samples collected from the same localities as the hand specimens

only sparse amounts of galena have been found in the ore. For this reason it is possible that the silver content of this chalcopryrite is somewhat anomalous. The silver content of 64-3 sphalerite might be somewhat high due to contamination by tetrahedrite and chalcopryrite.

The contention that gold occurs only in arsenopyrite is shown by these preliminary results to be unwarranted. Although arsenopyrite does contain significant amounts of gold, tetrahedrite and pyrrhotite have even higher gold contents, and all ore minerals tested, except perhaps galena, contain some gold. The data are too few to draw firm conclusions, but they serve to point out that all the metallic minerals of the sulfide vein deposits are potential sources of precious metals. Although no analyses were made on minerals from the gold-bismuth deposit, free gold is

common as isolated specks in gangue material and as grains along the cleavage planes of josite. Thompson, 1949, has also identified calaverite from this deposit.

Pyrrhotite

Distribution and Description

Pyrrhotite is widespread. In sulfide ores of the intermediate zone it is the most abundant iron sulfide. Although far less abundant than pyrite, it is also an important constituent of the molybdenum deposit. Using detailed mapping, D. Davidson and J. Jonson of Climax Molybdenum Corp. (personal communication) have shown that pyrrhotite is more abundant near the limits of molybdenum deposition. The writer has confirmed their observation. In those parts of the metamorphic aureole which have not been affected by alteration related to molybdenum deposition, pyrite is very sparse. In these areas pyrrhotite is widespread as a minor constituent, in veinlets, as disseminations, and as small masses in alteration clots and vugs. In the barren zone some of the quartz veins contain minor amounts of pyrrhotite.

In the southern part of the district pyrrhotite and pyrite seem to be antipathetic. In vein deposits on the southwest slopes of Hudson Bay Mountain they tend to be in separate stringers in the sheeted fracture zones. Pyrrhotite tends to be more closely associated with sphalerite and chalcopyrite, whereas pyrite is more closely associated with arsenopyrite and quartz. On the southeast side of the mountain most deposits contain either one or the other iron sulfide but not

both. In the molybdenum deposit there are veins that contain abundant pyrrhotite and abundant pyrite, but most contain either one or the other so to some degree there is an antipathetic relationship. But many of the veins and replacement bodies on the northwest side of the mountain contain abundant pyrrhotite and pyrite, indicating a S_2 and T conditions such that they were stable together.

Pyrrhotite is invariably massive but ranges from very coarse-grained to very fine-grained. Unterminated crystals up to three inches in diameter have been observed in some deposits. The coarse grained pyrrhotite on the Mammoth and Neepawa properties is associated with coarse sphalerite and lesser amounts of coarse chalcopyrite that is concentrated between the two minerals. An unusual vermicular intergrowth of pyrrhotite and sphalerite has been developed on the Iron Vault property by selective replacement of pelecypod shell fragments. In some deposits pyrrhotite has been deformed by movements along the ore-bearing faults. Pyrite, arsenopyrite and to a lesser degree sphalerite have reacted in a relatively brittle manner while the pyrrhotite and galena have deformed plastically, flowing around breccia fragments and boudins of the other minerals. In the deformed ores pyrrhotite is generally fine grained and in polished section displays well developed deformation twinning.

Experimental Techniques

The composition of natural pyrrhotites that crystallized in equilibrium with pyrite was proposed by Arnold (1962) as a possible geothermometer. Recent work (Carpenter and Desborough, 1964; Desborough and Carpenter, 1965; Clark, 1966; Arnold, 1966 and 1967, etc.) has shown, however, that owing to solid state equilibration, most natural pyrrhotites are low temperature structural types. Pyrrhotite cannot be used in geothermometry unless it is possible to evaluate its post-depositional history. Yet since pyrrhotite is an important constituent of the ores in the district, and shows some diversity of occurrence, and because Arnold (1966 and 1967) has suggested some improved methods for studying pyrrhotite, the writer x-rayed a total of sixteen pyrrhotites and studied thirty in polished surfaces by the etching technique outlined by Arnold (1966 and 1967).

Diffractometer traces of the " $d_{(102)}$ " peak were made with and without a quartz internal standard. The superior peak resolution without the internal standard greatly facilitated the identification of hexagonal and monoclinic mixtures. This x-ray method was used in conjunction with polished surfaces etched for approximately one hour with a saturated solution of chromic acid (Arnold, 1966). Very small amounts of one type of pyrrhotite in another could be detected. Runs with the quartz internal standard made it possible to employ the $d_{(102)}$ spacing method of Arnold and

Reichen (1962) and Arnold (1966) to determine the composition of predominantly hexagonal samples. The d spacing of the hexagonal peak was measured only in those samples where the $d(20\bar{2})$ monoclinic peak was insignificant. A summary of the findings of the x-ray and microscopic analyses is given in Table 9.

Although it is possible to determine the bulk composition of hexagonal-monoclinic mixtures by heating the samples in evacuated silica tubes, such work was not done in this study. Nevertheless, Carpenter and Desborough's (1964 and 1965) and Arnold's (1967) work indicates that the bulk composition of such mixtures varies within fairly small limits, (46.5-47.5%). Hence it is possible to make a reasonable estimate of the bulk composition of the sample by determining the relative amounts of hexagonal and monoclinic pyrrhotite. It was found, however, that in all cases where several polished surfaces were available from one deposit, the ratio of hexagonal to monoclinic pyrrhotite varies greatly from one section to the next. Moreover, in some specimens it was noted that the etch reaction is partly dependent on grain size and orientation. For these reasons no attempt was made to determine accurately the relative amounts of the various phases.

Table 9 - Summary of Pyrrhotite Data

Prop. No.	Property Name	Sample No.	1) Structure Types	2) Atomic % Metals	Main Associated Minerals in Sample
10	Unnamed	64-60A, 64-60B	H T	47.5 ⁵⁾	asp, sp, ccp
9	Glacier Gulch N. Side	63-104	H M	47.2	sp, asp, ccp
16	Iron King	65-20	H M	47.5	sp, asp, ccp
30	Mamie	65-23	H M	47.2	sp, asp, ccp
49	Iron Vault	64-110, 64-111, 66-83 & 4 drill core samples	H M	47.6 ⁶⁾	py, sp, ccp, asp, gn
5	Unnamed	65-74	H M		asp, ccp
26	Mayflower #2 claim - Hend. vein system	64-26	H M	47.5 ⁷⁾	sp, ccp
52	"T" Fraction	65-85	H M		asp, py, ccp, sp, gn
50	Mammoth Claim	65-101	H M		py, asp, sp, ccp, gn
14	Josie Claim	65-94	H M		sp, py, ccp
1	Glacier Gulch Molybdenum (surface)	64-78 65-99	H, M H, M		py, ccp
24	Neepawa	65-137	H, M		sp, ccp, gn, ms
1A	Glacier Gulch Molybdenum 3500 Level ³⁾	66, 68, 66-69, 66-70, 66-71	H, M		
52	Copper Queen Claim	63-206, 65-121	M H		asp, sp, py, ccp
1A	Glacier Gulch Molybdenum 3500 Level ⁴⁾	66-76	M H		shee, ccp, sp, bn, ty, mo
1	Glacier Gulch	DD#39-990'	M H		mo, py
5	Unnamed	65-73	M H		ms
12	Unnamed	64-43	M H		asp, ccp

Symbols - T-troilite; H-hexagonal; M-monoclinic; asp-arsenopyrite; bm-bismuthinite; ccp-chalcopyrite; gn-galena; mo-molybdenite; ms-marcasite; py-pyrite; shee-scheelite; sp-sphalerite; ty-tetradymite

- 1) arranged in approximate order of increasing percentage of monoclinic pyrrhotite
- 2) -determined by $d(102)$ spacing method after Arnold and Reichen (1962) and Arnold (1966)
 - combined hexagonal-monoclinic peaks were measured below the point separation
 - None of the samples were heated; therefore, the composition has not been given for samples containing much monoclinic pyrrhotite. However, from Arnold's work (1967) and Carpenter and Desborough's work (1964), it can be expected that the bulk composition for hexagonal-monoclinic mixtures varies from about 47.5 to 46.5 atomic per cent metals with increasing monoclinic pyrrhotite content.
- 3) pyrrhotite that occurs disseminated (up to 20% of the rock) in black argillites and metavolcanic rocks
- 4) in a tungsten-rich vein near the limit of molybdenum deposition
- 5) $d(102)$ spacing of the troilite phase was found to be 2.0930A which, as shown by Toulmin and Barton (1964), is very close to stoichiometric FeS.
- 6) Carpenter and Desborough's Silver Creek Sample (p. 1355, 1964)
- 7) Arnold's Henderson Mine sample (p. 35, 1967)

Interpretation of the Results

Perhaps the most remarkable feature of the pyrrhotites studied is the fact that no single phase pyrrhotites were found. This supports the contention that at low temperatures 2-phase fields (troilite + hexagonal and monoclinic + hexagonal) predominate in the composition range 46.5 to 48.5 atomic per cent metals. The bulk compositions show a general relationship with structural type, the presence or absence of pyrite, and the position of the pyrrhotite in the district. Samples with significant percentages of monoclinic pyrrhotite occur only in the molybdenum deposit or in areas near the outer limit of the intermediate zone where the pyrrhotite is associated with pyrite. Predominantly hexagonal pyrrhotites (relatively metal-rich ones) occur in or very close to the metamorphic aureole. These features indicate that pyrrhotite bulk compositions are indeed related to conditions that prevailed at the time of ore formation. However, it is misleading to emphasize this relationship too strongly since it is apparent that in some samples, such as 63-104 (Figure 37), the formation of much of the monoclinic pyrrhotite was related to supergene processes that lead to the formation of marcasite and limonite. On the other hand, however, the fact that lamellae in some pyrrhotite have no apparent relationship to marcasite veinlets is further evidence to suggest that the two had different origins (Figure 38). Because of the overall pattern of pyrrhotite distribution it is tentatively

suggested that lamellae such as the troilite in sample 64-60A (Figure 35) and the hexagonal and monoclinic lamellae in sample 65-74 and 64-26 (Figures 36 and 38) formed by exsolution mainly in a response to cooling and not because of compositional changes in the environment (i.e., a change in the fugacity of sulfur). However, it is equally apparent that lamellae of monoclinic pyrrhotite can form in hexagonal pyrrhotite by supergene alteration and presumably by any process that would cause an increase in sulfur fugacity. It is obvious that each sample, deposit, or even district should be evaluated on its own merits. It would be advantageous to have some criteria whereby the cooling history could be traced.

In the Hudson Bay Mountain district distribution of pyrite and pyrrhotite gives some indication of the general conditions at the time of ore deposition. The molybdenum deposit is characterized by relatively sulfur-rich assemblages, whereas other areas within the metamorphic aureole are in sharp contrast with their sulfur-poor assemblages. Outside the metamorphic aureole the sulfur-poor assemblages grade to assemblages richer in sulfur until pyrrhotite stability limits were exceeded and pyrite was deposited. This pattern of iron sulfide occurrence is almost certainly due to fugacity of sulfur and temperature gradients that existed during the period of ore deposition, (see Figure 54), and it is possible to evaluate the pyrrhotite composition within this framework.

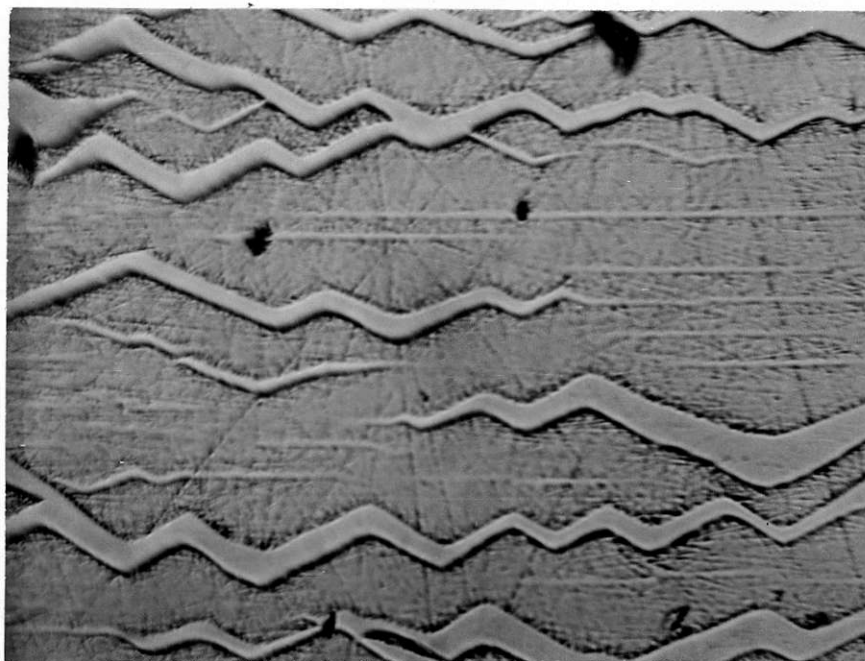


Figure 35 - "Zig-zag" troilite lamellae in hexagonal pyrrhotite from a sulfide vein (64-60A) to the north of the Toboggan Glacier. Note that the "zig-zag" amplitude is approximately proportional to the lamellae width. Surface was etched with a saturated solution of chromic acid. Mag. 450x.



Figure 36 - Intergrowth of monoclinic pyrrhotite (dark) in hexagonal pyrrhotite (light). The light bands in the monoclinic pyrrhotite are probably twin lamellae. Specimen (65-74) is from property no. 5. Surface was etched with a saturated solution of chromic acid. Mag. 675x.

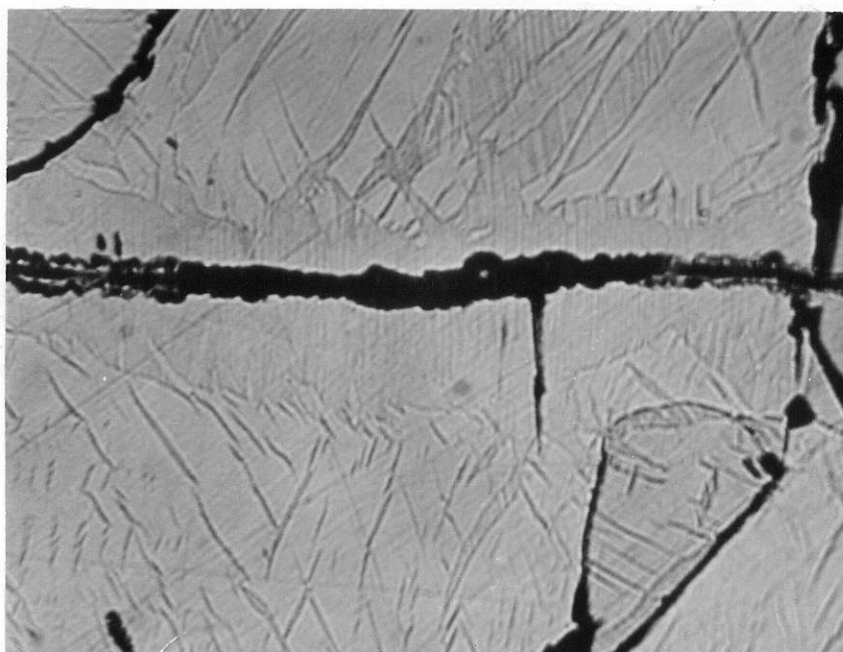


Figure 37 - Monoclinic pyrrhotite (dark) formed in hexagonal pyrrhotite (limonite) along a secondary fracture with limonite and marcasite. Specimen (63-104) is from the Glacier Gulch North Side property. Surface was etched with a saturated solution of chromic acid. Mag. 300x.



Figure 38 - Lamellae of monoclinic pyrrhotite (dark) in hexagonal pyrrhotite (light and medium gray) showing no apparent relationship to the marcasite veinlets. Specimen (64-26) is from property no. 25. Surface was etched with a saturated solution of chromic acid. Mag. 150x.

Pyrrhotites of the molybdenum deposit probably have bulk compositions from about 46.7 to 47.2 atomic per cent metals. This is based on the assumption that Arnold's (1967) findings for natural pyrrhotites would hold for these pyrrhotites. If, as might be expected, these pyrrhotites crystallized in or almost in equilibrium with pyrite, the minimum temperature of formation estimated from the pyrrhotite-pyrite solvus (Arnold, 1962) would be about 450° to 350° C. Using the same reasoning, similar minimum temperatures can be obtained for the Mamis, Iron Vault, "T", Mammoth, Josie, and Copper Queen properties. It is not unreasonable to consider that the pyrrhotite equilibrated with pyrite down to these temperatures, but in view of the rapid reaction rates of pyrrhotite in the solid state it is even more surprising that the pyrrhotite, at least in some areas, did not equilibrate at even lower temperatures, forming assemblages of only monoclinic pyrrhotite and pyrite. The mere fact that the pyrrhotite with pyrite is not solely monoclinic pyrrhotite is strong evidence to suggest that most if not all of these ores crystallized above 300° C. However, any definitive use of pyrrhotite in geothermometry in the district should be deferred pending further work in the Fe-S system.

Even with all uncertainties that have currently been raised concerning interpretation of pyrrhotite relations, mineral assemblages in the Fe-S system certainly are useful indicators of the general conditions (a_{S_2} and T) of ore depositions in the Hudson Bay Mountain district.

Sphalerite

Introduction

The relatively slow reaction rates of sphalerite in the solid state, its large range in composition, the abundant available information on its phase relations, and its widespread distribution in the district make it a very useful mineral in the study of ore-forming processes. For this reason considerable effort was expended in collecting representative material from as many deposits as possible.

Distribution and Description

Sphalerite has been found in all zones of the district, but it is most abundant in the sulfide ores of the intermediate and outer zones. Traces are present in the molybdenum deposit. It occurs as exsolution (?) stars and blebs in some chalcopyrite, but it occurs mostly in quartz, carbonate veins that cut the molybdenite-bearing quartz vein stockwork. Its deposition was therefore not directly related to that of the molybdenite. In one sample (66-76) taken on the 3500 foot level sphalerite is associated with molybdenite, but the two minerals are not in contact.

Sphalerite typically forms dark brownish-black, fine- to coarse-grained, massive, anhedral aggregates or grains intimately intergrown with other ore and gangue minerals. Terminated crystals of sphalerite were not found. Regular polysynthetic twinning is prominent on some fresh cleavage surfaces of coarse grained material, and on polished sur-

faces etched with saturated chromic acid solutions (Figure 40). Pyrite, pyrrhotite, arsenopyrite, galena, chalcopyrite, tetrahedrite, bournonite, quartz, calcite, and dolomite are common associated vein minerals.

Small amounts of light-colored sphalerite were found in many deposits. In general it constitutes only a minor portion of the total sphalerite; in deposits such as the veins on the Silver Lake claims (property no. 48), it is a main constituent. At most localities the light sphalerite occurs as blebs and pods in darker sphalerite. It probably crystallized in cavities or replaced material after the dark sphalerite had formed.

In polished "thick sections"--sections slightly thicker than normal thin sections--regular growth zoning is relatively rare. Intricate growth zoning such as that described by Sawkins (1964) in Providencia district, Mexico, and Roedder (1965) and Barton, et al. (1963) at Creede, Colorado was not found. Nevertheless, a few specimens exhibit some growth zoning. Typically the transparent sphalerite is in reasonably sharp contact with opaque sphalerite. In many specimens, areas of light sphalerite are blotchy and contain numerous zones of opaque ("dusty") inclusions.

Polished sections reveal that some sphalerites contain intergrown pyrrhotite and chalcopyrite, both as irregular blebs and as crystallographically oriented blades (Figure 39). Etched sphalerite surfaces show that most unoriented

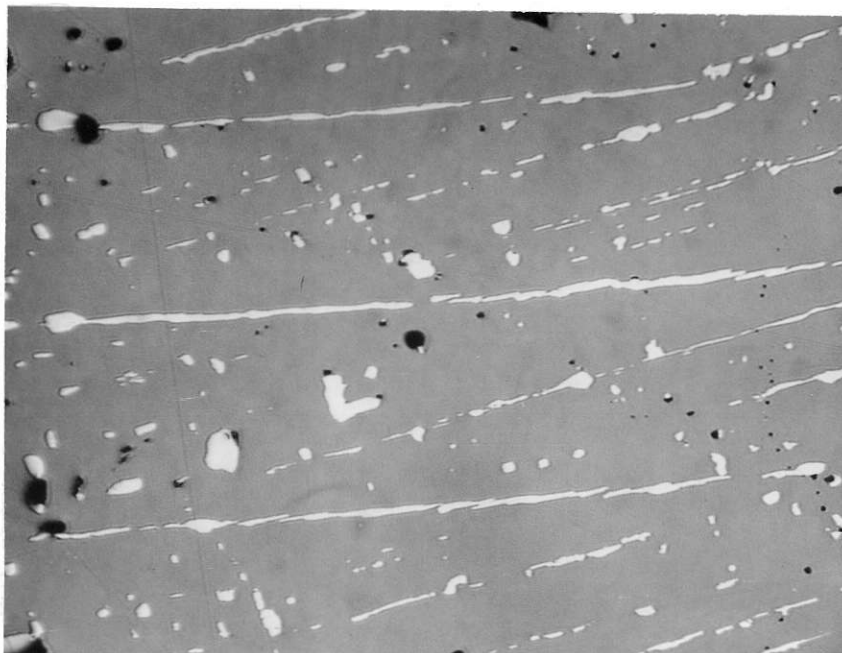


Figure 39 - Oriented lamellae and blebs of chalcopyrite in unetched sphalerite (65-111) from the Empire property. Mag. 150x.

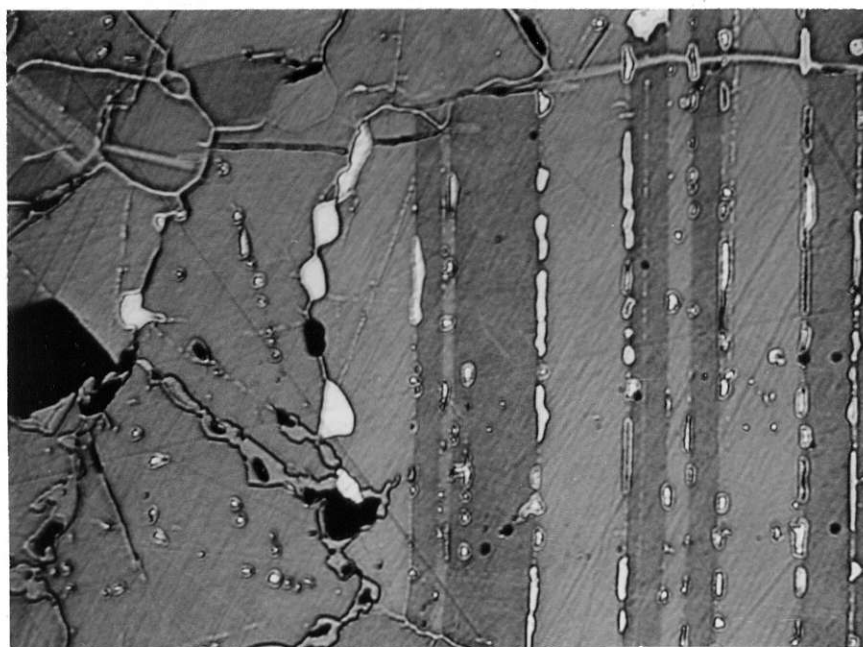


Figure 40 - Same as Figure 39 except the surface was etched with a saturated solution of chromic acid. Note that the oriented chalcopyrite lamellae lie along twin planes, and that the unoriented lamellae lie along grain boundaries. Also note that a rim of sphalerite stands in relief along the grain boundaries. Mag. 300x.

blebs occur along grain boundaries, while the oriented blebs occur along crystallographic planes within crystals; for example, along twin lamellae (Figure 40). In many of the etched surfaces narrow rims of sphalerite along grain boundaries and irregular vein-like structures stand in relief after etching (Figure 40). The reason for this is unknown.

Chemically Analyzed Sphalerite Standards

Sixteen sphalerite samples, to serve as standards for electron microprobe and x-ray analyses, were analyzed for Zn, Fe, S, Cd, Mn, and Cu. Pure samples representing a wide range of iron content were sought. In general satisfactory samples were found; however, because several grams of material were required, and because some microscopic impurities could not be avoided, the analyses at best are only very close approximations of the bulk composition of what was later shown by microprobe analyses to be heterogeneous material.

The variation shown in the duplicate analyses of sample 65-109G is undoubtedly due to the heterogeneous nature of the sample, not to poor analytical procedure. Indeed, the fact that the analyses show a very high degree of linear correlation (+ .999) with the electron microprobe analyses indicates that the chemical and microprobe bulk compositions are in general reliable.

The following is a brief summary of analytical methods used:

Zinc. Sample was dissolved in $\text{HNO}_3 + \text{KCl}_3$, interfering elements were removed, and zinc was titrated with a standard $\text{K}_4\text{Fe}(\text{CN})_6$ solution. Analysis by R.S. Young.

Sulfur. Sample was dissolved with a mixture of KBr and Br_2 , and the resulting sulfate was precipitated with BaCl_2 and weighed as BaSO_4 . Analysis by R.S. Young.

Iron. Sample was fused with Na_2O_2 and the fusion leached with water. After acidification and removal of interfering elements iron was reduced and titrated with a standard $\text{K}_2\text{Cr}_2\text{O}_7$ solution using diphenylamine sulfonic acid as end-point indicator. Analysis by S. Metcalfe.

Manganese. Sample was put in a sulfuric acid solution and manganese was oxidized to permanganate with KIO_4 . The absorbancy of the colored solution was measured on a Beckman spectrophotometer. Analysis by R.S. Young.

Copper. In some sphalerites copper was determined by N. G. Colvin by x-ray fluorescence and in other samples by R. Hibberson using an A.R.L. spectrograph.

Cadmium. It was determined by N.G. Colvin using x-ray fluorescence.

The results are given in Tables 10, 11, and 12. The major elements should be accurate within a few tenths of one per cent.

Semi-quantitative analyses of some of these samples showed trace amounts of Sb, In, Ti, Ni, and Co but failed to reveal any Sn or Ge.

Table 10- Chemical Analyses of Sphalerite Standards

Sample No.	Zn	Fe	Cd	Mn	S	Cu	As	Pb	Total
65-109C	64.20	2.44	0.58	0.08	32.64	0.01	-	-	99.95
65-109F	61.38	5.16	0.55	0.06	32.86	0.015	-	-	100.02
65-109G1	61.04	5.70	0.58	0.05	32.54	0.03	-	-	99.94
65-109G2	61.04	5.28	0.57	0.05	32.87	0.02	-	-	99.83
65-111	56.40	9.04	0.48	0.27	33.26	0.32	-	-	99.77
64-3A	50.35	9.31	0.34	0.43	30.89	0.43	-	2.02	93.77
63-176	55.80	9.50	0.28	0.20	32.90	0.03	-	-	98.71
64-154C	53.45	10.51	0.38	0.27	32.84	0.09	-	-	97.54
64-5	52.41	10.46	0.39	0.22	32.67	0.11	-	1.37	97.63
64-39C	49.80	11.40	0.39	0.30	32.11	0.25	1.30	1.65	97.20
65-23A	54.48	11.60	0.35	0.26	32.42	0.08	-	-	99.19
64-26	52.41	11.98	0.36	0.34	33.12	0.24	-	-	98.45
65-114	52.68	13.16	0.32	0.60	33.08	0.07	-	-	99.91
65-20	51.98	14.04	0.25	0.49	33.02	.16	-	-	99.94
63-104	46.53	16.87	0.53	0.31	33.39	0.28	-	-	97.91

-Done by the Analytical Branch of the British Columbia Department of Mines

-Samples collected during 1965 are of higher purity than those collected during 1963 and 1964

Electron Microprobe Analyses

X-ray and electron microprobe techniques were used to determine the iron content of sphalerite. However, because of the overwhelming superiority of the latter technique, the x-ray methods of analysis were abandoned. Williams (1965) has presented a good discussion of the relative merits of the various methods of sphalerite analysis.

Table 11 - Sphalerite Analyses Corrected for Impurities
and Recalculated to 100 Weight Per Cent

Sample No.	Zn	Fe	Cd	Mn	S
65-109C	64.25	2.43	.58	.08	32.66
65-109F	61.39	5.15	.55	.06	32.85
65-109G1	61.13	5.68	.58	.05	32.56
65-109G2	61.18	5.27	.57	.05	32.93
65-111	57.50	8.46	.49	.28	33.27
64-3A	56.29	9.47	.38	.48	33.38
63-176	56.58	9.60	.28	.20	33.34
64-154C	54.94	10.72	.39	.28	33.67
64-5	54.75	10.82	.41	.23	33.79
64-39C	54.37	11.06	.43	.33	33.81
64-26	53.61	12.04	.37	.35	33.63
65-114	52.83	13.14	.32	.60	33.11
65-20	52.39	13.85	.25	.49	33.02
63-104	48.05	17.00	.55	.32	34.08

- calculated on the basis $Zn + Fe + Cd + Mn + S = 100 \text{ wt. } \%$
- amounts of included pyrrhotite and chalcopyrite blebs were determined from polished sections
- all Cu was assumed to be in chalcopyrite ($CuFeS_2$)
- all Pb was assumed to be in galena (PbS)
- all As was assumed to be in arsenopyrite ($FeAsS$)
- pyrrhotite composition was assumed to be FeS
- minor corrections for pyrrhotite impurities were made for samples 65-111, 64-3A, 64-39C, 65-20, 63-104

Table 12 - Calculated Mole Per Cent Sulfides in Sphalerite Standards

Sample No.	ZnS	FeS	CdS	MnS
65-109C	95.14	4.21	0.50	0.15
65-109F	90.53	8.89	0.47	0.11
65-109GI	89.66	9.75	0.50	0.09
65-109G2	90.31	9.11	0.49	0.09
65-111	84.53	14.56	0.42	0.49
64-3A	82.58	16.26	0.33	0.83
63-176	82.94	16.47	0.24	0.35
64-154C	80.73	18.44	0.34	0.49
64-5	80.61	18.64	0.35	0.40
64-39C	80.01	19.05	0.36	0.58
65-23A	79.56	19.71	0.29	0.44
64-26	78.45	20.62	0.32	0.61
65-114	76.45	22.26	0.26	1.03
65-20	75.57	23.38	0.21	0.84
63-104	69.99	28.99	0.47	0.55

-Calculated on the basis $ZnS + FeS + CdS + MnS = 100\%$

The main purpose of the microprobe analyses was to determine the iron content of sphalerite from as many deposits as possible and correlate it with the zonal distribution of metals. Early in the work, however, it was recognized that individual deposits showed a wide range of sphalerite composition. Sampling the material to give the most meaningful results, therefore, became a problem. Presumably the average iron content would be most representative of the overall physicochemical conditions prevailing during ore deposition. Nevertheless, to determine these conditions from the sphalerite phase relations, it is necessary to establish that equilibrium existed between sphalerite and an iron sulfide. In lieu of well developed growth zoning or crustiform layering the only satisfactory way to determine equilibrium compositions is to analyze sphalerite that grew in contact with an iron sulfide. However, it is still possible that sphalerite isolated from iron sulfide grains crystallized in equilibrium with an iron sulfide. On the other hand, mere coexistence of sphalerite and an iron sulfide in a deposit or even the same hand specimen is not sufficient evidence that equilibrium was obtained, although such evidence has been accepted in other studies. The writer's studies suggest that a rim of sphalerite 1 mm or less in thickness around an iron sulfide grain was sufficient to prevent it from reacting with subsequently deposited sphalerite. A good example is shown in sample 64-110, in which sphalerite

with less than 1 mole per cent FeS occurs only a few millimeters away from pyrite and pyrrhotite. Under no conditions is it conceivable that the sphalerite reached equilibrium with the pyrrhotite.

Time requirements and the nature of the available material precluded a study that would satisfy all requirements. In general it was easiest to select material from which the average composition of the sphalerite of the sample and hence the deposit could be estimated. For this purpose, sphalerite grains were selected from as many locations as possible in the hand specimens. Most specimens consist of several chunks and chips from several places at the sample locality. If color zoning was prominent, separate samples were prepared from each zone. The grains were then mounted in either epoxy or plastic in one inch cylindrical epoxy blocks made to fit in the sample holders of the microprobe. These blocks were polished by normal diamond polishing techniques and buffed with chromic oxide.¹ The polished surface was evenly coated with a thin layer of carbon to conduct away the bombarding electrons. As a rule, ten separate grains were measured from each sample, and if the zoning was

¹ Although chromic oxide buffing was used throughout this study, some duplicate samples were buffed with chromic acid solution using the method suggested by Cameron and Van Rensburg (1965). The results indicated that the chemical-mechanical buffing did not cause any significant change in the composition.

pronounced, more grains were measured.

To evaluate compositions of sphalerite that might have crystallized in equilibrium with an iron sulfide, compositions of sphalerite adjacent or reasonably close to iron sulfide grains are given in column 5 of Table 13. However, the mere proximity of the grains is no assurance that sphalerite crystallized in equilibrium with the associated iron sulfides. In fact in some cases, as cited on p. 52, there is reason to believe that the sphalerite crystallized in equilibrium with pyrrhotite that was subsequently replaced by pyrite. Moreover, on textural grounds it is difficult to determine the relative ages of the minerals. For a few properties separate samples were prepared to determine the sphalerite compositions adjacent to iron sulfides.

Instrumentation and Analytical Procedure

The Applied Research Laboratories Electron Microprobe of the Department of Geology of the University of Wisconsin was used for the analyses. The acceleration voltage for all runs was 15 KeV and the sample current was about .05 MA. FeK_{α} and ZnK_{α} peaks were measured using LiF analyzing crystals. Since optical resolution is poor for carbon-coated surfaces, simultaneous measurement of zinc eliminated the possibility of mistaking other iron-bearing sulfide minerals for sphalerite. A method employing counts per 100,000 counts of beam current eliminated the need for drift corrections commonly used in standard x-ray fluorescence analysis.

Most measurements required 15 to 20 seconds.

As a rule 6 or 7 sphalerite samples were run between measurements of a homogeneous sphalerite standard. A sphalerite obtained from B.W. Evans of the University of California at Berkley was used for this standard, since no sphalerite of sufficient purity from the Hudson Bay Mountain district was found during the early stages of the work. Evans (indirect communication) reported the iron content, as found by wet chemical techniques, to be 11.4 weight per cent. However, from Figure 41 it can be seen that this analysis is probably too high. The same grains were measured each time the standard was run.

All analyses were corrected for background, determined by measuring the background an equal distance on either side of the peak and averaging the results. The background was normally measured at the end of a day's run. An average value, determined for both high-iron and low-iron sphalerites, was used.

For some samples S, Cd, Mn, Cu, and As were also determined by procedures essentially the same as those used for Fe and Zn, except that pure metal standards were used for the As and Cu analyses.

Splits from the samples sent for chemical analysis were employed to establish an iron calibration curve for Hudson Bay Mountain sphalerites. To obtain the curve shown in Figure 41 the chemically analyzed sphalerites were run

several times over a period of three months. The curve was calculated by least squares regression analysis forcing the curve through the origin.¹ The constant for the regression equation is known very accurately ($\pm .0010$; Figure 41); hence, although the samples used for calibration show some dispersion from the curve, their heterogeneity is not a limiting factor of the accuracy of the method.

Williams (1967) pointed out that if natural sphalerites are to be used for probe standards, one should not only have a library of standards analyzed for Fe, but should also have analyzed samples displaying a range of Cd and Mn contents. Undoubtedly variations in Cd and Mn will affect the accuracy of the results. However, the effects should be very minor indeed for Hudson Bay Mountain sphalerites since Cd + Mn is usually less than 1 per cent, Cd content does not generally vary more than .25 per cent, and Mn varies with Fe. Williams suggests that for most work pure metals standards would be most satisfactory. However, use of natural sphalerite standards is far faster and need not be any less accurate. Goresy (1967) used ZnS, FeS, and MnS standards to good advantage in analyzing sphalerites in meteorites.

The precision or reproducibility of the analyses was evaluated by measurement of the same grains of samples of a low- and high-iron sphalerite five times over the three-

1 Sample 63-176 was not used for the calculations.

month period of analysis. The standard deviation for the low-iron sphalerite was found to be ± 0.01 weight per cent Fe or 0.4 per cent of the amount present, while that for the high-iron sphalerite was found to be ± 0.16 weight per cent Fe or 1.23 per cent of the amount present. Since the calibration curve is known with confidence, the accuracy of the analytical technique is probably limited by the precision.

Barton and Toulmin (1966) in their analysis of synthetic sphalerites used a Fe/Zn count ratio and related it to a FeS/ZnS mole ratio. One should, however, be cautioned against using this method for natural sphalerites since the analysis is based on the assumption that FeS + ZnS = 100 per cent. Natural sphalerites invariably contain some Cd and/or Mn which necessarily causes the results to be consistently high. For example Hudson Bay Mountain sphalerites determined by this method yielded results that were consistently .1 to .4 mole per cent FeS higher than the values calculated from Fe counts alone.

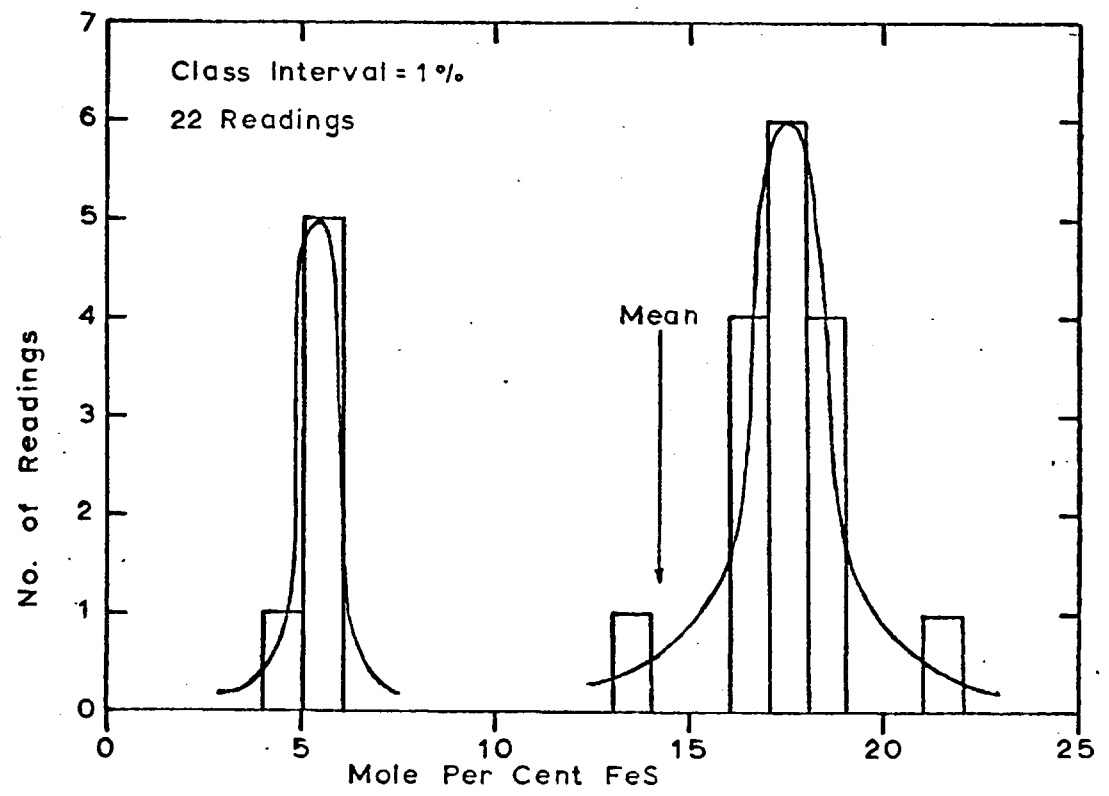
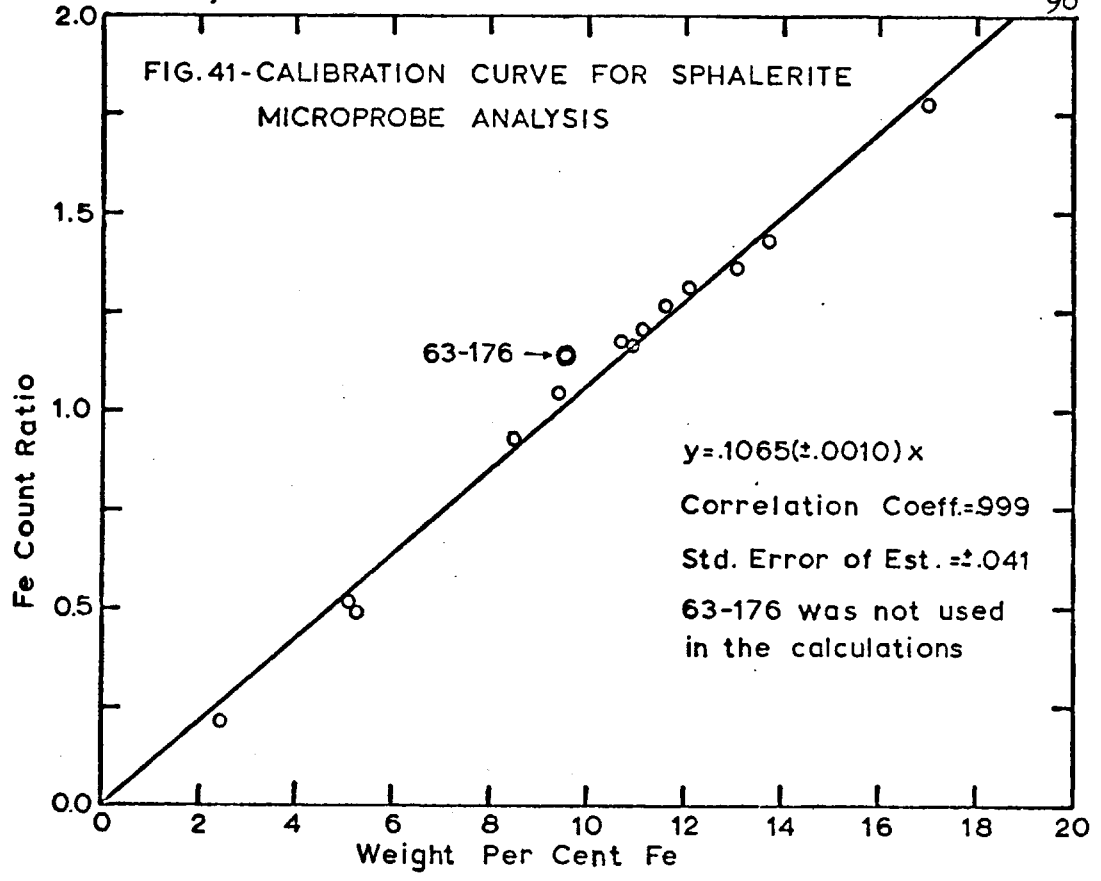


FIG. 42-FREQUENCY DISTRIBUTION OF FeS IN SPHALERITE FROM SAMPLE 63-174A

Discussion of the Results

Iron contents of sphalerite from microprobe analyses are given in Table 13. Most of the analyses can be accepted at face value, but the method of presenting the data fails to reveal erratic values or mixed populations of differing compositions. Figure 42, for instance, shows an extreme case of a bimodal population. The arithmetic mean (average) is not very representative of the sphalerite compositions. At first it was thought that the marked break in composition had genetic significance; that is, there was a definite discontinuity in sphalerite deposition. However, iron contents in the range 6 to 13 mole per cent were found in samples 65-61, 65-62, and 65-63 taken from the same property, indicating that the bimodal nature of the population is probably a function of the sampling procedure. This points up the shortcomings of the analytical method in determining the mean sphalerite composition of a sample and of an entire deposit.

Even with these limitations, the microprobe data are far superior to those obtained by other available analytical methods. Only the purest of sphalerite samples can be analyzed with confidence by wet chemical techniques, and the results are only averages of a composite sample.

Measurement of the cell edge by x-ray diffraction has been used extensively in the past to determine the Fe content, but the method has very serious drawbacks, as pointed

Table 13 - Summary of Electron Microprobe Data for Sphalerite

1 Prop No	2 Sample No	Mole % FeS				7 Occurrence	8 Main Assoc Ore Minerals in Sample
		3 Sample 1) Av	4 Observed 2) Range	5 Adjacent 3) Fe Sulf	6 Est 4) Prop Av		
1	64-87	12.3	8.0-16.0	8.0-16.07		mainly barren post-mo qtz-carb vn	py, ccp
	65-98	0.4	0.1- 0.9			"	py, ccp, bo?
	65-138	1.25	0.5- 2.0		15.3 ⁵⁾	"	py, gn, bo?
1A	66-76A	15.3	13.7-16.7			W-rich vn at fringe of Mo dep	shee, po, ccp, bn, ty, mo
	66-76B	15.8	12.5-17.8	17.0-17.8 ⁸⁾		"-sp adj po	"
2	65-71	12.9	11.0-15.4		12.9	probably a late carb vn	ccp, bo, asp
3	65-68	19.1	17.0-19.7	19.0-19.7	19.1	mainly barren qtz vn	asp, po, ccp
4	65-67	20.7	18.0-22.3		20.7	"	alt po?, asp, py, bo
6	65-77	10.25	0.5-25.0 ⁹⁾		10.0	probably late carb veinlets	py, gn
8	63-104	28.5	24.8-30.5	24.8-30.5	27.0	sulf vn ⁶⁾	po, asp, gn, ccp
	65-41A	0.7	0.4- 1.6			sulf lense-h s l sp	asp, po
	65-41B	9.6	6.0-11.2			" -h s m sp	asp, po
	65-41C	10.8	11.5-26.4	? -26.4		" -h s d sp	asp, po
9	65-3 ¹⁰⁾	4.0	1.0- 7.07		4.0	probably a late carb vn	gn, asp, bo
10	64-58	26.0	20.3-28.0		26.5	sulf vn	asp, py, ccp
	64-58A	27.6	25.4-29.2	25.4-29.2		"	po, ccp, ms
	64-60A	26.1	22.8-27.5	22.8-27.5		"	po, asp
	64-60B	25.9	18.3-26.0	25.8-26.0		"	po, ccp
11	65-116	22.7	18.3-26.0	24.0-26.0	24.0	"	po, ccp
	65-117	25.4	22.7-27.6	22.7-27.6		"	asp, po
13	64-66	22.0	21.3-23.5	21.3-23.5	22.0	sulf veinlets	po+py in wall rock
14	64-132A	19.5	18.8-21.2		21.5	sulf vn	po
	64-132B	21.3	20.7-22.0	19.0-22.0		"	po
	65-94	22.2	20.0-24.0	20.0-24.0		"	po, py, ccp
15	65-93	12.9	12.3-13.5		17.5	"	gn, ccp
	65-114	21.7	21.4-24.0	21.4-24.0		"	po, gn, ccp
16	65-16	21.6	19.2-23.1	19.2-23.1	23.0	sulf veinlets	asp, po
	65-17	23.5	21.9-25.0	21.9-25.0		widely scattered vein- lets in meta rks	asp, po
	65-20	23.1	21.0-25.4	21.0-25.4		sulf vn	po, asp, ccp
17	65-64	19.4	18.9-19.8		19.4	sulf vn	asp, ccp, py
18	64-39	19.6	19.0-19.7	19.0-19.7	19.4	"	asp, py, gn, ccp
	64-39C	19.3	18.8-19.7	18.8-19.7			
19	63-181	12.1	9.5-13.7	11.0-13.7	15.0	"	py, asp, gn
	64-35	16.2	15.3-19.2	15.3-19.2			asp, py, gn, ccp
20	65-113	5.2	0.3- 8.8		7.0	sulf vn	asp, py, gn
	66-77	9.9	5.4-12.4	5.4-12.4		"	gn, ccp, py, asp, td
	66-78	11.7	7.0-17.4			sulf frag in late qtz	py, gn
	66-79	7.7	7.4- 8.4	7.4- 8.4		sulf vn	gn, ccp, py, asp, td
22	61120 ¹¹⁾	9.1	8.0-10.3			carb vn	gn, ccp, py
23	63-195	5.5	1.2-10.1		12.0	sulf vn	gn, py, asp
	65-111	14.9	11.0-21.1	11.0-21.1		"	py, gn, asp, ccp
	665-112	6.4	4.9- 8.2	4.9- 8.2		frag in late qtz	py, gn
24	65-136	19.4	18.3-20.8	18.3-20.8	19.7	sulf vn	po, ccp, gn, ms, asp
	65-137	20.0	19.0-21.8	19.0-21.8		"	po, ccp, gn, ms

Table 13 - continued

1 Prop No	2 Sample No	Mole % FeS				7 Occurrence	8 Main Assoc Ore Minerals in Sample
		3 Sample Av	4 Observed Range	5 Adjacent Fe Sulf	6 Est Prop Av		
25	63-189 65-26	20.9 18.5	20.2-21.7 17.3-19.1	17.3-19.1	19.5	sulf vn " -asp+py in se- parate veinlets	asp, py po, ccp
26	63-188 64-26 64-27	10.7 21.1 18.7	7.5-12.7 20.0-21.9 18.1-20.0	10.0-12.7 20.0-21.9 18.1-20.0	20.0	sulf vn (poor sample) sulf vn "	asp, ccp, py po, ccp, py?, asp po, py, ccp, asp
28	64-30	21.8	20.7-23.4	20.7-23.4 ⁷⁾	21.8	"	py, asp
29	65-14	20.25	19.0-21.0		20.3	"	py, asp
30	65-22 65-23 65-24 65-25	20.4 20.2 18.2 20.7	19.7-20.9 19.5-21.1 17.9-18.7 19.8-21.4		19.7	" " " "	asp asp, ccp, po, py asp, ccp asp
31	65-21	16.7	15.0-20.0	15.0-20.0	16.7	"	asp, py, ccp
32	65-13	16.8	16.2-17.6	16.2-17.6	17.0	"	gn, py, asp, ccp
33	63-28 64-2 64-3 64-34	18.2 14.8 16.9 16.8	12.5-20.0 9.7-19.7 14.0-18.1 16.2-17.5	12.5-20.0 ? -19.7 ? -18.1 16.2-17.5	16.5	" " " "	py, asp, ccp, gn, bo? asp, gn asp, gn, cpy, py asp, gn, cpy, py
34	64-17 64-21 64-154C 64-154D 64-154E 64-155 64-155C 64-155D	23.5 19.0 18.8 18.8 18.5 18.2 17.7 15.1	21.9-25.0 18.7-19.6 18.0-19.7 18.2-19.5 18.3-19.3 17.6-18.7 16.9-18.1 8.1-16.9	21.9-25.0 18.7-19.6 18.0-19.7 18.2-19.5 17.6-18.7 16.9-18.1	18.5	" " " " " " " -h s d sp " -h s d sp	py, gn, po py, gn, asp, ccp py, asp py, asp py, asp gn, asp, ccp, py gn, asp, py, ccp gn
35	64-5	18.7	18.2-19.4		18.5	"	asp, py, gn, ccp
36	63-26 65-32A 65-32B 65-33	18.5 7.1 15.3 24.7	15.4-20.7 0.4- 7.6 13.1-19.0 19.2-27.8	? -20.7 ? -19.0	15.0	" " -h s m sp " -h s d sp "	asp, gn, ccp, py asp, gn, py, ccp asp, gn, py, ccp asp, gn, po
37	63-36 65-34A 65-34B	17.3 5.2 11.7	14.6-22.5 0.5-10.3 9.7-13.5	? -22.5	10.0	" " -h s m sp " -h s d sp	asp, ccp, gn, py gn, asp, ccp gn, asp, ccp
38	65-30 65-31A 65-31B 65-31C	14.4 1.2 6.6 11.7	13.7-15.0 1.0- 1.4 0.7-15.7 6.9-16.7		13.0	" " -h s l sp " -h s m sp " -h s d sp	gn, ccp, bo, asp gn, asp, ccp, bo gn, asp, ccp, bo gn, asp, ccp, bo
39	64-6	16.0	13.2-18.6	13.2-18.6	16.5	"	asp, py, gn, ccp
40	64-7 64-152C 64-152D 64-152A 64-157A 64-157B 65-38 65-39 65-40A 65-40B	16.8 11.0 9.0 0.7 10.3 15.0 15.3 9.7 14.4	16.0-17.5 10.6-15.1 5.4-10.7 0.1- 3.7 9.2-11.5 7.5-19.3 12.8-16.2 3.7-17.9 11.7-16.0	16.0-17.5 ? -11.5	14.0	" " -h s d sp " -h s m sp " -h s m sp " -h s d sp " " " -h s m sp " -h s d sp	asp, py, gn, ccp asp, py asp, py py, asp py, asp gn, asp gn gn, asp gn, asp
41	64-10	7.4	2.8-17.8	? -17.8	7.4	carb vn	py, gn, asp, ccp
42	63-176	18.3	3.9-18.9		18.3	carb-sulf veinlets	gn, py

Table 13 - continued

1 Prop No	2 Sample No	Mole % FeS				7 Occurrence	8 Main Assoc Ore Minerals in Sample
		3 Sample Av	4 Observed Range	5 Adjacent Fe Sulf	6 Est Prop. Av		
43	63-174	14.1	4.7-21.1	7 -21.1	8.0	carb-sulf veinlets	gn, ccp, py, asp
	65-61	5.7	3.7- 7.8			gn, ccp, py	
	65-62	9.9	5.2-15.8				
	65-63	5.6	3.3- 9.5			gn, ccp, py, bo?	
45	65-134	5.2	1.8-11.0		5.2	sulf veinlet	
48	64-117	20.8	19.7-21.4	19.7-21.4	10.0	sulf vn	asp, py, ccp, gn
	65-107A	1.0	0.7- 1.6	0.7- 1.6		-h s l sp	gn, ccp
	64-107B	1.7	1.1- 2.4			-h s l sp	gn, ccp
	65-107C	2.3	1.0- 5.7			-h s m sp	gn, ccp
	65-108	9.7	7.5-12.7				gn, ccp
	65-109C	3.5	3.2- 4.9			-large xtl	gn, ccp
	65-109F	8.4	6.9-10.5			-large xtl	gn, ccp
	65-109G	8.0	7.3-10.1			-large xtl	gn, ccp
	66-80A	1.9	1.2- 2.2			-h s l sp	ccp, gn, po
	66-80B	2.4	1.2- 4.0			-h s m sp	ccp, gn, po
	66-80C	15.9	14.8-17.3			-h s d sp	ccp, gn, po
	66-80D	19.7	18.1-21.7	18.1-21.7		not adj po	ccp, gn, po
	49	63-213	17.9	17.5-18.5		17.5-18.5	18.5
64-110A		0.8	0.6- 1.0		adj po	po, py, asp, ccp	
64-110B		19.1	18.1-19.5	18.1-19.5	repl body in lm	po, py, asp, ccp	
64-111		19.3	18.1-21.0	18.1-21.0	-h s l sp	po, py, asp, ccp	
65-92		15.8	14.2-18.5		-h s d sp	gn, ccp	
65-129		17.7	16.7-18.5	16.7-18.5	sulf vn	py	
65-130		18.2	18.0-19.5	18.0-19.5	repl body in lm	py, po, ccp	
66-83		18.7	18.3-19.4	18.3-19.4		po, py, gn, ccp, asp	
DDH1		18.2	16.8-19.3	16.8-19.3	sulf vn	py, po, asp, gn	
DDH2		18.6	11.3-18.9	18.0-18.9	repl body in lm	py, asp, po	
DDH4A		17.9	17.2-18.9	17.2-18.9		po, py	
DDH4B		19.2	18.8-19.6	18.8-19.6	sulf vn	po, py, asp, ccp	
DDH7		18.3	18.1-18.5	18.1-18.5	repl body in lm	po, py	
DDH8		18.3	17.7-18.5	17.7-18.5		po, py, ccp	
DDH15		18.6	17.4-19.4	17.4-19.4		py, po	
DDHU4	18.2	16.2-19.3	16.2-19.3		gn, py, po		
50	65-101	20.0	18.3-20.5	18.3-20.5	20.0	sulf vn	po, py, asp, ccp, gn
51	65-121	19.6	19.1-20.0	19.1-20.0	19.5	"	asp, po, py, ccp
52	65-85	17.2	16.0-18.2	16.0-18.2	17.2	"	asp, po, py, ccp, gn
58	65-91	3.0	0.2- 6.2		3.0	"	tn, ccp
59	65-104	9.4	6.9-13.7	7 -23.7	7.0	"	py, gn
	65-105	4.7	0.1-11.7			"	py, gn, asp

Abbreviations - adj - adjacent; asp - arsenopyrite; bm - bismuthite; bo - bournonite; carb - carbonate; ccp - chalcopyrite; dep - deposit; est - estimate; Fe - iron; frag - fragments; gn - galena; h s d sp - hand-sorted dark sphalerite; h s l sp - hand-sorted light sphalerite; h s m sp - hand-sorted medium sphalerite; lm - limestone; meta - metamorphic; min - mineral; mo - molybdenite; Mo - Molybdenum; ms - marcasite; no - number; po - pyrrhotite; prop - property; py - pyrite; qtz - quartz; repl - replacement; rk - rock; shee - scheelite; sp - sphalerite; sulf - sulfide; td - tetrahedrite; tn - tennantite; ty - tetradymite; vn - vein; W - tungsten; xtl - crystal

- 1) Many samples have pronounced bimodal and even polymodal distributions. Hence, the average may not be very representative.
- 2) In many samples the range is controlled by one or two erratic values.
- 3) Column 5 is given to aid in evaluation of the phase relations in the Fe-Zn-S system. However, it is not necessarily implied that the sphalerites with the compositions cited were in equilibrium with the associated iron sulfides.
- 4) This was the value used in the statistical study. It is probably within 0.5-3.0 mole per cent of the actual value for most properties, but in deposits containing abundant strongly zoned sphalerite the estimate could be off by as much as 5 mole per cent. The value given in this column was usually tempered by the writer's knowledge of the deposits and the samples.
- 5) These sphalerites, although occurring in the molybdenum deposit, were not directly related to molybdenite deposition.
- 6) Quartz and carbonate minerals are important gangue minerals in the sulfide veins.
- 7) A few small pyrrhotite inclusions were found in the pyrite. Possibly the sphalerite crystallized in equilibrium with pyrrhotite that was later replaced by pyrite.
- 8) The FeS content drops to about 15 mole per cent about 100 microns from pyrrhotite contact.
- 9) Most of the sphalerite in this sample contains less than 1.5 mole per cent FeS except for a few high erratic values near 24-25 mole per cent. As far as can be ascertained only low-iron sphalerite occurs near the pyrite.
- 10) Determined by x-ray techniques.
- 11) University of Wisconsin Economic Geology Collection number.

out by Williams (1965). Skinner (1961) has shown minor amounts of cadmium and manganese have a profound effect on determination of the iron by this method. For instance, the writer measured the cell dimensions of about fifty sphalerite samples from the Hudson Bay Mountain district using an x-ray diffractometer and NaCl as an internal standard. It was found that if no corrections were made for cadmium or manganese the iron content determined by x-ray diffraction was generally 5 to 8 mole per cent higher than that determined by the microprobe. The deviation was usually greater the higher the iron content of the sample. This deviation is what would be expected from the known cadmium and manganese contents of the samples.

The microprobe determinations of cadmium and manganese were, in general, in agreement with the values cited in the chemical analyses in Table 11.

Boyle and Jambor (1963, p. 488) suggest that arsenic may substitute for sulfur in sphalerite lattice. Since arsenic is abundant (in arsenopyrite) in the Hudson Bay Mountain district, the writer thought that this would offer an excellent opportunity to see if arsenic does in fact enter the sphalerite structure. Of the ten samples tested for arsenic none gave counts significantly above background. Since the exact detection limits were not determined it can only be concluded that the arsenic content is probably less than a few hundredths of one per cent.

Copper was also analyzed for in the same samples as the arsenic. In all the samples tested it was found to be low, probably less than .01 per cent, but distinctly above background. This is in good agreement with the findings of Toulmin (1961) and Sims and Barton (1961). High-iron sphalerite samples were tested both away from and near lamellae of chalcopyrite. No significant difference was found. This evidence plus the fact that most of the intergrown chalcopyrite blebs occur along grain boundaries lend support to Toulmin's contention that sphalerite cannot take sufficient copper into solid solution to permit a significant amount of chalcopyrite exsolution. The oriented nature of the chalcopyrite blebs has been explained by Toulmin (1961) and Sims and Barton (1961) to be the result of epitaxial crystal growth. Of course the possibility remains that initial solid solution copper completely exsolved as chalcopyrite in the natural environment, leaving no evidence of its former solid solution. Heating experiments could be used to test this possibility. It should also be pointed out that no copper values approaching those reported in the wet chemical analyses were found. This is further evidence that the copper found by wet chemical analysis occurs actually as intergrown chalcopyrite.

District-wide Variations in the FeS Content of Sphalerite

The average FeS content of sphalerite from most deposits in the district lies between 5 and 30 mole per cent. Therefore, all sphalerites of the district have formed at activities of sulfur and temperatures somewhere in the band about the pyrite-pyrrhotite solvus shown in Figure 43. From Barton and Toulmin's data (1966) this interval corresponds to activities of FeS in the range 0.1 to 0.7. Although this only sets very broad limits on the conditions of sphalerite formation, it serves to establish a general framework within which various possible conditions of formation can be considered.

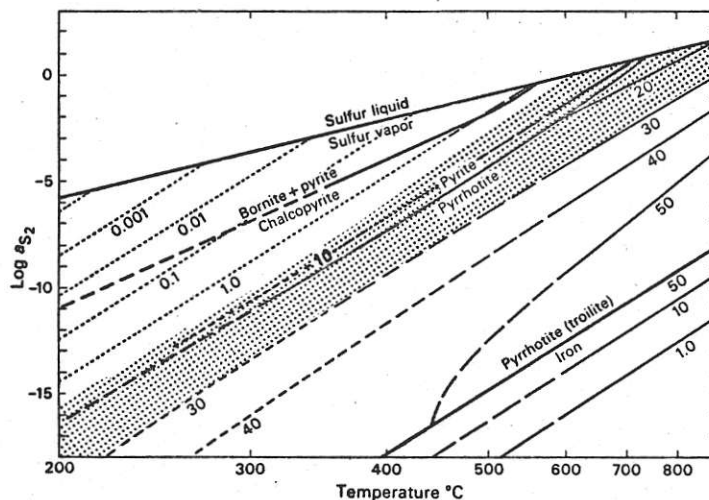
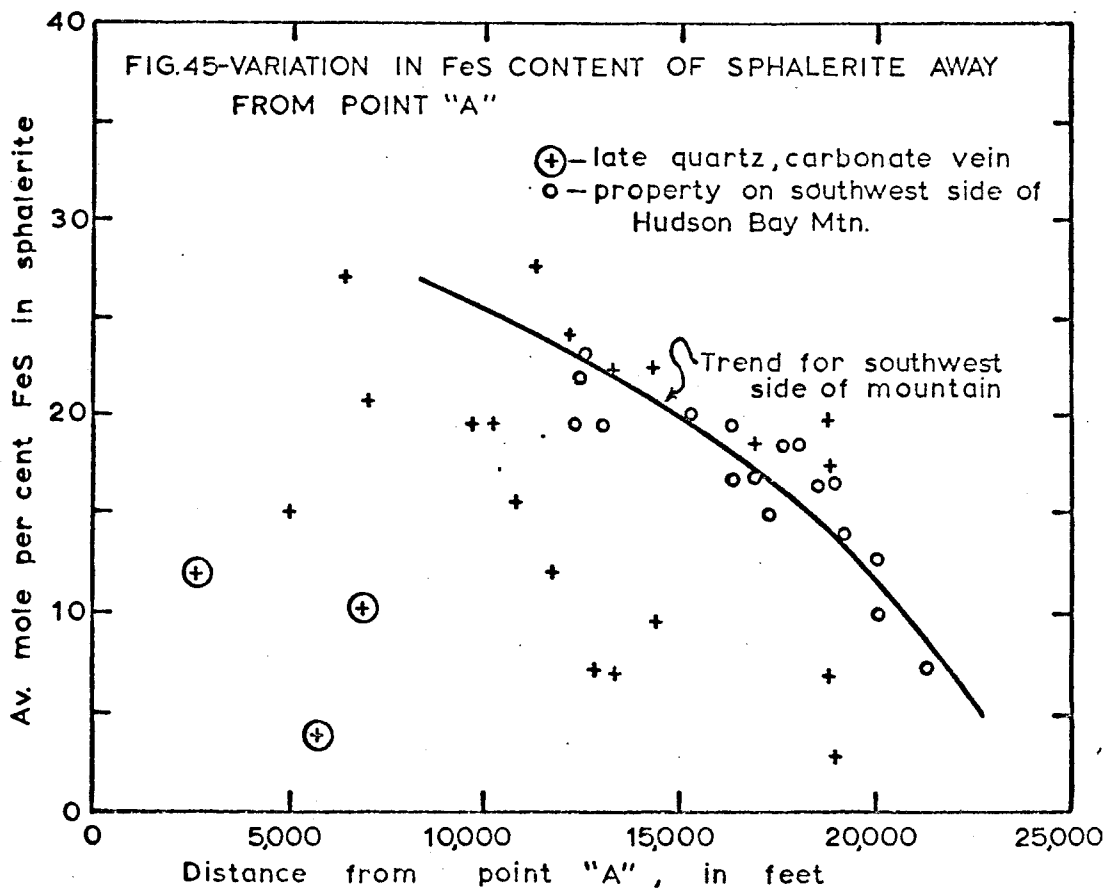
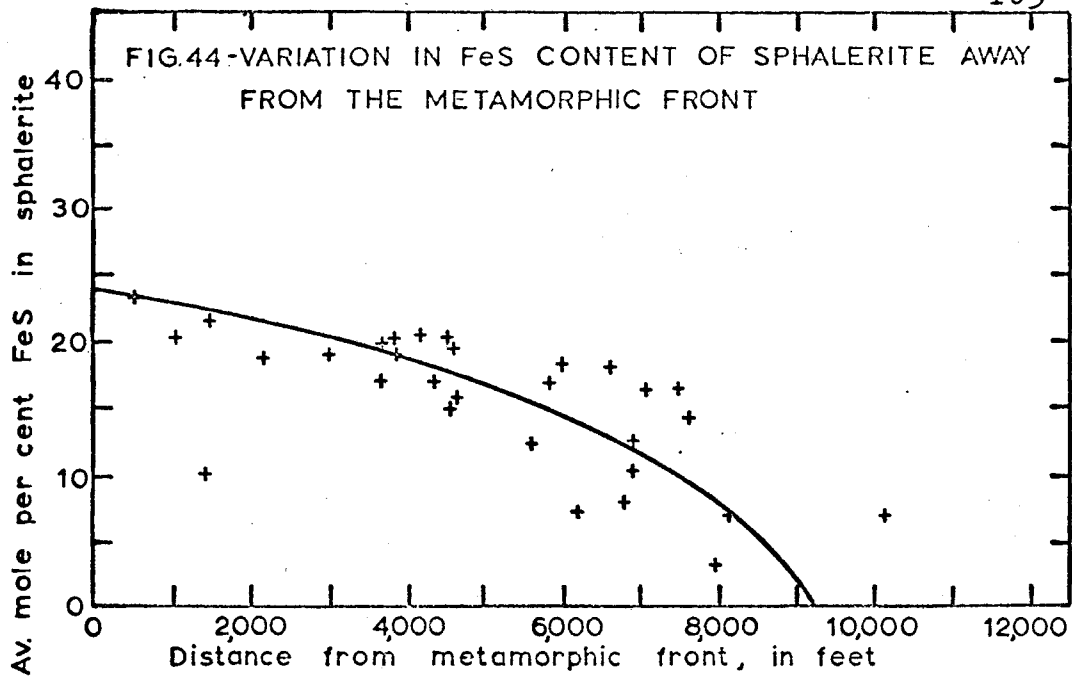
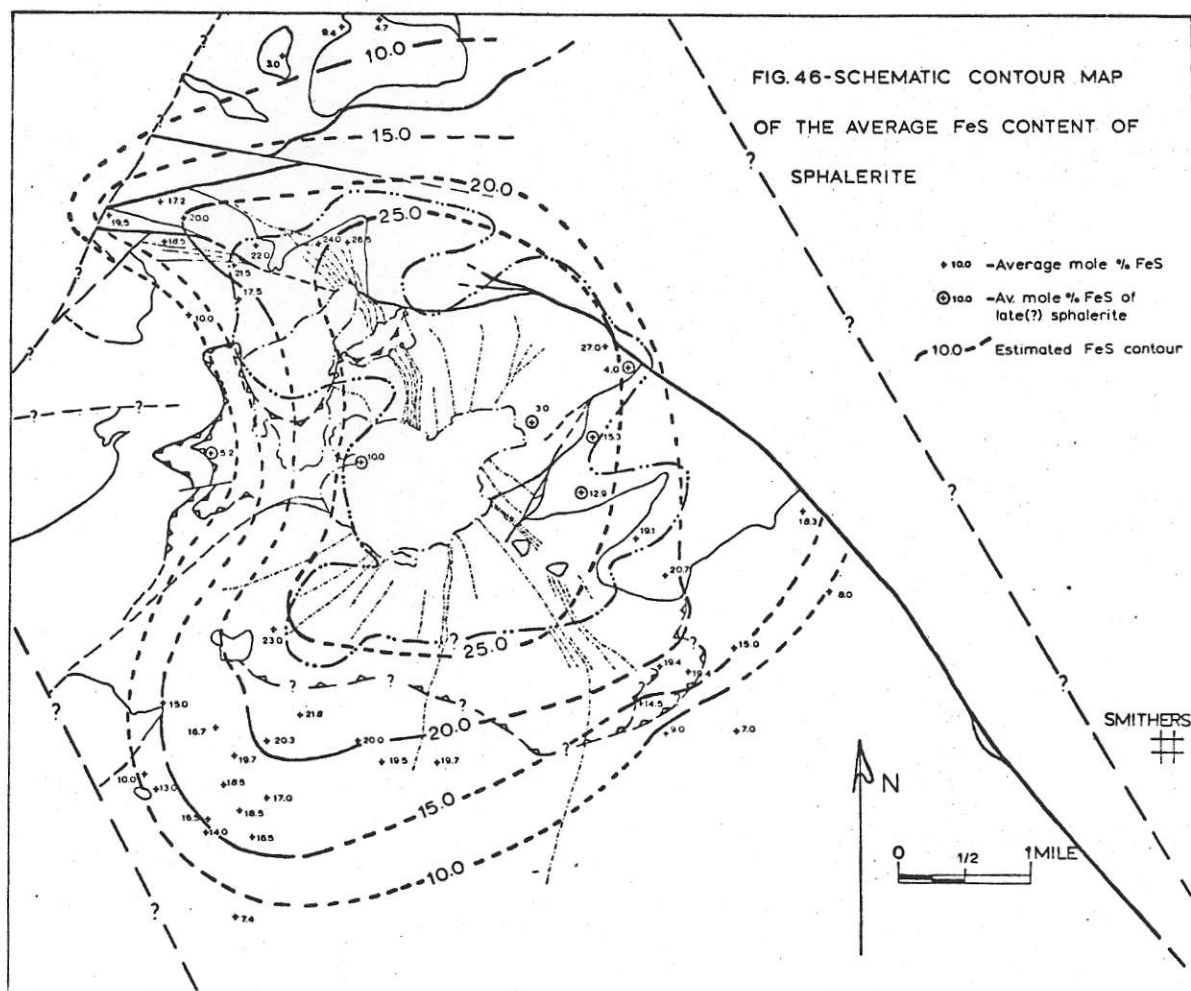


Fig. 43 - FeS contents of sphalerites in mole per cent contoured on an activity of S_2 -temperature plane. The sulfur liquid + sulfur vapor, bornite + pyrite + chalcocopyrite, pyrite + pyrrhotite and pyrrhotite + iron buffer curves are plotted for reference. (modified slightly from Barton & Toulmin, 1966, using Boorman's data, 1967)-Shaded area shows possible range of H.B.Mtn. sphalerite-bearing ores.

The sphalerite adjacent to pyrrhotite in sample 66-76 from the scheelite-rich quartz vein near the outer limit of the molybdenum deposit may be of use in geothermometry. This was the lowest iron content (17.0-17.8%) found immediately adjacent to pyrrhotite. If, as Boorman (1967) contends, the sphalerite-pyrrhotite-pyrite curve in the Fe-Zn-S system does not reverse its slope below 500°C, then from Barton and Toulmin's data (1966) it is apparent that if the sphalerite crystallized in equilibrium with the pyrrhotite, it probably formed above 600°C. The possibility of high pressures causes some uncertainty in this estimate.

Figures 44, 45, and 46 show that there is a reasonably systematic variation in the FeS content of sphalerite in the Hudson Bay Mountain district. It should be noted, however, that most of the sphalerite was collected from sulfide deposits; hence the variations discussed are mainly restricted to variations in these ores. By comparing Figure 12 with 46 and Figures 16 to 23 with Figure 44 it can be seen that the variation of FeS approximately parallels the general zonal distribution of ores in the district. This lends support to the conclusion that the underlying causes for both are directly or indirectly related. Barton and Toulmin (1966) have pointed out that the iron content of sphalerite is primarily a function of the activity of FeS which is dependent on the activity of sulfur and temperature. Therefore, either variations in the activity of sulfur and temperature were responsible for the zoning or else parameters that did not vary





independently from the activity of sulfur and temperature were responsible for the zonal distribution of the sulfide ores.

The regularity of the district-wide pattern of the FeS content of sphalerite (Figures 44 and 46) suggests that spatial variations were more important than temporal variations in the sulfide ores. The heterogeneous nature of individual sphalerites, nevertheless, indicates that there were some temporal variations in ore deposition. Marked temporal changes, such as those described by Sawkins (1964)

for the Providencia district in Mexico, were volumetrically, apparently not very important.

Early in the study of the district the writer became aware that the sulfide ores seemed to show a closer relationship to the metamorphic aureole than to the molybdenum deposit. To test this possibility the FeS content of sphalerite was plotted as functions of distance from both (Figures 44 and 45). It is readily apparent that the FeS content of sphalerite is, in fact, more closely related to the metamorphic front than to the molybdenum deposit (point "A"). The trend shown in Figure 45 is for sphalerites from the southwest side of Hudson Bay Mountain. It could also simply reflect variation away from the metamorphic aureole.

In some manner the metamorphic aureole must be related to the compositional variations of sphalerite. It is most reasonable to consider that at the time of sphalerite deposition in the sulfide ores, the metamorphic aureole was still at elevated temperatures. The resulting regional thermal-hydrothermal regime, with its physicochemical gradients was conceivably responsible for district-wide zonation of sphalerite and the sulfide ores. The fact that the molybdenum deposition at least in part followed the metamorphism (p. 16) and the zonation is not primarily a function of distance from the molybdenum deposit, supports the contention that the molybdenum deposit was formed later in the magmatic history of the area.

Arsenopyrite

Distribution and Description

Arsenopyrite is widespread in the district. It is probably the most abundant ore mineral in the intermediate zone and inner part of the outer zone. It is less predominant near the periphery of the outer zone where low-iron sphalerite is abundant. Arsenopyrite is virtually absent in the molybdenum deposit. 65-144 was the only sample in which molybdenite and arsenopyrite were observed together.

Arsenopyrite in many ores is closely associated with quartz. Although in part it replaces quartz and wall rock it seems to have been mostly deposited with quartz. Some deposits contain cockade layers of quartz and arsenopyrite around breccia fragments of wall rock. Both fine and coarse-grained crystals are common, and in some deposits terminated crystals of arsenopyrite occur with clear euhedral quartz crystals in vugs. In the Dome vein there are terminated arsenopyrite crystals up to $\frac{1}{2}$ inch in diameter.

From microscopic textural relations arsenopyrite appears to have been deposited relatively early. It was veined and partially replaced by most other ore and gangue minerals. In polished surfaces etched with nitric acid, arsenopyrite displays very complex twinning (Figure 47) and possibly intergrowth patterns. The twinning makes it difficult to establish the presence or absence of well developed growth zoning. Nevertheless, growth zoning was observed in a few crystals (Figure 48).



Figure 47 - Twinned arsenopyrite crystals veined by pyrrhotite (light gray), chalcopyrite (slightly darker gray) and quartz (dark gray). Specimen (65-85) is from property no. 52. Surface was etched with nitric acid. Mag. 100x.

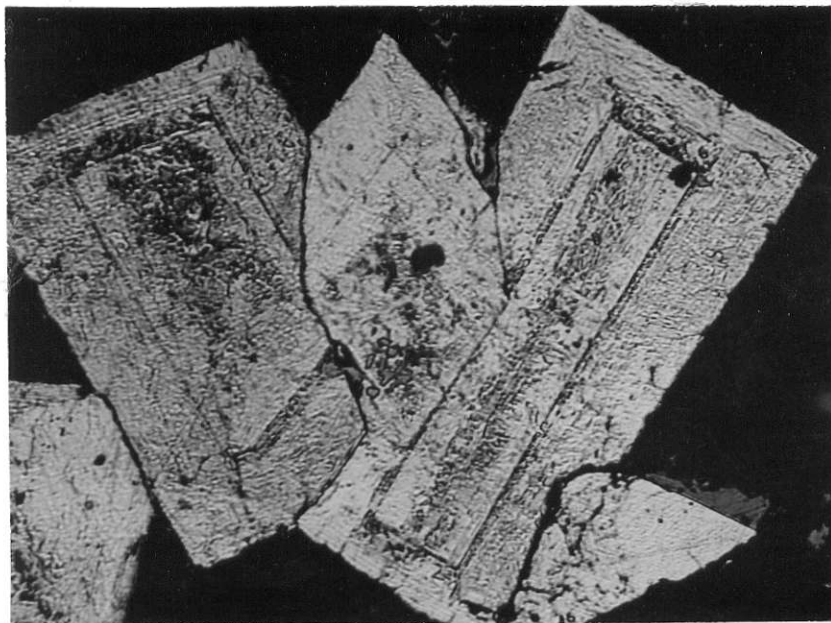


Figure 48 - Zoned arsenopyrite crystals from the Iron Vault property. Surface was etched with nitric acid. Mag. 150x.

Arsenopyrite geothermometer-geobarometer

Clark (1960a, 1960b) studied in detail portions of the Fe-As-S system which are of geologic interest. He suggested that arsenopyrite may be useful as a geobarometer and/or geothermometer. In view of this it is surprising that so little subsequent work has been done on arsenopyrite field relations or in the Fe-As-S system. Because of our lack of knowledge on the applicability of the experimental studies to natural systems, it is still not possible to use arsenopyrite relations with confidence in geobarometry or geothermometry. At present the best one can do is to see if arsenopyrite relations are compatible with other features of the geology. If, however, subsequent work shows that arsenopyrite can be used to determine the PT conditions of ore formation, then its importance cannot be overemphasized. For instance, if it becomes possible to determine the temperature of mineral formation to $\pm 5^{\circ}\text{C}$ using oxygen isotopes (Taylor, 1967), the composition of arsenopyrite should be the best pressure indicator available for ore studies.

The slow reaction rates of arsenopyrite in the solid state (Clark, 1960a & b, Barton, et. al., 1963, and Skinner and Barton, 1967) increase its potential usefulness in geothermometry and geobarometry, but they have also made it very difficult to study arsenopyrite in the laboratory. Clark (1960a & b), for instance, was only able to approach equilibrium from one direction. It should also be pointed out that he used rigid silica glass tubes for his initial studies and encountered vapor in all runs.

Bulk compositions could have been affected to some extent, since some elements, such as As and S, would be differentially partitioned in the vapor phase. Moreover, since vapor could not be avoided, pressures would vary, making it only possible to determine the supposed "condensed system" (see Kullerud and Yoder, 1959) which does not truly represent the phase relations.¹ Without further work in the Fe-As-S system it is hazardous to rely too heavily on Clark's findings.

Chemical Analyses

Four arsenopyrites to be used as standards for x-ray and microprobe analyses were chemically analyzed. Clark (1960a & b) and Morimoto and Clark (1961) have shown that the $d_{(131)}$ spacing of arsenopyrite is a function of the As/S ratio. They state that provided the combined minor element content is less than one per cent, the composition can be determined to within one atomic per cent. The four analyzed samples were used to check their findings.

The samples for analysis were hand picked under a binocular microscope. Polished sections were used to determine the presence or absence of internal impurities. Many samples that seemed megascopically satisfactory were rejected because of numerous, microscopic veinlets of other minerals. Sample 65-144 was etched with FeCl_3 and x-rayed to determine whether

¹ Clark was aware of these problems.

or not it contained any loellingite contamination. As might be expected from the chemical analysis, none was found. Some quartz contamination was noted in samples 64-2 and 65-21, and minor chalcopyrite was noted in sample 65-21. Otherwise no other impurities were recognized.

The following is a brief description of the wet chemical analytical technique:

Arsenic. Sample was decomposed with $K_2SO_4 + H_2SO_4$ and arsenic was distilled as the trichloride, which was titrated with a standard $KBrO_3$ solution using methyl orange as the end-point indicator. Analysis by R.S. Young.

Sulfur. Sample was dissolved with a mixture of KBr and Br_2 , and the resulting sulfate was precipitated with $BaCl_2$ and weighed as $BaSO_4$. Analysis by R.S. Young.

Iron. Sample was dissolved with HCl and Br_2 , interfering elements were removed and iron was titrated with a standard $K_2Cr_2O_7$ solution using diphenylamine sulfonic acid as the end-point indicator. Analysis by R.S. Young.

Nickel. After solution, nickel was extracted as nickel dimethyl-glyoxime into chloroform, and the absorbancy was measured on a Beckman spectrophotometer. Analysis by S. Metcalfe.

Cobalt. After solution of the sample and removal of interfering elements, the nitroso-R-salt method was applied, and the absorbancy was measured on a Beckman spectrophotometer. Analysis by R.S. Young.

Copper and Bismuth. Analysis by R.J. Hibberson using an A.R.L. Spectrograph.

Antimony. Analysis by N.G. Colvin using Phillips x-ray fluorescence equipment.

The results of the analyses are shown in Table 14.

Table 14 - Chemical Analyses of Arsenopyrite Standards

	64-2		64-39B		65-21		65-144	
	a	b	a	b	a	b	a	b
Fe	34.88	35.39	34.80	35.52	34.45	34.60	33.85	33.88
S	21.68	22.00	21.29	21.73	21.30	21.39	19.08	10.09
As	41.92	42.54	41.81	42.68	43.76	43.94	46.94	46.98
Sb	0.07	0.07	0.07	0.07	0.07	0.07	0.04	0.04
Bi	n.d.	-	n.d.	-	0.002	-	0.01	0.01
Co	trace	-	trace	-	0.0011	-	0.0042	-
Ni	trace	-	trace	-	0.0021	-	0.0011	-
Cu	-	-	-	-	0.04	-	0.015	-
Totals	98.55	100.00	97.97	100.00	99.625	100.00	99.94	100.00

- done by the Analytical Branch of the British Columbia Department of Mines

a - chemical analysis

b - recalculated assuming Fe+S+As+Sb+Bi+Co+Ni = 100 weight per cent

- a second sample from specimen 65-144 was found to contain 46.90 per cent As

- n.d. = not detected

X-Ray Analyses

The x-ray analyses were carried out using a Norelco diffractometer. CuK_{α} radiation at 35 KeV and 18 MA was used with four degree slits and a scanning speed of $\frac{1}{4}$ degree 2θ per minute. Chart speed was $\frac{1}{2}$ degree 2θ per inch. A natural fluorite with cell dimension of $5.4630^{\pm} .0003 \text{ \AA}$ (R. Thorpe, personal communication) was used as an internal standard. Five to ten oscillations were made over the (311) and (131) peaks of fluorite and arsenopyrite, respectively. ΔK_{α} , (131)-(311) and ΔK_{α} , were measured to closest .005 degree 2θ (that is, .01 inches). The average of all measurements was used

to determine the $d_{(131)}$ spacing to approximately $\pm .0004$ Ångstrom units. This variation is equivalent to about ± 0.4 atomic per cent arsenic.

The results are shown in Figure 49 and Table 15.

Table 15 - Summary of X-ray Data for Arsenopyrite

Prop. No.	Sample No.	$d_{(131)}$	Indicated Atomic % As ($\pm 1\sigma$) ¹⁾	Main Assoc. Ore Minerals in Sample ²⁾	Indicated P.T. Limits ³⁾
1	65-144	1.6332-1.6338	33.25-33.9	mo, py?	
2	65-71	1.63087	30.9	sp, ccp, bo-no nearby	
4	65-66	1.6331	33.15	sp, py-po nearby	0-1000 bars < 450° C
5	65-74	1.63235	32.4	po, ccp	>1400 bars > 500° C
8	65-41	1.63095	31.0	sp, po	
10	64-58	1.63112	31.2	sp, py, ccp-ms+po nearby	
11	65-117	1.63112	31.2	sp+po nearby	
12	64-43	1.63124	31.8	ccp-po nearby	
16	65-20	1.6316	31.6	po, sp, ccp	> 2200 bars > 520° C
17	65-64	1.6312	31.2	sp, ccp, py	
18	64-39	1.6305	30.5	py, sp, gn, ccp	> 500 bars 470° C ⁴⁾
19	63-181		31.0 ⁵⁾	sp, py, gn	0-2000 bars > 320°-500° C ⁴⁾
20	65-113	1.6303	30.3	py, gn, sp	
27	64-28	1.6326	32.65 32.1 -33.25		
28	64-30	1.63167	31.7	py, sp	< 2200 bars 360°-420° C
30	65-23, 65-25	1.63098 1.63112	31.0 31.2	sp, ccp, po, py sp	
31	65-21	1.6305	30.5	sp, py, ccp	> 400 bars < 470° C
33	64-2	1.63042	30.4	sp, gn-ccp, py nearby	> 500 bars < 470° C ⁴⁾
51	65-121	1.63087	30.9	po, sp, py, ccp	0-2000 bars 310°-520° C
52	65-85	1.6310	31.0	po, py, ccp, sp, gn	0-2000 bars 320°-520° C ⁴⁾
55	64-48	1.6320	32.0	ccp	

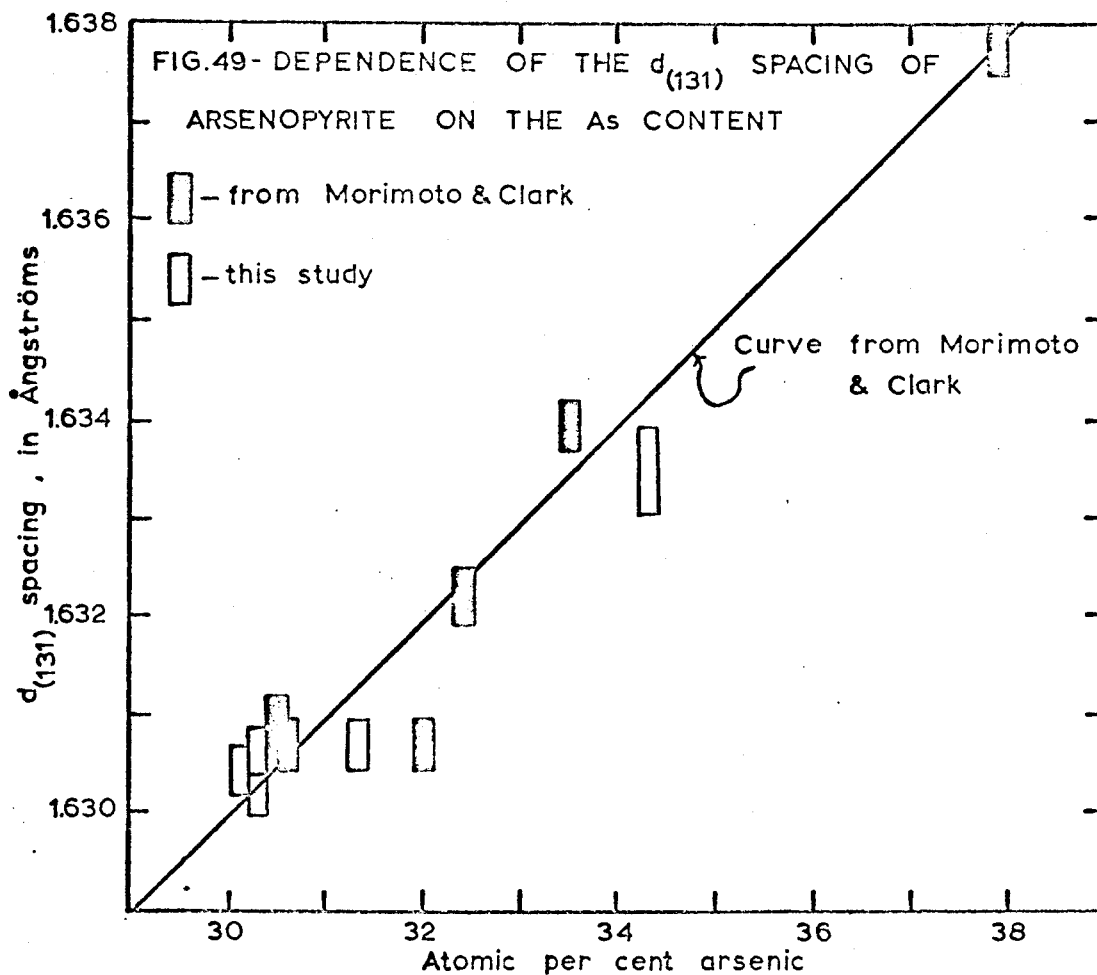
1)-from the relationship $d_{131} = 1.6006 + 0.0098x$, after Morimoto and Clark, 1961
-x is the atomic per cent arsenic (the equation is misprinted in the original paper)

2)-abbreviations same as Table 13,
-Underlined iron sulfides are intimately intergrown with the arsenopyrite.

3) The assumption has been made that the arsenopyrite in question crystallized in equilibrium with the associated iron sulfides.

4) -for reasonable pressures

5) -electron microprobe analysis



Discussion of the Results

From Table 14 it is apparent that samples 64-2, 64-39B, and 65-21 have very similar compositions and only sample 65-144 is significantly different. The deficiency in the analyses of 64-2 and 64-39B is most probably due mainly to quartz contamination.

It can be seen that the Hudson Bay Mountain arsenopyrites are remarkably low in minor elements. It is improbable that any samples studied contain more than 0.1% combined trace elements.

Sample 65-144 has a significantly higher arsenic content than would be predicted by Morimoto's and Clark's (1961) equation: $d_{131} = 1.6006 + 0.00098x$, where x is the atomic per cent arsenic (Figure 49). This, plus the fact that Morimoto and Clark have little control for their curve at higher arsenic values, prompted the writer to check and recheck this $d_{(131)}$ determination. A second sample submitted for arsenic analysis showed a difference of only .04%. Polished surfaces showed no arsenic-bearing impurities. The cell dimension of the fluorite standard was checked on the diffractometer using NaCl ($a_0 = 5.64028\text{\AA}$) as an internal standard. It was found to be $5.4631 \pm .0004\text{\AA}$ which is within the limits given by Thorpe. A complete diffractogram was made of the arsenopyrite to check its structure against the structure of samples studied by Morimoto and Clark. It was found that 65-144 arsenopyrite has features intermediate between the synthetic and Freiberg arsenopyrites (Fig. 1 of Morimoto and Clark). Most of the peaks are very similar to those of the Freiberg arsenopyrite except that the $\bar{3}21, 202$ and $\bar{1}23$ reflections are not split.

Several runs on separately prepared samples were made on the diffractometer to determine the $d_{(131)}$ spacing. Although some variation was found, all runs gave arsenic values significantly below those indicated by chemical analyses.

The data are meager, but permit certain inferences. Morimoto and Clark used only five natural and one synthetic arsenopyrite to calibrate their curve; hence, their control is not much better than the writer's. The 65-144 arsenopyrite sample is remarkably free from contamination and is very low in minor elements.¹ However, it should be remembered that they state that this method is not overly sensitive--that is, it can only be used to determine the arsenic composition to within one atomic per cent. Since the overall range in arsenic content of natural arsenopyrites is only about 8 atomic per cent, this is not particularly good accuracy. Even if Morimoto and Clark's curve is slightly in error, x-ray determined compositions should still be acceptable for the study of arsenopyrite phase relations, since Clark (1960a & b) used the x-ray spacing method in his experimental studies. However, in the future it will probably be important to know the position of this curve more accurately when the electron microprobe and possibly other techniques are used to determine arsenopyrite compositions.

In this study, x-ray measurements of the $d_{(131)}$ spacing were in general fair, but some arsenopyrites gave very poor $d_{(131)}$ peaks. A $\pm .0004\text{\AA}$ deviation is a reasonable value for the precision of most measurements. Some 131 peaks, nevertheless, are very broad and only an average "composition" could be determined. It is possible that this

¹ Some of the samples studied by Morimoto and Clark contain significant amounts of minor elements.

broadening is due to zoning. Some compositional variations were noted in microprobe analyses but regular zonal patterns have not been verified.

Reasonable ranges of PT conditions for arsenopyrite intimately associated with iron sulfides are given in Table 15. Ranges were only estimated for these samples because there is no just reason to expect that the other arsenopyrites had obtained equilibrium with a particular iron sulfide. Even intimate intergrowth is not conclusive evidence that these minerals crystallized in equilibrium, but it is the only criterion that is available.

It is very difficult to establish the exact paragenetic relations between pyrite and arsenopyrite. Many deposits contain abundant highly fractured and veined pyrite and arsenopyrite, indicating that these minerals probably had comparable histories. However, there is evidence to suggest that pyrite and arsenopyrite were also deposited during later episodes. For example terminated arsenopyrite and pyrite crystals in vugs are reasonably abundant and there are also arsenopyrite "veins?" that apparently cut other sulfides. Such an example is arsenopyrite in sample 65-41. In hand specimen it appears to be in a vein that cuts both sphalerite and pyrrhotite, but the high power of crystallization of arsenopyrite makes it difficult to evaluate this relationship under the microscope. It is significant, however, that this and other samples removed from the regression analysis

(Figure 50) do not contain the veinlets of other sulfides that are so numerous in arsenopyrite from other ores. Despite the lack of evidence on the exact depositional timing of these minerals, Clark's work (1960a & b) indicates that either the arsenopyrite and/or pyrite was formed below $491 \pm 12^\circ \text{C}^1$.

In all polished sections containing abundant intergrown arsenopyrite and pyrrhotite, the pyrrhotite veins and replace the arsenopyrite. Therefore, there is some doubt whether arsenopyrite crystallized in equilibrium with pyrrhotite. The district-wide distribution of pyrrhotite and pyrite suggests, however, that most of the arsenopyrite in the barren and intermediate zones probably crystallized in equilibrium with pyrrhotite rather than pyrite. Failing conclusive evidence for equilibrium of arsenopyrite with associated iron sulfides, it is still reasonable to expect that most if not all arsenopyrite of the district crystallized near its sulfur-rich limit (Clark, 1960).

District-wide Variations in the Composition of Arsenopyrite

Figure 50 shows the arsenic content of arsenopyrite plotted against the approximate distance from the metamorphic front. If samples 64-58, 65-41, 65-71, and 65-117 are removed, it is apparent that there is a reasonably systematic decrease in the arsenic content outwards in the district.

¹ This is at 1 bar. At higher pressures this temperature is slightly higher.

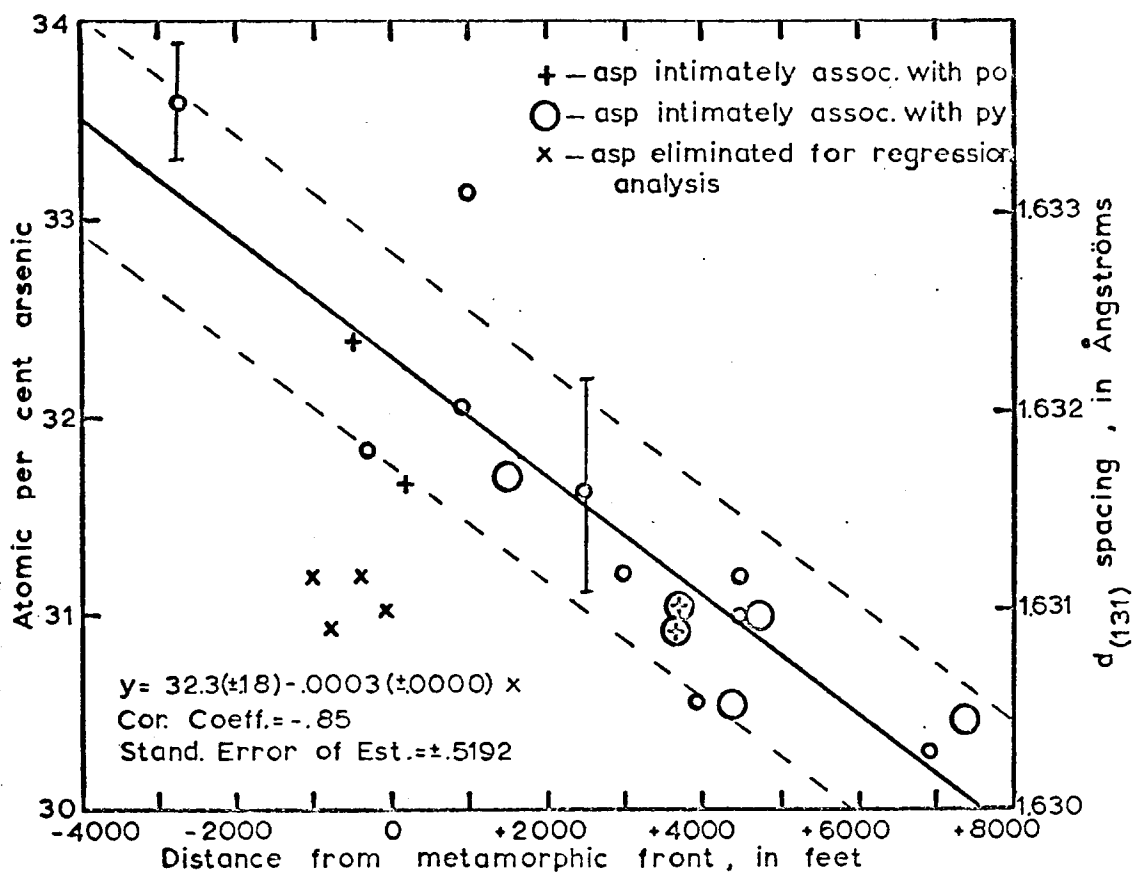


FIG. 50-VARIATION IN THE AS CONTENT OF ARSENOPIRYTE AWAY FROM THE METAMORPHIC FRONT

This variation at present seems most probably due to a decrease in temperature. Nevertheless, the change could reflect a decrease in lithostatic pressure systematically away from the center of the district, but this is unlikely since most of the deposits studied in the outer areas are at lower elevations than those in the inner zones. Another interesting possibility is that ore solutions decreased in pressure outwards because of successive zones of throttling. Determinations of the temperature of arsenopyrite deposition by some independent means would shed light on this possibility.

If one assumes that the decrease in arsenic content of arsenopyrite corresponds to a decrease in temperature, that the pressure was reasonably constant, and that most arsenopyrite crystallized near its sulfur-rich limit, from Figure 51 it is possible to evaluate the general PT conditions of the district. The transition from arsenopyrite (min. $d_{(131)}$ about 1.6320) in the intermediate zone associated with pyrrhotite without pyrite to arsenopyrite (max. $d_{(131)}$ about 1.6319) in the outer zone associated with pyrite with or without pyrrhotite might correspond to crossing of the arsenopyrite + pyrite + pyrrhotite + liquid univariant curve

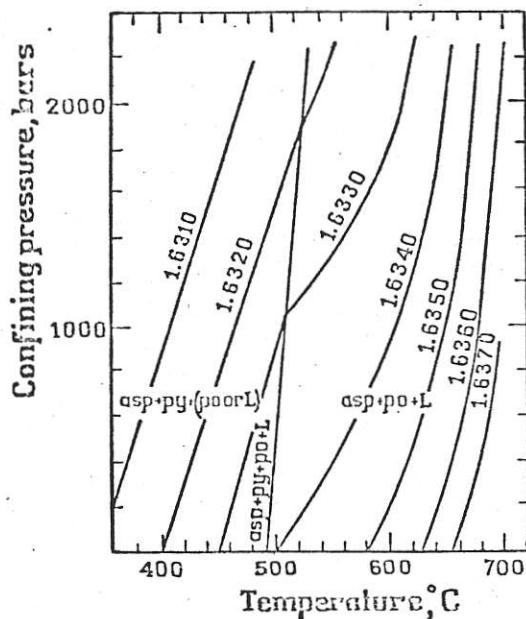


Fig. 51—Lines of constant 131 spacing, and As:S ratio, projected from the sulphur-rich P-T-X surface of the arsenopyrite stability field, and plotted as contours on the P-T projection. The upper stability curve of the pyrite-arsenopyrite assemblage (L. A. Clark, 1960 a) is also shown; the contour positions on the low-temperature side of this curve are approximate because pressure data were not obtained below 500°C. (After L. A. Clark, 1960 b).

in the Fe-As-S system. From Figure 51 it is apparent that the univariant curve would be crossed somewhere in the vicinity of 2000 bars. Most individual estimates of temperatures and pressures also indicate high pressures of formation (Table 15). For rocks with a density about 2.7, a lithostatic pressure of 2000 bars is equivalent to a depth of about 5 miles. Since rocks of the district have not been regionally metamorphosed above lowest greenschist facies, and since drusy cavities are common in many veins, such a pressure seems excessive. Because general geologic relationships do not seem compatible with deep burial, the writer is reluctant to accept such high pressures of formation. Nevertheless, it is interesting to entertain the possibility that ores of the district formed under high pressures.

Fluid Inclusions

An extensive search was made to find fluid inclusions suitable for geothermometry. Thermometric information gained from such inclusions would aid greatly in the interpretation of the sulfide relations. Many polished "thick" sections (slightly greater than 3 mm) were made of quartz and transparent sphalerite, but usable material was hard to find. The quartz studied was almost devoid of inclusions or had a maze of secondary inclusions. The sphalerite generally contained only very small, dark inclusions which were very difficult to see into because of total reflection from their walls. Moreover, since well developed growth

zoning is rare in either mineral, and since many of the inclusions are aligned along crystallographic planes that could not be related to crystal faces, primary inclusions could not be distinguished from secondary or "pseudo-secondary" inclusions (Roedder, 1965). Nevertheless, the writer feels that many inclusions, especially isolated ones, are probably primary.

Besides the limitations set by the nature of available material, the study was also hampered by problems in calibrating the heating stage. The main problem lay in the fact that the thermocouple used for temperature measurement conducted much more heat into the cell than did the air surrounding the sample. From metals and alloys with known melting points, it was determined that the thermocouple was generally from 10 to 60 degrees higher in temperature than the sample. Some samples that were placed close to the upper window of the cell, on the other hand, were actually lower in temperature than the thermocouple. The poor reproducibility of the results precluded accurate measurement of fluid inclusion filling temperatures.

Despite the severe limitations placed on this study, some significant discoveries were made. It was found that many of the inclusions in quartz from the molybdenum deposit contain daughter minerals. Transparent cubes, such as the one shown in Figure 52, are by far the most common. Since these cubes have relatively slow rates of solution on heating

it can be expected that they are NaCl rather than KCl. The presence of a salt daughter mineral indicates that the solution contained greater than 40 equivalent weight per cent NaCl (Roedder, 1965). This means that some of the ore solutions were very concentrated brines rather than relatively dilute hydrothermal solutions. The absence of daughter minerals in other inclusions, however, indicates variability in concentrations of the solutions. Roedder and Creel (1966) have noted similar brine-filled inclusions in quartz from Bingham, Utah, and Roedder (1967) states that very concentrated saline solutions are a characteristic feature of porphyry copper deposits.

Although most of the daughter minerals are cubes, transparent crystals with acicular and other habits have been observed. In one inclusion in quartz, there are small opaque specks, and in one in sphalerite from the Silver Creek property there is a cubic daughter mineral, presumably NaCl.

Most filling temperatures of inclusions in quartz from the molybdenum deposit were quite inconsistent and ranged from 120-250°C. For instance the filling temperature of the inclusion shown in Figure 52 was about 150°C. However, the daughter mineral persisted above 200°C. The writer cannot offer a satisfactory answer for this relationship. Even though it is obviously a very concentrated saline solution, a considerable pressure correction presumably has to be applied to the filling temperature to determine the actual

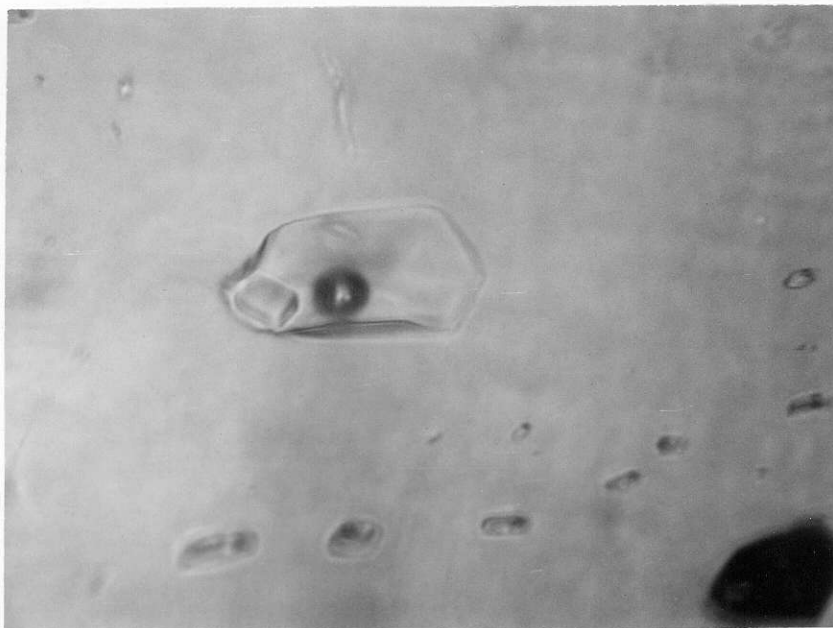


Figure 52 - Fluid inclusion with a sodium chloride daughter mineral. Quartz crystal (Sample 66-76) from scheelite-rich vein near the outer limit of molybdenum mineralization in Climax's exploration adit. Mag. 200x.

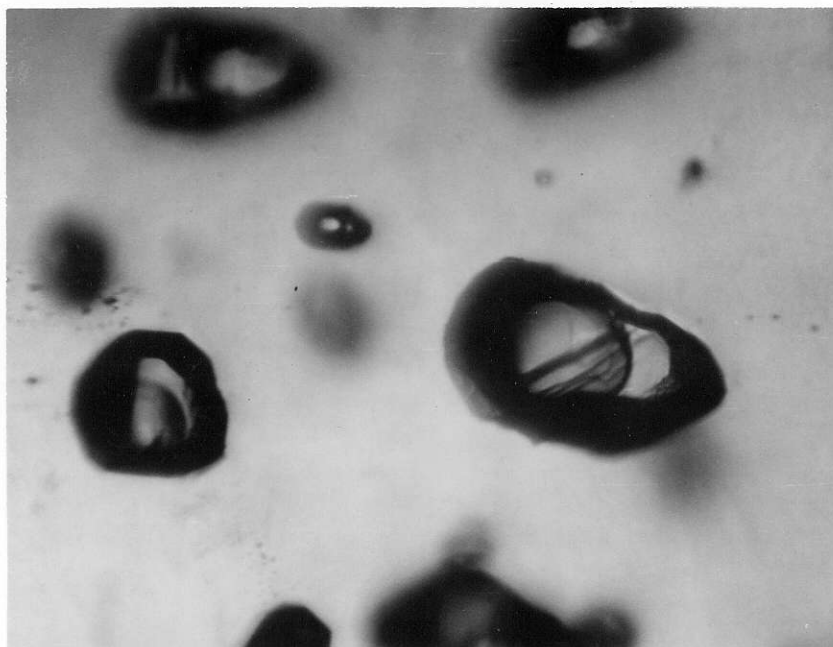


Figure 53 - Typical fluid inclusions in sphalerite from the Henderson vein (Sample 64-155D). Note large vapor bubbles. Mag. 700x.

temperature of formation.

Inclusions shown in Figure 53 are typical of some found in sphalerite from the outer and intermediate zones. Although filling temperatures of these inclusions were not measured, it can be expected that they would be considerably higher than those in quartz from the molybdenum deposit. Groups of these inclusions seem to have similar liquid/vapor ratios.

In some quartz crystals from the molybdenum deposit and from the sulfide veins, groups of inclusions contain highly variable liquid/vapor ratios, and some appear to be filled entirely by gas. This could be an indication that boiling occurred during ore deposition. However, this line of evidence is inconclusive since variable liquid/vapor ratios could also be the result of leakage or "necking-down" of large inclusions.

SOME THEORETICAL CONSIDERATIONS OF ORE GENESIS

The close spatial and temporal relationship of the ores to the Tertiary porphyries and to the metamorphic aureole presumably related to the Tertiary porphyries, leaves little doubt that the ores are genetically related to the porphyries. But many of the details of the relationship remain somewhat conjectural. For instance, although it is apparent that silicic magmas were the source of the heat or energy that drove the system, the exact nature and origin of the transporting media, the source of the sulfur, heavy metals, and gangue constituents, and the depositional controls are still in doubt. From the data at hand, however, it is possible to offer some answers to these important questions.

Pressure Estimates of Ore Formation

Besides partial pressures of volatile components, there are two main pressures, lithostatic and hydrostatic, to be considered in deducing conditions of ore formation. If the ore solutions were in contact with freely circulating groundwater then the pressure predominating would be hydrostatic. But if the solutions were trapped in contact with a magma it is reasonable to consider that fluid pressures could have built up to the point where they equalled or exceeded the lithostatic pressure. Pressures in the district during ore deposition were probably between the hydrostatic and lithostatic.

Although it is impossible to estimate the depth of ore formation by reconstructing the stratigraphy, minimum depths can be estimated from the present topography. Also, arsenopyrite compositions possibly give some indications of pressures that might have existed during ore deposition. Hudson Bay Mountain is 8500 feet high. Most of the ore deposits occur below 5500 feet elevation and some occur below 2000 feet. Therefore, if it is assumed that the deposits were covered by rocks at least level with the top of the mountain, there were from 3000 to 6500 or more feet of cover at the time of ore deposition. However, this assumption, although very reasonable, may not be acceptable since the land may not have been flat while plutonism was taking place during the Tertiary. Lateral zonation in most ores seems more marked than vertical zonation; hence, it is a distinct possibility that slopes of the range during the Tertiary were much the same as they are now.

From Table 15 it can be noted that some arsenopyrites may have formed under pressures greater than 2000 bars. If these pressures were essentially lithostatic, and the cover rocks were of normal density (2.7), the pressure would be equal to a depth greater than five miles. Although such a depth based on other geologic features seems excessive, the possibility of depths greater than five miles should not be ruled out. For purposes of speculation on the processes of ore deposition, it is reasonable to conclude that ores of

the district could have formed at depths ranging from two to five miles. These would be equivalent to lithostatic pressures of 800 and 2000 bars, and hydrostatic pressures of 300 and 800 bars.

Thermal Pattern in the District

Variations in mineralogy and metal content of the ores in respect to the metamorphic aureole strongly suggest that all ores of the district despite their timing were deposited under the same general thermal regime. That is, the core of the district was relatively hot and the peripheral parts of the district were relatively cool. This thermal regime was controlled by the emplacement of Tertiary porphyries. Although it is not possible to determine precisely the temperature of ore formation in space or time, some reasonable temperature estimates can be made. Some of the more important temperature data are as follows:

1. Based on the depth estimates in the previous section and on reasonable geothermal gradients, minimum temperatures in the district at the time of ore formation were probably somewhere between 250 and 400°C.
2. The minimum melting temperature of water-saturated, granitic magma at 2000 bars is about 700°C. This is a satisfactory maximum temperature for most deposits.
3. The common occurrence of the assemblage magnetite + pyrite gives a maximum temperature for most of the molybdenum deposit of 675°C (Barnes and Kullerud, 1961).
4. Kullerud (1966) has also shown that pyrite and molybdenite cannot coexist above 732°C, and Kullerud and Yoder (1959) have shown that pyrite melts incongruently at 742°C. These reactions further substantiate the maximum temperatures of ore formation in the molybdenum deposit.

5. Absence of arsenopyrite from the molybdenum deposit could be an indication that temperatures in the deposit were in excess of 500°C, exceeding the stability limits of arsenopyrite in a sulfur-rich environment. However, this line of reasoning is inconclusive, since the molybdenum deposit may have evolved from solutions significantly different in nature from those that deposited the sulfide ores.
6. Composition of ankerite in sample 65-98 (p. 66) may be an acceptable indication that it crystallized above 425°C, which could be taken as a minimum temperature for molybdenum deposition in that area.
7. The composition of sphalerite adjacent to pyrrhotite in sample 66-76 from a tungsten-rich quartz vein near the outer limit of molybdenum mineralization indicates a possible temperature of formation in excess of 600°C (Barton and Toumin, 1966, and Boorman, 1967).
8. The common assemblage of arsenopyrite + pyrite indicates a maximum temperature of about 500°C for the crystallization of the outer zone (Clark, 1960a).
9. The transition of the assemblage arsenopyrite + pyrrhotite in the intermediate zone to arsenopyrite + pyrite in the outer zone must have occurred below 500°C (Clark, 1960a, see Fig. 54). However, the mineralogic transition might have occurred as the temperature dropped below 500°C if the solutions were near the pyrite-pyrrhotite solvus.
10. The compositions of some arsenopyrites from the intermediate zone indicate temperatures of formation in excess of 500°C.
11. Presence of hypogene marcasite and kaolin in the outer zone indicates that this stage of mineralization took place below 430°C (Kullerud, 1966 and Roy and Osborne, 1954).
12. Tennantite melts at 640°C and tetrahedrite at 555°C which give maximum temperatures of formation for these minerals.
13. The pyrrhotite compositions indicate that probably all the pyrrhotite formed initially above 300°C.
14. The exsolution of matildite from galena must have occurred below 215°C (Craig, 1967).

Although the data are not conducive to rigorous interpretation, the following generalizations on temperatures of can be made:

1. All ores of the district were probably deposited between 250 and 700°C.
2. The quartz vein stockwork of the molybdenum deposit probably formed between 400 and 700°C.
3. Ores of the intermediate zone were probably formed between 400 and 600°C; however, there are few reliable temperature indicators for this zone.
4. Ores of the outer zone probably formed mainly in the range 250-500°C.
5. Compared to other deposits of the district temperatures of formation of the Cu-Fe-Ag deposits were probably relatively low but they can only be inferred from general geologic relationships.

The Concept of Monoascendent and Polyascendent Zoning

Kutina (1957) proposed that zoned ores should be separated into monoascendent types, those derived from a single period of interrupted ascending solutions, and polyascendent types, those derived from interrupted ascending solution, possibly from unrelated sources. Since his proposal there has been considerable discussion of the relative importance of monoascendent and polyascendent solutions in the development of zoned deposits and districts. Much of the two volumes generated from the symposium on "Problems of Postmagmatic Ore Deposition" held in Prague, Czechoslovakia is devoted to this question.

From findings of the present study the writer would caution against uncritical use of these terms. Kalliokoski (1965) has

noted the risk of obscuring the complex and variable nature of vein formation by using these terms, and even Kutina (1965a) has indicated the difficulty of unambiguous interpretation of geologic features in separating the two types of zoning.

As cited throughout this thesis, there is ample evidence indicating that there was at least some polyascendency of the ore solutions. However, it does not necessarily follow that polyascendency of solutions was responsible for the zonal distribution of ores. Cause and effect relationships should not be forgotten. From this study it appears as if neither monoascendent or polyascendent solutions were the cause of the zoning, but rather the zoning was a result of a thermal-hydrothermal regime developed by the emplacement of Tertiary intrusions.

Chemical Character of Ore Solutions in Terms of Activity of Sulfur and Temperature

Since most sulfide reactions are relatively insensitive to changes in pressure and are very sensitive to changes in the activity of sulfur and temperature, Sims and Barton (1961) and Barton and Skinner (1967) have shown that it is very convenient to show the stability fields of ore minerals on a_{S_2} -T diagrams. Figure 54 is such a diagram for ores of the Hudson Bay Mountain district. It can be noted that the stability positions of the various types of ores are strongly dependent on the temperatures used for plotting. As mentioned above, the temperature determinations for ores of the district

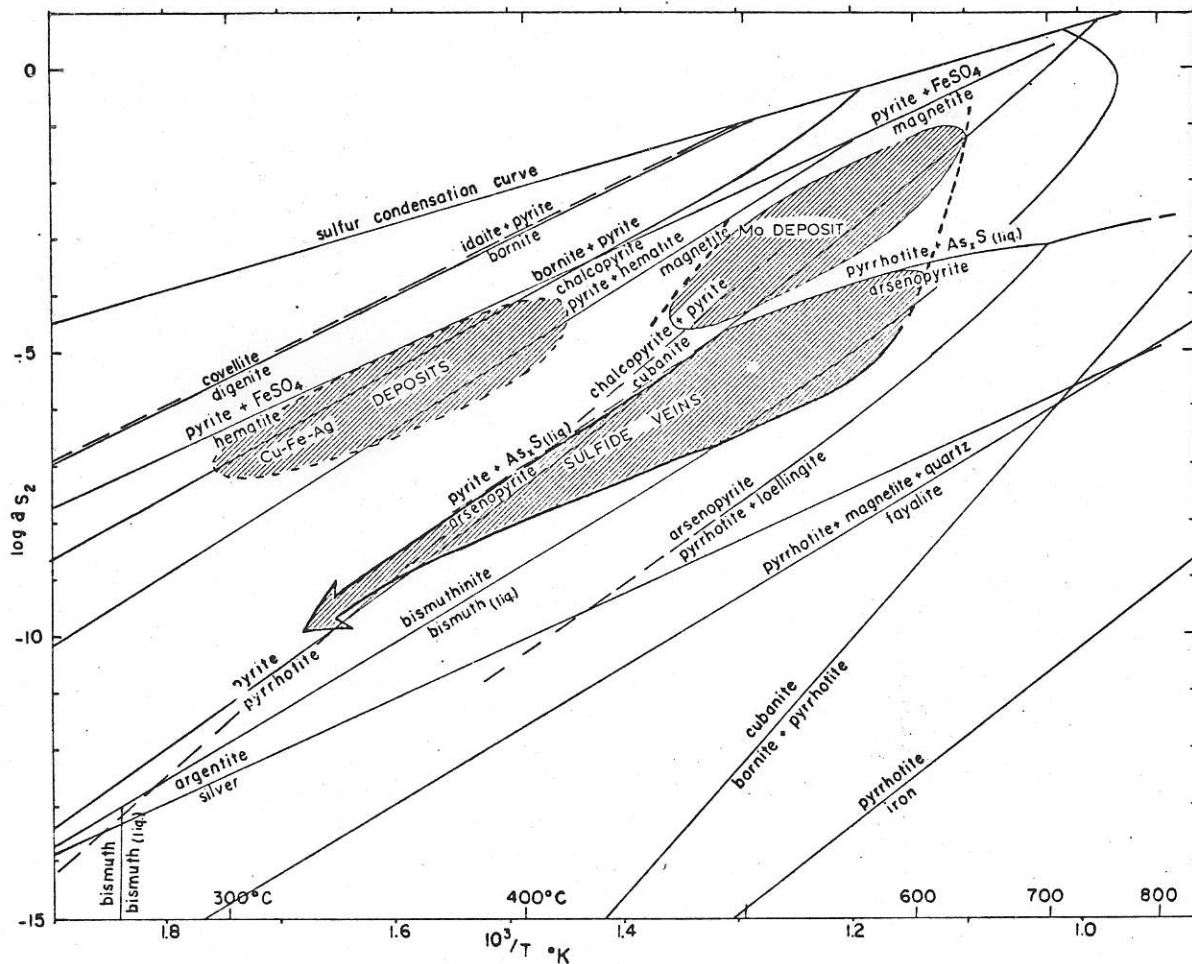


FIG.54-ACTIVITY OF S_2 -TEMPERATURE DIAGRAM FOR SELECTED SULFIDATION REACTIONS (after Barton & Skinner,1967)

Shaded areas are the most probable a_{S_2} -T regions for ores of the Hudson Bay Mtn. district.

may be subject to revision; however, it is reasonable to expect that the positions of the various ore types will not be changed drastically by future work.

The diagram serves to indicate that it is quite reasonable to assume that sulfide ores of the intermediate and outer zones were formed largely from monoascendent solutions that gradually changed in chemical character as they migrated away from the central part of the district. On the other

hand, it is equally apparent that, chemically, ores of the Cu-Fe-Ag deposits and molybdenum deposit, are significantly different from those of the "sulfide" deposits. Although it is not indicated on the diagram, it remains a possibility that the Cu-Fe-Ag deposits evolved from solutions that produced the molybdenum deposit but this is rather unlikely.

The exact relationship of ores of the molybdenum deposit to the sulfide veins of the intermediate and outer zones is not at all clear. At present the writer favors the hypothesis that the sulfide ores were formed at the same time or shortly after the development of the metamorphic aureole, and that the molybdenum deposit, with its pervasive alteration and bleaching, formed later during a more restricted period of magmatic activity.

Possible Mechanisms of Ore Deposition

Any process that could decrease the solubility of ore and gangue minerals could be responsible for ore deposition. Since the solubility of most minerals decreases with temperature,¹ processes which lead to a significant lowering of temperature could be effective in causing ore deposition.

Mixing of Solutions

Mixing of hydrothermal solutions with ground water could certainly be an effective means of cooling ore solutions. The drastic change in the chemistry of the sulfide ores near

¹ Carbonate minerals and anhydrite as shown by Holland (1967) are notable exceptions. Decreases in pressure would be the most effective way of precipitating these minerals.

the periphery of the district could be due to this process. As Sims and Barton (1961 and 1962) have indicated, such mixing may be accompanied by irreversible adiabatic expansion (throttling) of the solutions, which would further promote cooling. Even if mixing of solutions occurred near the periphery of the district, it is far less probable that such mixing could have been important in the central part of the district.

Throttling

Barton and Toulmin (1961), Toulmin and Clark (1967), and other authors, from theoretical considerations, have demonstrated how throttling may play a very important role in the cooling of hydrothermal fluids, and hence in causing ore deposition.¹ The principle may be explained as follows: when a fluid under high pressure passes through a constriction to an area of lower pressure, it is rapidly cooled by adiabatic expansion. Some throttling must have occurred in the district, but its importance in causing ore deposition remains to be demonstrated. It may have been responsible for development of ore shoots along sulfide vein systems, but more important, it could have been the main factor in the localization of ores of the molybdenum deposit.

The writer previously (1966) stated that fractures which are occupied by quartz veins of the molybdenum deposit could

¹ Solubility of most substances also decreases tremendously as density of a supercritical fluid decreases.

have been "formed during cooling following thermal metamorphism or possibly from relaxation of the magmatic forces that caused the doming." But this is rather an unsatisfactory explanation on several counts. It fails to answer the question why the prominent joints of the molybdenum deposit (Figure 8) are not characteristic of other parts of the metamorphic aureole. Moreover, the profusion of cross-cutting veins indicates that the jointing was actually an integral part of the mineralizing process.

Secor (1965) has demonstrated, using theoretical models, that fluids under high pressures, especially when they approach load pressures, can be very effective in jointing rocks or re-opening existing fractures. It is very reasonable to consider that near the magma chamber in Glacier Gulch, fluid pressures built up to the point that the fluids actually fractured the rock. As the fluids migrated out through the fractures, pressures would be released and the solutions were effectively throttled. The resulting decreases in temperature and pressure of the solutions would have promoted deposition of ore and gangue minerals, eventually sealing off the fractures, again making it possible for fluid pressures to increase. The banded Type I molybdenum veins were probably formed in fractures that were repeatedly opened. This is a very satisfactory way of explaining the localization of the wide and continuous Type I veins which control zones of higher grade molybdenum ore in the

granodiorite sheet approximately parallel to the base of the sheet, and a main thrust fault. The fractures would simply have been pre-existing, structurally weak zones that were continuously re-opened by the hydrothermal fluids. From Figure 25 it can be seen that at least some of the banded veins were re-opened.

In envisioning such a system it is easy to see how the solutions of the area would have been mechanically very unstable, and quite variable in their physicochemical nature. This is consistent with the great diversity of vein and alteration types in the deposit.

If such a system were responsible for the development of the molybdenum deposit, it is a necessary requisite that hydrothermal fluids migrated away from the magma and not towards it. The short distance of travel through the volcanic host rocks would also support the contention that much of the molybdenum was derived from the magma and not from other parts of the hydrothermal system. Turekian and Wedepohl, 1961, indicate that the average igneous rock of intermediate composition contains about 1 ppm Mo. This is far too low to account for the several hundred to over 2,000 ppm Mo contained in as much as $\frac{1}{2}$ or possibly 1 cubic mile of rock in the molybdenum deposit.

The throttling model developed for the localization of the molybdenum deposit should be considered only a first approximation. In order to fully understand the mechanisms

of deposition one would have to know the absolute and relative temperatures of hydrothermal solutions and wall rock, as well as the pressures involved. Moreover, the salinity of the solutions would certainly affect the throttling mechanism. Although the necessary quantitative thermal data on concentrated complex solutions is lacking, Toulmin and Clark (p. 446, 1967) state:

Broadly speaking, however, the thermal effect of throttling is greatest in the general vicinity of the critical point. The effect of dissolved solids will in general be to displace this region to higher temperatures and lower pressures and so restrict the region of geological likelihood of the throttling process.

Chemical Control of Wall Rocks

Most recent workers such as Barton and Toulmin (1961), Parker (1962), and Toulmin and Clark (1967) have concluded that heat exchange with host rocks and wall rock alteration are not effective means of cooling hydrothermal solutions. But this does not exclude the possibility that chemical exchange with wall rocks could be an important factor in decreasing the solubility of some ore constituents, thus leading to ore deposition. It is a well established fact that lime-rich rocks can play an important role in ore deposition. Most ores of the district occur in lime-poor rocks, but it is obvious that limestone lenses and limy graywackes on the northwest side of the district were very important in localizing ores. Here sulfides have replaced limestone near limestone-vein intersections and have caused the localization

of ore shoots in the veins where they cut these rocks. Such a chemical control on ore deposition may be the reason why ores in this area are telescoped.

Cu-Fe-Ag ores commonly occur in red and purple volcanic rocks rich in supergene or diagenetic iron oxides. As indicated by the limited size of these deposits and their alteration halos, the volume of ore solution was probably relatively small. Thus they could easily have been affected by reactions with the wall rock. It is quite possible that the iron oxides of the wall rock (largely hematite?) were effective in buffering the solutions, causing a significant increase in fO_2 , thus permitting the formation of the unique mineral assemblages. The Last Chance property, the only one of this type with abundant magnetite, occurs in volcanic rocks that do not contain as much hematite (?). The complete pseudomorphic replacement of early hematite by magnetite in this deposit, indicates that reactions with the wall rocks in the early stages of ore deposition could have caused the deposition of hematite, but that with increasing hydrothermal activity, compositions of the solutions were able to override the initial, dominating effects of the wall rocks.

Structural Control

Structural control of ore deposition is apparent in the sense that permeable structures that had access to the hydrothermal solutions were favored sites for ore formation. For instance, ore occurs in subsidiary fractures along the

main fault on the east and north sides of Hudson Bay Mountain, and in the subparallel set of fractures on the southwest side of the mountain. These fracture systems must have had access and been permeable to the hydrothermal solutions. Ore shoots along vein systems were probably localized mainly in the most permeable areas (possibly due to throttling). Volcanic and intrusive rocks, in general, were better hosts than sedimentary rocks, with the exception of limy rocks. The reason for this is simply that, being more brittle, the former were more highly fractured and thus provided better access routes for ore solutions.

Possible Model of Ore Formation in the District

Although it is obvious that the ore-forming processes in the district were very complex, it is possible to offer a generalized model consistent with observed relationships. Burnham (1967), based on experimental data, has given a detailed discussion of the possible relationships of hydrothermal fluids and granitic magmas. His diagram, shown in Figure 55, can be used to trace the history of a hypothetical magma as it migrates towards the earth's surface. If it is assumed that, at depth, the magma contained about five per cent H_2O , then it is apparent that the P_{H_2O} would equal P_{total} when the P_{total} was decreased to just less than three kilobars. At this point the magma would boil and a water-rich phase would separate as droplets which would move upwards. The subsequent decrease in water content would promote crystallization of the magma--perhaps producing the

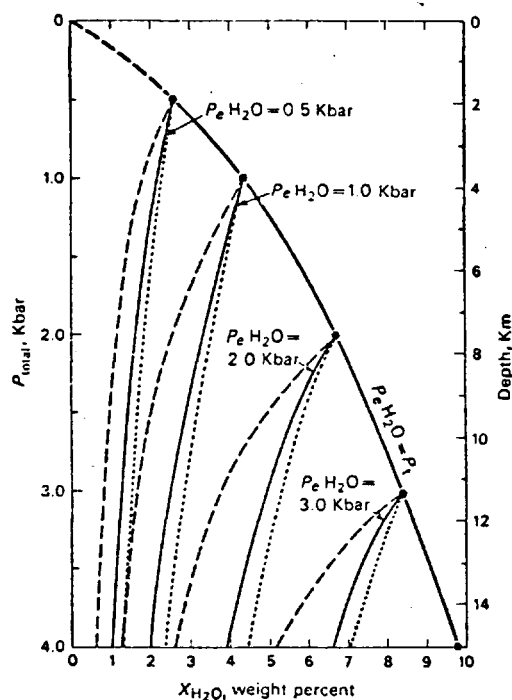


Fig. 55 - Isothermal (945°C) P - X projection of the L-V boundary in the system $\text{NaAlSi}_3\text{O}_8$ - H_2O showing the calculated effects of P_t on $P_{e,\text{H}_2\text{O}}$ of melts undersaturated with water. The solid curves are the calculated $P_{e,\text{H}_2\text{O}}$ isobars assuming an effective molecular weight of 65.5 grams/mole, whereas the dashed isobars are for a molecular weight of 262 grams/mole. The dotted curves represent isobars calculated using weight percent H_2O after Burnham (1967)

phenocrysts so characteristic of porphyry copper deposits. Crystallization would decrease the amount of silicate melt and hence promote "second boiling" which would cause a further separation of water from the melt. It is this initial water-rich phase that the writer envisions as facilitating the extensive thermal metamorphism and possibly being responsible for sulfide ores of the intermediate and outer zones. This thermal-hydrothermal activity could have preceded the magma on its advance towards the surface. Following this stage, the magma or perhaps small portions

of the magma, then could continue upwards until it reached a Ptotal of about 2 kilobars. Possibly further intrusion of the magma was inhibited by the granodiorite sheet. During this stage the writer believes that the bodies of magma were smaller than those of earlier magmas, but possibly the amount of hydrothermal fluid being evolved was considerably greater. Whereas earlier pressures of the hydrothermal fluids had been gradually dissipated as the fluids migrated away from the magma, pressures of these fluids were permitted to build up to a point of sudden release. This stage of activity caused development of a throttling zone that led to formation of the quartz vein stockwork of the molybdenum deposit.

Although as viewed here, the molybdenum deposit was formed after the sulfide ores from smaller bodies of magma, the central positioning of all the magmas and the maintenance of a regional thermal-hydrothermal regime permitted the zonal distribution of the ores.

Admittedly this model is over simplified but it is consistent with the major features of the district. It explains the relationship of the ores to the Tertiary porphyries, metamorphic aureole, and the overall regime of the district. It also explains the relative timing of the main types of ores; the drastic chemical, mineralogic, and structural differences between ores of the molybdenum deposit and ores of the intermediate zone; and it is consistent with the observed spatial and temporal relationships of porphyries and molybdenum mineralization.

CONCLUSIONS

All deposits of the Hudson Bay Mountain district are spatially, temporally, and genetically related to Early Tertiary porphyry intrusions. Most deposits were formed under the same general thermal regime, except perhaps the quartz, carbonate veins of the molybdenum deposit which probably formed under waning conditions. The overall zonal pattern of ores was developed by chemical evolution, in space and time, of hydrothermal solutions that migrated outwards from a magmatic center during a prolonged period of magmatic and hydrothermal activity. Temporal, mineralogic, chemical, and structural features of the deposits suggest that there were at least two main periods of ore deposition--an early one that led to the formation of the sulfide ores and a later one that led to the formation of the molybdenum deposit.

The sulfide veins were probably synchronous with the thermal metamorphism which resulted from the emplacement of a relatively large intrusion that has not yet been unroofed. The formation of the molybdenum deposit coincided with a period of pervasive hydrothermal activity and fracturing and the emplacement of small porphyry intrusions in the Glacier Gulch area. This restricted period of magmatic activity largely followed the period of thermal metamorphism.

The maintenance of a regional thermal-hydrothermal regime about a magmatic center was probably the reason for the zonal deposition of ores. Monoascendency and polyas-

cendency of ore solutions were important in the district, but neither was solely responsible for causing the zoning. The Hudson Bay Mountain area is perhaps a suitable example of a zoned district in which polyascendency of ore solutions was important.

Most of the ore solutions were probably magmatically derived, concentrated brines. Interaction of the hot brines with ground water near the periphery of the district could have been the main reason for ore deposition and the drastic change in metal values and metal ratios in these areas. Throttling might also have been an important factor in causing deposition of these ores. Throttling of fluids under very high pressure as they were released from a magma chamber could have been a key factor in the formation and localization of the molybdenum deposit. Chemical interaction of the ore solutions with wall rocks apparently was not an important factor causing deposition, except perhaps on the northwest side of the district where lime-rich host rocks caused the precipitation of sulfides. Such a chemical control could have been responsible for the telescoping in this area.

BIBLIOGRAPHY

- Armstrong, J.E., 1944, Preliminary map, Smithers, British Columbia: Geol. Survey of Canada, Paper 44-23.
- Arnold, R.G., 1962, Equilibrium relations between pyrrhotite and pyrite from 325° to 743°C: *Econ. Geol.*, v. 57, p. 72-90.
- , 1966, Mixtures of hexagonal and monoclinic pyrrhotite and the measurement of the metal content of pyrrhotite by x-ray diffraction: *Am. Mineralogist*, v. 51, p. 1221-1227.
- , and Reichen, Laura E., 1962, Measurement of the metal content of naturally occurring, metal-deficient hexagonal pyrrhotite by an x-ray spacing method: *Am. Mineralogist*, v. 47, p. 105-111.
- Barnes, H.L., 1962, Mechanisms of mineral zoning: *Econ. Geol.*, v. 57, p. 30-37.
- , ed., 1967, *Geochemistry of Hydrothermal Ore Deposits*: Holt, Rinehart and Winston, Inc., New York, 670p.
- , and Czamanske, G.K., 1967, Solubilities and transport of ore minerals: in *Geochemistry of Hydrothermal Ore Deposits*, H.L. Barnes, ed., Holt, Rinehart and Winston, New York, p. 334-381.
- , and Kullerud, G., 1961, Equilibrium in sulfur-containing aqueous solutions, in the system Fe-S-O, and their correlation during ore deposition: *Econ. Geol.*, v. 56, p. 648-688.
- Barton, Paul B., Jr., Bethke, P.M., and Toulmin, Priestley, III, 1963, Equilibrium in ore deposits: *Min. Soc. of America, Spec. Paper 1*, p. 171-185.
- , and Skinner, Brian J., 1967, Sulfide mineral stabilities: in *Geochemistry of Hydrothermal Ore Deposits*, H.L. Barnes, ed., Holt, Rinehart and Winston, New York, p. 236-333.
- , and Toulmin, Priestley, III, 1961, Some mechanisms for cooling hydrothermal fluids: *U.S. Geol. Survey Prof. Paper 424-D*, p. D348-D352.
- , and ----, 1964, Experimental determination of the reaction chalcopyrite + sulfur = pyrite + bornite from 350° to 500°C: *Econ. Geol.*, v. 59, p. 747-752.
- , and ----, 1966, Phase relations involving sphalerite in the Fe-Zn-S system: *Econ. Geol.*, v. 61, p. 815-849.

- Berry, L.G., and Thompson, R.M., 1962, X-ray powder data for ore minerals: the Peacock atlas: Geol. Soc. America, Memoir 85, 281p.
- Boorman, Roy S., 1967, Subsolidus studies in the ZnS-FeS-FeS₂ system: Econ. Geol., v. 62, p. 614-631.
- Boyle, R.W., and Jambor, J.L., 1963, The geochemistry and geothermometry of sphalerite in the lead-zinc-silver lodes of the Keno Hill-Galena Hill area, Yukon: Can. Min., v. 7, part 3, p. 479.
- Brett, R., 1961, A magmatic-pegmatitic-hydrothermal sequence at Lacorne, Quebec: Econ. Geol., v. 56, p. 784-789.
- , 1964, Experimental data from the system Cu-Fe-S and their bearing on exsolution textures in ores: Econ. Geol., v. 59, p. 1241-1270.
- Brown, A.S., 1960, Geology of the Rocher Deboule Range: B.C. Dept. of Mines, Bull. 43, 78p.
- , 1965, Lucky Ship molybdenum property: Minister of Mines, B.C., Ann. Rept., p. 84-87.
- , 1966, Big Onion copper-molybdenum property: Minister of Mines, B.C., Ann. Rept., p. 83-86.
- Burnham, C. Wayne, 1967, Hydrothermal fluids at the magmatic stage: in Geochemistry of Hydrothermal Ore Deposits, H.L. Barnes, ed., Holt, Rinehart and Winston, New York, p. 34-76.
- Buseck, P.R., 1967, Contact metasomatism and ore deposition: Tem Piute, Nevada: Econ. Geol., v. 62, p. 331-353.
- Cameron, E.N., and Van Rensburg, W.C.J., 1965, Chemical-mechanical polishing of ores: Econ. Geol., v. 60, p. 630-632.
- Carpenter, R.H., 1965, A study of the ore minerals in cupriferous pyrrhotite deposits in the Southern Appalachians: unpublished Ph.D. thesis Univ. of Wis., 70p.
- , and Desborough, G.A., 1964, Range in solid solution and structure of naturally occurring troilite and pyrrhotite: Am. Mineralogist, v. 49, p. 1350-1365.
- Chace, F.M., 1956, Abbreviations in field and mine geological mapping: Econ. Geol., v. 51, p. 712-723.

- Clark, A.H., 1965, The composition and conditions of formation of arsenopyrite and löllingite in the Ylöjärvi copper-tungsten deposit, southwest Finland, Bulletin de la Commission Geologique de Finlande, no. 217, 56p.
- , 1966, Equilibrium temperature, PS_2 and PO_2 during formation of the Marmoraton pyrometasomatic iron deposit: Econ. Geol., v. 61, p. 780-783.
- Clark, L.A., 1960a, The Fe-As-S system: Phase relations and applications: Econ. Geol., v. 55, p. 1345-1381, and 1631-1652.
- Clark, S.P., ed., 1966 Handbook of physical constants: Geol. Soc. America, Memoir 97, 587p.
- Craig, J.R., 1967, Phase relations and mineral assemblages in the Ag-Bi-Pb-S system: Mineralium Deposita, v. 1, p. 278-306.
- Desborough, G.A., and Carpenter, R.H., 1965, Phase relations of pyrrhotite: Econ. Geol., v. 60, p. 1431-1450.
- Edwards, A.B., 1954, Textures of the ore minerals: Aust. Inst. Min. and Met., Melbourne, 242p.
- Ellis, A.J., 1967, The chemistry of some explored geothermal systems: in Geochemistry of Hydrothermal Ore Deposits, H.L. Barnes, ed., Holt, Rinehart and Winston, New York, p. 465-514.
- Fryklund, V.C., and Fletcher, J.D., 1956, Geochemistry of sphalerite from the Star Mine, Coeur d'Alene district, Idaho: Econ. Geol., v. 51, p. 223-247.
- Galloway, J.D., 1923, Hudson Bay Mountain: Minister of Mines, B.C., Ann. Rept., p. 107-111.
- , 1924, Victory group: Minister of Mines, B.C. Ann. Rept., p. 109-110.
- Goldsmith, J.R., and Graf, D.L., 1958, Relation between lattice constants and composition of Ca-Mg carbonates: Am. Mineralogist, v. 43, p. 84-101.
- , and ----, 1958, Structural and compositional variations in some natural dolomites: Jour. Geol., v. 66, p. 678-693.
- Goresy, A.E., 1967, Quantitative electron microprobe analyses of coexisting sphalerite, daubreelite and troilite in the Odessa iron meteorite and their genetic implications: Geochim. et Cosmochim. Acta, v. 31, p. 1667-1676.

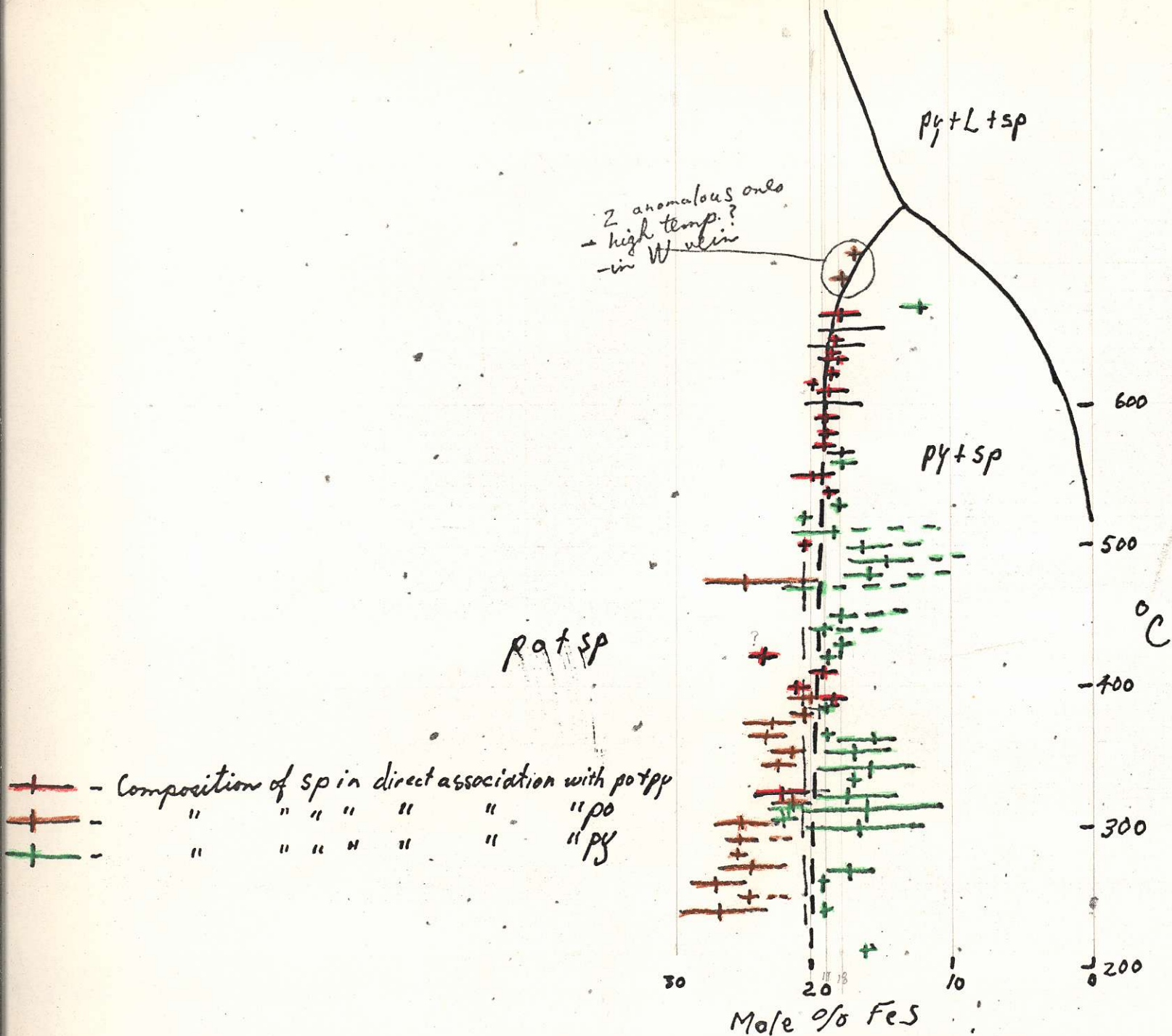
- Greenwood, R., 1943, Effect of chemical impurities on scheelite fluorescence: *Econ. Geol.*, v. 38, p. 56-64.
- Helgeson, Harold C., 1964, *Complexing and Hydrothermal Ore Deposition*: Pergamon Press, New York, 123p.
- Hemley, J.J. and Jones, W.R., 1964, Chemical aspects of hydrothermal alteration with emphasis on hydrogen metasomatism: *Econ. Geol.*, v. 59, p. 538-569.
- Holland, H.D., 1959, Some applications of thermochemical data to problems of ore deposits. I. Stability relations among the oxides, sulfides, sulfates and carbonates of ore and gangue metals: *Econ. Geol.*, v. 54, p. 184-233.
- , 1965, Some applications of thermochemical data to problems of ore deposits. II. Mineral assemblages and the composition of ore-forming fluids: *Econ. Geol.*, v. 60, p. 1101-1166.
- , 1967, Gangue minerals in hydrothermal deposits: in *Geochemistry of Hydrothermal Ore Deposits*, H.L. Barnes, ed., Holt, Rinehart and Winston, New York, p. 382-436.
- Holland, S.S., 1964, Landforms of British Columbia, a physiographic outline: *Dept. of Mines, Bull. 48*, 138p.
- Jones, R.H.B., 1925, Geology and ore deposits of Hudson Bay Mountain, Coast District, B.C.: *Can. Geol. Survey Sum. Rept.*, 1925, Part A, p. 120-143.
- Kalliokoski, J., 1965, On monoascendent and polyascendent zoning: in *Symposium on Problems of Postmagmatic Ore Deposition*, v. II, *Geol. Survey of Czechoslovakia*, p. 192-193.
- Kindle, E.D., 1948, Duthie Mine in structural geology of Canadian ore deposits: in *Can. Inst. Min. and Met. Symposium*, p. 131-137.
- , 1954, Mineral resources, Hazelton and Smithers areas, Cassiar and coast districts, British Columbia: *Geol. Survey, Canada, Memoir 223*.
- Kirkham, R.V., 1966, Glacier Gulch Molybdenum deposit: *Minister of Mines, B.C., Ann. Rept.*, p. 86-91.
- Koch, G.S., Jr., and Link, R.F., 1963, Distribution of metals in the Don Tomas Vein, Frisco Mine, Chihuahua, Mexico, *Econ. Geol.*, v. 58, p. 1061-1070.

- Krauskopf, K.B., 1964, The possible role of volatile metal compounds in ore genesis: *Econ. Geol.*, v. 59, p. 22-45.
- , 1967, Source rocks for metal-bearing fluids: in *Geochemistry of Hydrothermal Ore Deposits*, H.L. Barnes, ed., Holt, Rinehart and Winston, New York, p. 1-33.
- Krumbein, W.C., and Graybill, F.A., 1965, *An Introduction to Statistical Models in Geology*: McGraw-Hill, New York, 475p.
- Kullerud, G., 1953, The FeS-ZnS system, a geological thermometer: *Norsk Geol. Tidsskr.*, v. 32, p. 61-147.
- , 1966, The Fe-Mo-S system: *Ann. Rept. of the Director Geoph. Lab.*, p. 337-342.
- , 1966, The Fe-S-O-H system: *Ann. Rept. of the Director Geoph. Lab.*, p. 352-354.
- , 1967, Sulfide studies: in *Researches in Geochemistry*, v. 2, P.H. Abelson, ed., John Wiley and Sons, p. 287-321.
- , and Buseck, P.R., 1962, The Fe-Mo-S system: *Carnegie Inst. Washington Yearbook* 61, p. 150-151.
- , and Yoder, H.S., Jr., 1959, Pyrite stability relations in the Fe-S system: *Econ. Geol.*, v. 54, p. 533-572.
- Kutina, J., 1957, The zonal theory of ore deposits: *Econ. Geol.*, v. 52, p. 316-319.
- , 1965, The concept of monoascendent and polyascendent zoning: in *Symposium on Problems of Postmagmatic Ore Deposition*, v. II, *Geol. Survey of Czechoslovakia*, p. 47-55.
- , Park, C.F., and Smirnov, V.I., 1965, On the definition of zoning and on the relation between zoning and paragenesis: in *Symposium on Problems of Postmagmatic Ore Deposition*, v. II, *Geol. Survey of Czechoslovakia*, p. 589-595.
- Meyer, Charles, and Hemley, J.J., 1967, Wall rock alteration: in *Geochemistry of Hydrothermal Ore Deposits*, H.L. Barnes, ed., Holt, Rinehart and Winston, New York, p. 166-235.

- Morimoto, N., and Clark, L.A., 1961, Arsenopyrite crystal-chemical relations: *Am. Mineralogist*, v. 46, p. 1448-1469.
- Orville, P.M., 1963, Alkali ion exchange between vapor and feldspar phases: *Am. J. Sci.*, v. 261, p. 201-237.
- , 1967, Unit-cell parameters of the microcline-low albite and the sanidine-high albite solid solution series: *Am. Mineralogist*, v. 52, p. 55-86.
- Parker, P.D., 1962, Some effects of environment on ore deposition: *Econ. Geol.*, v. 57, p. 293-324.
- Richards, S.M., 1963, The abundances of copper, zinc, lead and silver in the discordant hydrothermal orebody of the Conrad Mine, N.S.W.: *Aust. Inst. Min. and Met. Proc.*, no. 208, p. 43-54.
- Roedder, E., 1965, Evidence from fluid inclusions as to the nature of the ore-forming fluids: in *Symposium on Problems of Postmagmatic Ore Deposition*, v. II, *Geol. Survey of Czechoslovakia*, p. 375-384.
- , 1965, Report on S.E.G. symposium on the chemistry of the ore-forming fluids: *Econ. Geol.*, v. 60, p. 1380-1403.
- , 1967, Fluid inclusions as samples of ore fluids: in *Geochemistry of Hydrothermal Ore Deposits*, H.L. Barnes, ed., Holt, Rinehart and Winston, New York, p. 515-574.
- , and Creel, J.P., 1966, Fluid inclusions at Bingham, Utah: *U.S. Geol. Survey Prof. Paper 550A*, p. 153-154.
- Rosenberg, P.E., 1963, Subsolidus relations in the system $\text{CaCO}_3\text{-FeCO}_3$: *Am. J. Sci.*, v. 261, p. 683-690.
- , 1967, Subsolidus reactions in the system $\text{CaCO}_3\text{-MgCO}_3\text{-FeCO}_3$ between 350 and 550 C: *Am. Mineralogist*, v. 52, p. 787-796.
- Roy, R., and Osborn, E.F., 1954, The system $\text{Al}_2\text{O}_3\text{-SiO}_2\text{-H}_2\text{O}$: *Am. Mineralogist*, v. 39, p. 853-885.
- Sato, M., 1966, Electrochemical method of geothermometry for ore and gangue minerals (abstract): *Geol. Soc. of America Program for Ann. Meeting*, p. 189-190.
- Sawkins, F.J., 1964, Lead-zinc ore deposition in the light of fluid inclusion studies, Providencia Mine, Zacatecas, Mexico: *Econ. Geol.*, v. 59, p. 883-919.

- Schmitt, H.A., 1954, The origin of the silica of the bed-rock hypogene ore deposits: *Econ. Geol.*, v. 49, p. 877-890.
- Scott, S.D., and Barnes, H.L., 1967, Sphalerite geothermometry at 330 to 580 C (abstract): *Econ. Geol.*, v. 62, p. 874.
- Secor, D.T., Jr., 1965, Role of fluid pressure in jointing: *Am. J. Sci.*, v. 263, p. 633-646.
- Shcherba, G.N., Gakova, V.D., Kudryashov, A.V., and Senchilo, N.P., 1964, Alkali feldspars from feldspar-quartz veinlets in molybdenum-tungsten deposits, Kazakhstan. Chapter IV. Quartz and feldspar-quartz vein and veinlets: *Geochemistry International*, p. 141-192.
- Sims, P.K., and Barton, P.B., Jr., 1961, Some aspects of geochemistry of sphalerite, Central City district, Colorado: *Econ. Geol.*, v. 56, p. 1211-1237.
- , and -----, 1962, Hypogene zoning and ore genesis, Central City district, Colorado: in *Buddington Volume*, *Geol. Soc. of America*, 660p, p. 373-395.
- , Drake, A.A., Jr., and Tooker, E.W., Economic geology of the Central City district, Gilpin County, Colorado: *U.S. Geol. Survey Prof. Paper* 359, 231p.
- Skinner, B.J., 1961, Unit cell edges of natural and synthetic sphalerites: *Am. Mineralogist*, v. 46, p. 1399-1411.
- , White, D.E., Rose, H.J., and Mays, R.E., 1967, Sulfides associated with the Salton Sea geothermal brine: *Econ. Geol.*, v. 62, p. 316-330.
- Souther, J.G., and Armstrong, J.E., 1966, North central belt of the Cordillera of British Columbia: *Can. Inst. Min. and Met.*, Special Volume no. 8, p. 171-184.
- Stanton, R.L., 1958, Abundances of copper, zinc and lead in some sulphide deposits: *Jour. Geol.*, v. 66, p. 484-502.
- , 1962, Elemental constitution of the Black Star orebodies, Mount Isa, Queensland, and its interpretation: *Trans. Inst. Min. and Met.*, v. 72, p. 69-124.
- , and Richards, S.M., 1961, The abundances of lead, zinc, copper and silver at Broken Hill: *Aust. Inst. Min. and Met. Proc.*, no. 198, p. 309-367.
- , and -----, 1963, The abundances of lead, zinc, copper and silver at Broken Hill - a reply to C.J. Hodgson: *Aust. Inst. Min. and Met. Proc.*, no. 206, p. 309-367.

- Stemprok, Miroslav, 1965, Genetic features of the deposits of tin, tungsten and molybdenum formation: in Symposium on Problems of Postmagmatic Ore Deposition, v. II, Geol. Survey of Czechoslovakia, p. 472-481.
- Taylor, H.P., 1967, Oxygen isotope studies of hydrothermal mineral deposits: in Geochemistry of Hydrothermal Ore Deposits, H.L. Barnes, ed., Holt, Rinehart and Winston, New York, p. 109-142.
- Thompson, R.M., 1949, The telluride minerals and their occurrence in Canada: *Am. Mineralogist*, v. 34, p. 342-382.
- Thorpe, R.I., 1967, Controls of hypogene sulfide zoning, Rossland, British Columbia: unpublished Ph.D. thesis Univ. of Wis., 131p.
- Tipper, H.W., 1959, Revision of the Hazelton and Takla Groups of central British Columbia: *Geol. Survey of Canada, Bull.* 47, 51p.
- Toulmin, Priestley, III, 1960, Effect of copper on sphalerite phase equilibria - a preliminary report (abstract): *Geol. Soc. of America Bull.*, v. 71, p. 1993.
- , and Barton, Paul B., Jr., A thermodynamic study of pyrite and pyrrhotite, *Geochim. et Cosmochim. Acta*, v. 28, p. 641-671.
- , and Clark, Sydney P., Jr., 1967, Thermal aspects of ore formation: in *Geochemistry of Hydrothermal Ore Deposits*, H.L. Barnes, ed., Holt, Rinehart and Winston, New York, p. 437-464.
- Turekian, K.K., and Wedepohl, K.H., 1961, Distribution of the elements in some major units of the earth's crust: *Geol. Soc. of America Bull.*, v. 72, p. 175-192.
- Vokes, F.M., 1963, Molybdenum deposits of Canada: *Geol. Survey of Canada, Econ. Geol. Rept. No.* 20, 332p.
- Wallace, S.R., Baker, R.C., Jonson, D.C., and MacKenzie, W.B., 1960, Geology of the Climax molybdenite deposit - A progress report: in *Guide to the Geology of Colorado, G.S.A. guidebook*, p. 238-252.
- Warne, S. St. J., 1962, A quick field or laboratory staining scheme for the differentiation of the major carbonate minerals: *Jour. Sed. Pet.*, v. 32, p. 29-38.
- Warren, H.V., and Thompson, R.M., 1945, Sphalerites from western Canada: *Econ. Geol.*, v. 40, p. 309-335.



quite possible
from esp
data

Ranges of Mole % FeS of H.B. Mtn. Spinelites, plotted with no regard to temperature or "absolute" evidence of equilibrium
 assume solvus is at 19 mole % according to Scott (1969) these sp Equil. @ the Fe sulphides at press. of at least 1 kb

West

East

Glacier

qz veins with
molybdenite

Jurassic
Volcanic Rocks

very approx.
1/2 mile

high silica
rock
(qz veins)

Intraminal
dykes

Quartz Monzonite
Porphyry
(67 m.y. old?)

It is younger than
most of the mineralization

Chilled magm.

Quartz Monz.
- Quartz habit
Porphyry

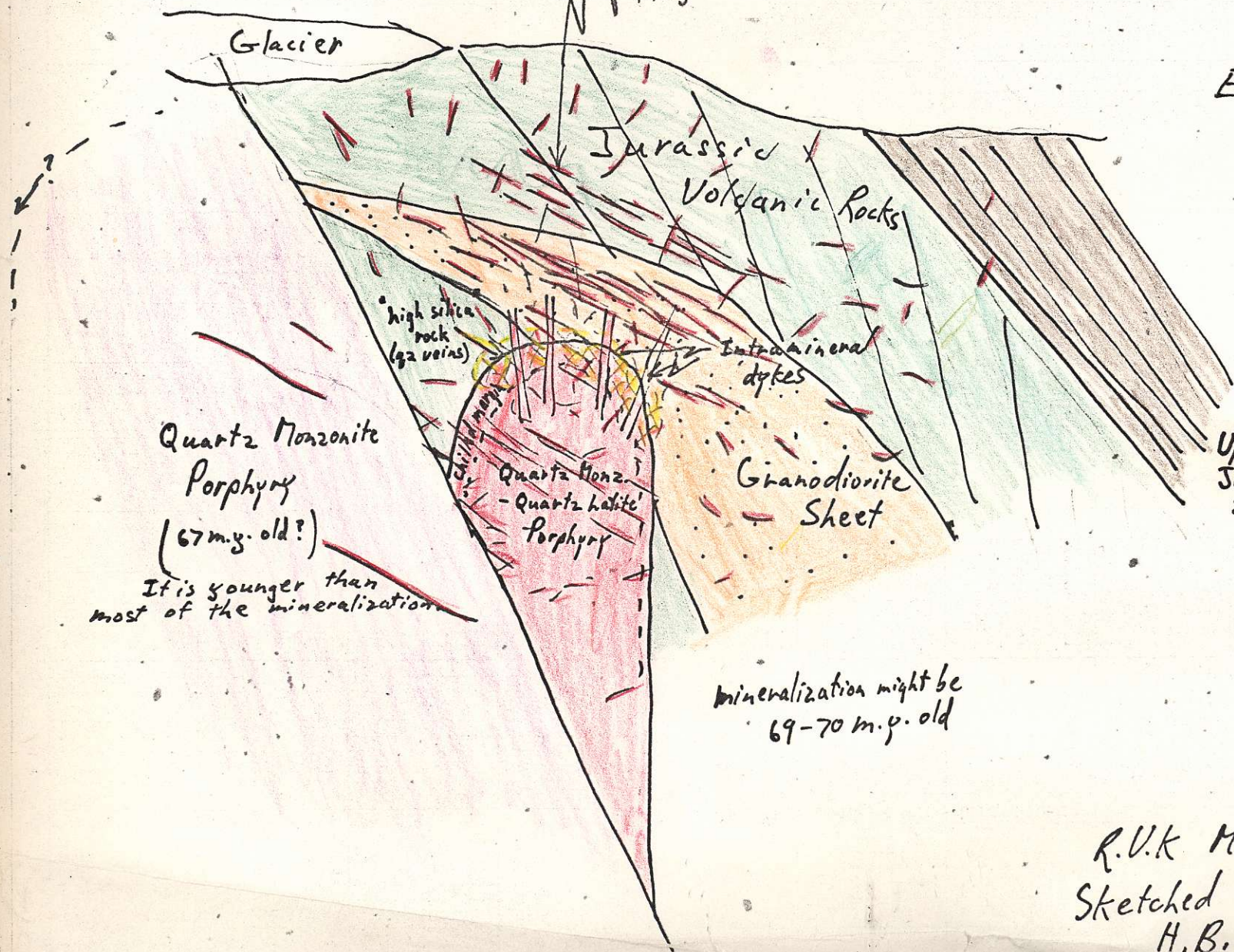
Granodiorite
Sheet

Upper
Jurassic
Sedimentary
Rocks

mineralization might be
69-70 m.y. old

Somewhere near
section BB in the
1966 Ann. Rept.

R.V.K. Mar. '69
Sketched Section through the
H.B. Mtn. Mo Deposit



White, W.H., 1966, Tectonic map of the western Cordillera, British Columbia and neighbouring parts of the United States: Can. Inst. Min. and Met., Special Volume no. 8.

Williams, K.L., 1965, Determination of the iron content of sphalerite (discussion): Econ. Geol., v. 60, p. 1740-1747.

----, 1967, Electron probe microanalysis of sphalerite: Am. Mineralogist, v. 52, p. 475-492.

Yund, R.A., and Kullerud, G., 1966, Thermal stability of assemblages in the Cu-Fe-S system: Jour. Pet., v. 7, p. 454-488.